BAKE HARDENING IN LOW AND MEDIUM CARBON STEELS

Sourav Das

BAKE HARDENING IN LOW AND MEDIUM CARBON STEELS

Thesis submitted to
Indian Institute of Technology, Kharagpur
for the award of the degree

of

Doctor of Philosophy

by

Sourav Das

under the guidance of

Dr. S. B. Singh and Dr. Ing. O. N. Mohanty

Department Of Metallurgical and Materials Engineering
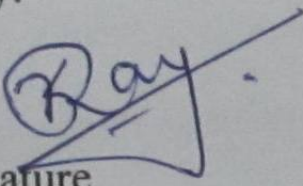
INDIAN INSTITUTE OF TECHNOLOGY, KHARAGPUR

May 2012

CERTIFICATE OF APPROVAL

--/--/--

Certified that the thesis entitled **Bake Hardening in Low and Medium Carbon Steels** submitted by SOURAV DAS to Indian Institute of Technology, Kharagpur, for the award of the degree of Doctor of Philosophy has been accepted by the external examiners and that the student has successfully defended the thesis in the viva-voce examination held today.
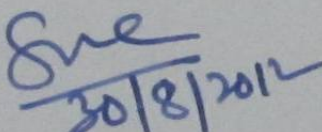
Signature

Name: K. K. Ray

(Member of the DSC)

Signature

Name: A. K. Chakraborty

(Member of the DSC)

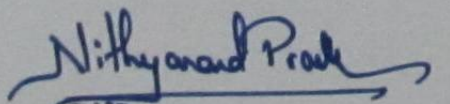Signature

Name   U. K. Chattrjee

(Member of the DSC)

Signature   30/8/2012
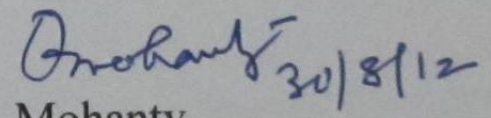
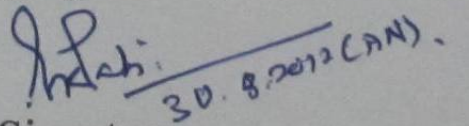Name : S. B. Singh

(Supervisor)

Signature   30/8/12

Name : O. N. Mohanty

(Supervisor)

Signature

Name N. PRABHU

(External Examiner)

Signature   30.8.2012 (AN).
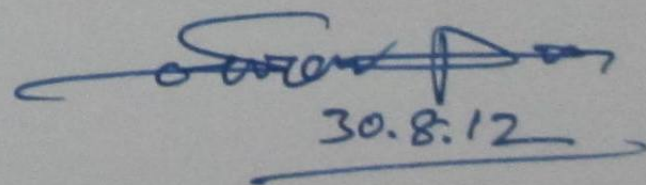
Name   S. K. PABI.

(Chairman)

DECLARATION

I certify that

a. the work contained in this thesis is original and has been done by me under the guidance of my supervisors.

b. the work has not been submitted to any other Institute for any degree or diploma.

c. I have followed the guidelines provided by the Institute in preparing the thesis.

d. I have conformed to the norms and guidelines given in the Ethical Code of Conduct of the Institute.

e. whenever I have used materials (data, theoretical analysis, figures, and text) from other sources, I have given due credit to them by citing them in the text of the thesis and giving their details in the references.

30.8.12

(Sourav Das)

भारतीय प्रौद्योगिकी संस्थान खड़गपुर

खड़गपुर – ७२१ ३०२, भारत

Indian Institute of Technology Kharagpur

Kharagpur - 721 302, India

Department of Metallurgical & Materials Engineering

CERTIFICATE

This is to certify that the thesis entitled **Bake Hardening in Low and Medium Carbon Steels** submitted by SOURAV DAS to Indian Institute of Technology, Kharagpur, is a record of bona fide research work under our supervision and is worthy of consideration for the award of the degree of Doctor of Philosophy of the Institute.

30/8/2012

_____
Supervisor

30/08/12

_____
Supervisor

Date: 30|8|2012

ACKNOWLEDGEMENT

It was a journey of a lifetime. This journey would not have come to an end if I did not get the support in many ways (technical, financial, mental *etc.*) from many persons in different times under various circumstances. It will not be fair if I do not acknowledge their support before proceeding any further.

At the very beginning, I would like to express my deepest regards and thanks to my Supervisors, Dr. O. N. Mohanty and Dr. S. B. Singh. They exposed me to the subject; they guided me how to progress in research and most importantly they trained me how to analyse the results. It is their patience and inquisitiveness what forced me to dive deep into the subject, understand it properly and in turn to develop a passion for it. They provided me every support I needed at times. It is their continuous thrive for excellence what brought me on the highway of becoming a metallurgist. I am grateful to have them as my Supervisor.

I also would like to consider Prof. H. K. D. H. Bhadeshia as my Supervisor as I spent one year under his supervision in University of Cambridge where a major portion of the current work was carried out. He taught me how to relentlessly work for good results and proper analysis of them. He also skilled me to work from theory to solve certain issue. I feel honoured to work under such a person. It would not have ever been possible to work with Prof. Bhadeshia had I not been awarded the Commonwealth Split-Site Doctoral Fellowship by the Commonwealth Scholarship Commission, United Kingdom for the year 2006-07 under the Commonwealth Scholarship and Fellowship Programme (CSFP). They provided all the expenses towards my study at University of Cambridge. I am grateful to them.

I always got enthusiasm and encouraging comments from my teachers, Prof. I Manna, Prof. S. Roy and Prof. K. K. Ray, from IIT-Kharagpur, Prof. P. Chackraborty and Prof. P. K. Mitra of Jadavpur University. Their constructive suggestions helped me a lot. I hereby also acknowledge the psychological support I received from Dr. S. Tarafdar, Dr. I. Chattoraj and Dr. S. Ghosh Chowdhury of National Metallurgical Laboratory, Jamshedpur. They always tried their best to console me and put me back into the proper energy level whenever it was needed.

This acknowledgement will be incomplete if I do not mention the help I got from my friends and peers in different locations and institutions. The person whom I first met in Cambridge University and who is was always a source of inspiration for me during my days in Cambridge is Saurabh Kundu. Though he is a good metallurgist to discuss any technical issue in detail, I will always remember our lengthy discussions on various topics during our dinner time. Matthew Pitt, Radu Dmitri, Stefan Forsik, Mohamed Sheriff, Hala Salmon Hasan, Andrew Barrow are the persons who made my life much easier and smoother within the Phase Transformation Group in University of Cambridge. Whenever I was stuck up with something, I always used to disturb either Matthew or Radu or Mohamed and they were always ready to provide a ray of light.

ABSTRACT

Bake hardening (BH) is a phenomenon where the strain aging is exploited in a positive way to improve the strength of formed automotive components. To measure the BH effect during the experiments, the samples are subjected to a tensile strain of 2% at room temperature, unloaded, aged at the required temperature (usually 170 ^{o}C) for the necessary time (usually 20 minutes) and then strained again in tension until failure. The difference between the lower YS after aging and the flow stress at 2% prestrain is the BH effect.

The current study was intended to investigate the BH response in different grades of steel, as a function of various parameters. Physical model based on the theory of strain aging and data-driven artificial neural network based models were developed in order to investigate the science behind such phenomenon as well as to predict the BH response under different situations. Bainitic transformation leaves higher than equilibrium carbon in bainitic ferrite and generates large amount of dislocations. This fact was exploited to induce BH response in novel TRIP-aided steel.

Different characterization techniques were used to critically analyse the experimental results on the effect of various parameters on BH in different automotive steels. Some interesting observations, *e.g.* inducing BH response in IF steel by changing the processing condition, were made. The physical model can very accurately predict the BH response for many different experimental cases. Contribution of Cottrell atmosphere and the precipitation towards the final BH response can be quantified and predicted with the help of this model. Outcomes of such calculations were logical and self-consistent. Data-driven neural network based models can effectively predict the experimental results for a large number of datasets. It was found that these ANN models can be used to predict the BH response for a wide range of composition as well as processing variables. However, when the prediction range is too far from the dataset value, the models show less confidence in prediction by incorporating large error bars. Kinetics of bainitic transformation was studied with different characterization techniques including XRD, 3-DAP *etc.* It was found that the dislocations generated during the bainite transformation can be exploited to induce the BH response in TRIP-assisted steel without providing any external predeformation.

CONTENTS

LIST OF SYMBOLS

A	A constant
A_1	Austenitisation temperature for steel
b	Burgers vector
B_s	Bainite start temperature
C_i	Amount of C in i phases in weight%
D	Diffusion co-efficient of C atoms in α-iron
E_a	Activation energy for the diffusion process
f_V	Volume fraction of the precipitates
f_v^{α}	Maximum volume fraction of precipitate
i_{ss}	Content of the element i in the solid solution in weight%
k	Boltzmann constant
k_C	Arrhenius type temperature dependent parameter
K_i	Proportionality constant that reflects the effect of element i in the solid solution on the Thermo Electric Power of pure iron
k_p	Temperature dependent Arrhenius parameter
$\overline{L}$	Inter-particle spacing
$M_{Cementite}$	Molar mass of cementite
M_C	Molar mass of carbon
M_s	Martensite start temperature
N_A	Avogadro constant
n_C	A constant (≈ 0.9)
N_m	Number of models in the committee
n_p	A constant
q	Concentration of impurities on a dislocation
R	Universal gas constant
S_{ss}	TEP of solid solution
S	Bake hardening constant
t	Aging time
T	Temperature in Kelvin

W_i	Weight fraction of each constituent phases in a microstructure
w_{ij}	Weight of neural network function
w_i^γ	Weight percent (wt%) of solute "i" in solution in austenite
y_i	Prediction made by a particular model
$\overline{y}$	Prediction of the committee model in neural network
α	Ferrite
$\dot{\gamma}$	Strain rate
γ	Austenite
γ_0	Factor representing the number of attempts at an elementary yielding
δ	A constant
δ-ferrite	Delta ferrite
$\Delta\sigma_{BH}$	Increment in strength due to bake hardening treatment
$\Delta\sigma_{Cottrell}$	Strength increment due to Cottrell atmosphere formation
$\Delta\sigma_{Max\_C}$	Largest possible increase in strength in the first stage of bake hardening
$\Delta\sigma_{Max\_P}$	Largest possible increase in strength in the second stage of bake hardening
$\Delta\sigma_{ppt}$	Strength increment due to the formation of precipitation
ε	Total strain due to plastic deformation
θ_i	Bias used in neural network
λ	Slip distance of the dislocation
ξ	A constant
ρ_d	Amount of dislocation density
ρ_p	Dislocation density for a given slip system resulting from the prestraining stage as mentioned by Berbenni *et al* [2004]
σ	Standard deviation
σ_v	Framework estimate of the noise level of the data used in neural network modeling
τ_1	Shear stress required for unpinning the dislocations from their Cottrell atmosphere
τ_2	Shear stress needed for shearing of clusters and precipitates

LIST OF ABBREVIATIONS

3-DAP	Three Dimensional Atom Probe
AHSS	Advanced High Strength Steel
ANN	Artificial Neural Network
BCC	Body Centered Cubic
BH	Bake hardening
CP	Complex Phase
CR	Cold Rolling/Rolled
CTE	Combined Test Error
DP	Dual phase
EDD	Extra Deep Drawing
ELC	Extra Low Carbon
FRT	Finish Rolling Temperature
HR	Hot Rolling/Rolled
HSLA	High Strength Low Alloy
IBT	Isothermal Bainite Transformation
IF	Interstitial Free
kJ	Kilo Joule
LPE	Log Predictive Error
MPa	Mega Pascal
MS	Martensitic Steel
ppm	Perts Per Million
TE	Test Error
TEM	Transmission Electron Microscope
TEP	Thermo Electric Power
TRIP	TRansformation Induced Plasticity
TTT	Time Temperature Transformation
ULC	Ultra Low Carbon
UTS	Ultimate Tensile Strength
VHN	Vickers Hardness Number
XRD	X-ray Diffraction
YS	Yield strength

LIST OF TABLES

LIST OF FIGURES

Chapter 4

Chapter 7

Chapter 1

Introduction

Chapter 1

Introduction

1.1 Introduction

The automobile manufacturers are now being forced to comply with the stringent safety and environmental norms. One way of achieving both these criteria is to increase the use of high strength steels with lower thickness. The increase in strength must be obtained without deteriorating the formability to any extent.

To meet this requirement of the automobile industry, many different grades of modern high strength steels have been developed; these include Dual Phase steel (DP steel), TRansformation Induced Plasticity steel (TRIP steel), Interstitial Free steel (IF steel) and IF High Strength steel, Complex Phase (CP) steel, Martensitic Steels (MS), Bake Hardening (BH) steel and High Strength Low Alloy (HSLA). These steels are having different combination of strength-elongation properties [Fig. 1.1].

These steels are used in different parts of a vehicle. Selection of the materials is done based on the specific purpose of a certain component. Level of strength required or formability, weldability, cost, are some of the aspects among others that are taken into consideration to decide the type of steel that should be used for a particular component. For example, to make the doors and the body panels of a car, a very good formability is required and therefore IF steels that have very good uniform elongation and formability are used.

The parts of the car body panel pass through a paint baking cycle that is done after all the forming operations are completed. In this paint baking cycle, the painted car body part is treated in an oven to dry and to allow the paint to bond to the substrate steel of the car. Depending on the quality and the amount of the paint required (as well as the luxury level of the car), this process (painting and paint baking) is repeated several times. The paint baking process not only gives the car an aesthetically pleasing look, but also positively influences on the strength of the material used for the car structure. The increment of strength which happens during such paint baking process is known as bake hardening effect. Such an increase in strength provides the automotive manufacturers an

option to improve the safety of the car and to reduce the gauge thickness of the steel used to reduce the environmental pollution. The BH effect is important also because of the fact that it is easier and cheaper to get the steel with good formability (low yield strength, r-value greater than 1, high n-value) to develop a component.
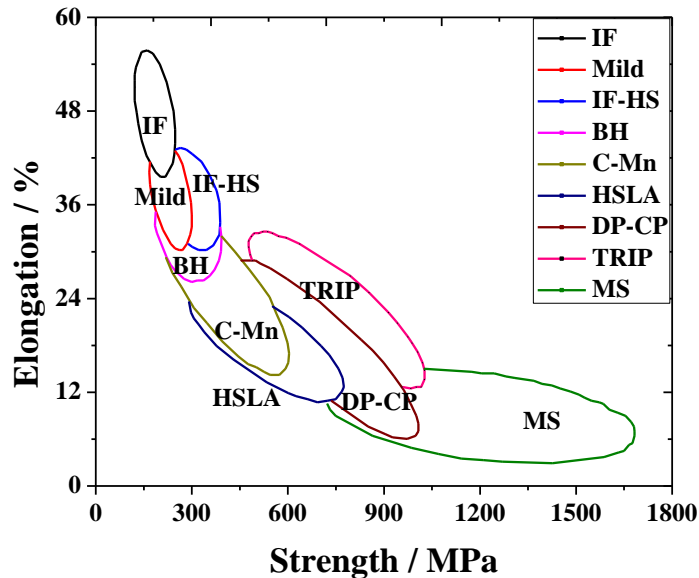
Fig. 1.1: *Schematic representation of strength-elongation combination of different steels commonly used in different parts of a passenger car [AHSS 2006]*

.

1.2   Objective

Bake Hardening is a general phenomenon and can be observed in many different grades of steels which can satisfy the requirements as discussed by Matlock *et al.* [1998]. Many studies have been carried out to investigate different aspects of this effect in different grades of steels. Yet there are certain issues that remain unanswered and need to be addressed in a comprehensive manner. Therefore, in the current work, an effort was made to have a closer look at the BH effect. Another major objective of the current project was to develop different models to predict the final BH effect so that this can be considered during the design procedure. In order to meet these objectives, different experimental schemes were designed with different steels with different intention. Different models were also developed to predict the final BH response. The model predictions were also compared with existing results to validate the accuracy in prediction.

1.3 Scope of the work

Existing knowledge provides some valuable inputs regarding which are the areas which need to be addressed, where understanding is not complete and how progress can be made in that particular direction. Keeping this in mind, in Chapter 2, a brief review of the current knowledge on BH is presented. This review touches the aspects of the microstructure-property correlation and examines the effect of various parameters on the bake hardening response with particular reference to the actual industrial production situation.

In Chapter 3, experimental observations on BH effect in some conventional automotive grade steels (IF, Extra Deep Drawing or EDD and BH grade) and in one AHSS (DP steel) are described. Dependencies of BH effect on the different process parameters are also examined. The results are explained in the light of the theories described in Chapter 2.

In order to improve the basic understanding of bake hardening process, a theoretical model was developed which is described in detail in Chapter 4. The model takes the amount of free solute carbon, prestrain and aging condition (temperature and time) as input parameters and predicts the BH response. The model was divided mainly into two parts, namely the Cottrell atmosphere and subsequent precipitate formation. The model was utilised to predict the BH response and the results were compared with the published literature data. It was found that the model predictions are very close to the experimental values with >98% of prediction within ±10 MPa. The individual contributions of Cottrell atmosphere and precipitate formation can also be quantified with the model.

Although the theoretical model developed in Chapter 4 gives a good representation of the amount of expected BH, Artificial Neural Network (ANN) is one of the best tools to pick up the underlying trend in any given set of data points. In Chapter 5, ANN technique was adopted to find out the effect of free carbon and aging condition on BH effect. Though, theoretically, BH effect is migration of the free carbon atoms under the influence of aging treatment, yet the process is a very complicated phenomenon where the final result depends on so many different variables which include the full chemistry of steels, processing conditions and aging conditions and so on. Considering all

these variables, another neural network model was developed and is discussed in details in Chapter 6.

A new grade of TRIP-assisted steel has recently been developed [Chatterjee 2006; Chatterjee *et al.,* 2007]. The microstructure of this steel at room temperature consists of a mixture of Delta-Ferrite (δ-ferrite) and a second micro-constituent which on high magnification reveals extremely fine pearlite. This alloy was found to have excellent mechanical properties when transformed into a microstructure consisting of δ-ferrite and a mixture of bainitic ferrite and carbon enriched austenite after austenitisation treatment carried out at higher temperature [Chatterjee 2006; Chatterjee *et al.,* 2007]. In the current work, an effort was made to study the BH behavior in this grade of steel. This work is described in details in Chapter 7.

Chapter 2

Bake Hardening: A Brief Review

Chapter 2

Bake Hardening: A Brief Review

2.1 Introduction

Bake hardening utilises the phenomena of strain aging in a positive way to provide an increase in the yield strength (YS) of formed components. In exposed autobody panels, this kind of strength increment is developed during low temperature (150-200 $^{\circ}$C) paint baking. The tensile properties of bake hardening steels are compared with those of other grades in Fig.1.1.

The increase in YS that occurs due to the thermal treatment during paint baking of already formed steel parts is known as the bake hardening (BH) effect. This operation improves the strength of the parts during the final stage of operation. This grade of steel is soft and shows excellent formability during the forming operations but it picks up strength during the subsequent paint baking stage. No requirement of additional shop floor facilities is another advantage of such strengthening. Increase in strength can be achieved by appropriate alloy design with the existing production line.

From the metallurgical point of view, bake hardening is essentially a strain aging process caused by the migration of interstitial solute atoms (mainly carbon and/or nitrogen) to the dislocation sites produced during the prior forming operations. As it is extremely difficult to control the increase in strength that takes place during storage of the steel due to the high diffusion rates of nitrogen to the dislocation sites even at room temperature [Leslie, 1981], all the nitrogen is precipitated out as AlN and removed from the solid solution and BH property is controlled by the amount of dissolved carbon (C) only [Baker *et al., 2002a*].

In the initial years, the carbon content of this kind of steels was higher than 0.05% by weight. However, with the development of vacuum degassing techniques, the production of steels containing 0.01 - 0.03% carbon by weight became possible. These steels are known as extra low carbon or ELC grade steel. The increasing demand for superior formability drove the lower carbon limit to 100 ppm level. Currently, ultra low carbon steels (ULC grade steels) containing less than 30 ppm carbon with excellent

formability are being produced on a regular basis. Further reduction in carbon level is possible but Hutchinson's work [Hutchinson *et al.,* 1990] has shown that reducing the total carbon content below 10 ppm by weight actually degrades the formability of the steel (Fig. 2.1). The amount of carbon must be controlled to avoid the room temperature aging prior to forming [Leslie, 1981]. It has been observed that 15-25 ppm carbon by weight in solid solution gives the optimum bake hardening effect and at the same time, avoids any room temperature aging.
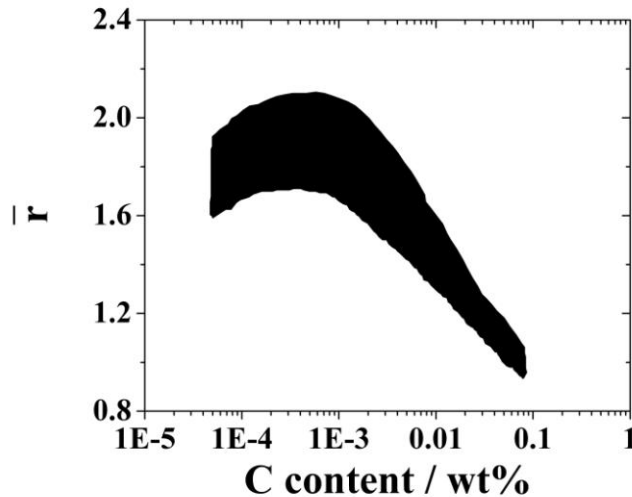
Fig. 2.1: *Effect of carbon content on formability of range of steels [Hutchinson et al., 1990]*

2.2   Determination of BH behaviour

The BH behaviour is measured with sample first prestrained up to 2% in tension at room temperature. The samples are then unloaded, aged at the required temperature (usually 170 ^{o}C) for a fixed time (usually 20 minutes) and then tensile tested again at room temperature. The difference between the lower YS after aging and the flow stress at unloading is due to the strain aging or BH effect and is known as the bake hardening response, $\Delta\sigma_{BH}$ (Fig. 2.2). In general, bake hardening of prestrained components can increase the YS generally by 30-40 MPa for ULC grade steels [De *et al.,* 2000; Zhao *et al.,* 2001] and sometimes, up to 100 MPa for DP and TRIP steels [De Meyer *et al.,* 2000; Bleck and Brühl 2008; Pereloma *et al.,* 2008 *a*; Pereloma *et al.,* 2008 *b*].
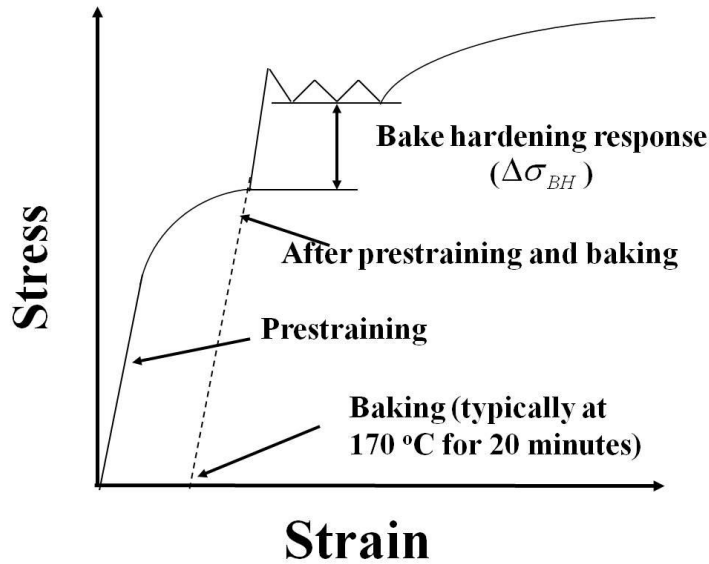
Fig. 2.2: Measurement of bake hardening response [Elsen and Hougardy, 1993]

2.3 Mechanism of Bake Hardening

Bake hardening is essentially related to a diffusion process and in 1948, Nabarro pointed out that this kind of diffusion can affect the mechanical properties of steel in three possible ways [Nabarro, 48]. These are as follows:

i. Stress induced ordering of carbon atoms among the possible sets of interstitial sites (Snoek effect),

ii. Segregation of carbon atoms to form the Cottrell atmosphere and

iii. The precipitation of iron carbide particles.

When an external elastic stress is applied on a crystal, it is expanded in the direction of applied stress and the interstitial atoms find it preferable to occupy the sites that are in direction of strain. With the removal of load, interstitial atoms are once again distributed randomly. This is the origin of anelasticity or internal friction in metals. This kind of stress-induced ordering was first observed by Snoek [1941] and the effect was named after him as the "Snoek effect". The activation energy for this kind of behavior has been reported to be 59 ± 9.6 kJ mol^{-1} [Seal, 2006]. It is well established that this kind of stress-induced ordering cannot be detected through the experiments which are carried

out above -12 ^{o}C [Wilson and Russel, 1959; Nakada and Keh, 1967] because it is complete even before the measurements are made. Therefore, this effect will not be considered any further and it will be omitted from any further discussion.

When the applied stress exceeds the elastic limit of the material, new set of dislocations are generated. If this strained material is now aged for a shorter time at higher temperature or for a prolonged period at a lower temperature, interstitial solutes (carbon and/ nitrogen) migrate to the newly generated dislocations and lock them. In this way, an atmosphere of interstitial solutes builds up around the dislocations [Cottrell, 1948; Cottrell and Bilby, 1949]. This atmosphere is called the "Cottrell atmosphere". It has been reported that the activation energy for the formation of "Cottrell atmosphere" is 87.1 ± 10 kJ mol $^{-1}$ [Seal, 2006] and it is essentially a diffusion controlled process [Bhadeshia and Honeycombe, 2006]. Long range diffusion of interstitial solute atoms to the dislocation core immobilises the dislocations that results in an increase in the yield and ultimate tensile strengths both. As this atmosphere formation follows $t^{2/3}$ rule [Cottrell, 1948; Cottrell and Bilby, 1949], it is far slower than the Snoek rearrangement that simply involves atomic jumps between the neighbouring sites making the process orders of magnitude faster than the segregation of solute atoms to form the Cottrell atmosphere. Elsen and Hougardy [1993] have designated this stage as the *"First stage of bake hardening"*.

With time, more and more solute atoms are attracted to the strain field of dislocations and in the extreme case, this may lead to lines of interstitial atoms along the cores of dislocations [Bhadeshia and Honeycombe, 2006]. Eventually this condensed atmosphere can act as nucleus for precipitates [Cahn, 1957; Dollins, 1970; Barnett, 1971]. However, this stage is reached only if all the dislocation sites allowing strong interactions are occupied by the interstitials. Previous workers have suggested that these precipitates, if they form, should be coherent [Wilson and Russel, 1960; Elsen and Hougardy, 1993]. Elsen and Hougardy [1993] also have concluded that the precipitation of coherent carbides gives rise to the *"Second stage"* of strengthening. De *et al.* [2001] have calculated the activation energy of such precipitation to be 74 ± 0.9 kJ mol^{-1}.

Defects like vacancies and dislocations are the preferred sites for the precipitation of carbides during low temperature aging [Leslie, 1981]. Transition ε-carbide rather than

cementite precipitates forms first at aging temperatures below the metastable ε-carbide solvus line because of better lattice matching between this carbide and ferrite [Leslie, 1981].The formation of ε-carbide takes place preferentially on the dislocations and this kind of carbides form along elastically soft {100} direction in bcc ferrite because it offers the minimum activation barrier to precipitation [Leslie, 1981; Bhadeshia and Honeycombe, 2006]. Previous researchers have reported the value of activation energy of 71.2 kJ mol^{-1} associated with such carbide formation [Abe and Suzuku, 1980]. In a study on aging in Al-killed low carbon steels, Abe *et al.* [1984] had reported the presence of ε-carbide up to 250 $^{\circ}$C. Comparing all these previous results, De and his co-workers [De *et al.,* 2001] have suggested the formation of ε- carbide during the second stage of bake hardening process, though the attempts to observe these particles using Transmission Electron Microscope (TEM) have been unsuccessful [De *et al.,* 1999]. The carbide particles, if they exist at all, are too fine to identify. Figure 2.3 schematically shows the different stages of bake hardening process [Farias, 2006].
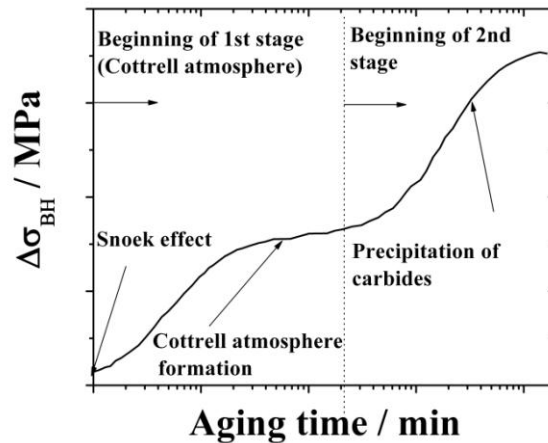
Fig. 2.3: Schematic representation of different stages of in bake hardening [Farias, 2006]

In the light of the discussion above, the criteria for achieving increase in strength after bake hardening can be summarised as [Matlock *et al.,* 1998; Jeong, 1998]:

    i.   Presence of mobile dislocations,

    ii.   Sufficient concentration of solutes to pin these dislocations,

    iii.   Solutes must be mobile at the baking temperature and

iv. Dislocation recovery during baking should be sufficiently slow to prevent any softening.

It was evident from the work of different researchers [Wilson and Russel, 1959; Nakada and Keh, 1967] that detecting the "Snoek ordering" stage above -12 ^{o}C is extremely difficult in routine experiments related to bake hardening and therefore this effect will not be discussed any further. In the remaining part, discussions will be limited to the "Cottrell atmosphere" and subsequent precipitation only and these processes will be treated as the first and second stages, respectively.

2.4   Factors affecting Bake Hardening

The bake hardening behaviour is influenced by different parameters, such as baking temperature and time, amount of prestrain, amount of solute carbon, grain size *etc*. These parameters may have an effect on the dislocation density, the kinetics of carbon diffusion *etc*.

2.4.1   Interstitial solute content

One of the basic requirements for BH grade steel is its *"shelf life"*. Automobile component makers are concerned about this particular property as this is the ability of the steel to resist room temperature aging during storage. The requirement is that the steel should possess sufficient *"shelf life"* so that the material should not undergo aging and deteriorate during transportation and storage before the final use. This parameter is important for the automakers in order to control the inventory and produce the components without any rejection. A minimum of 3 months *"shelf life"* is expected by the component manufacturers and this can be controlled mainly by controlling the diffusion of interstitial elements.

The most important interstitial solutes which may be found in steels are nitrogen and carbon. Between this two elements, nitrogen is very much deleterious because it causes room temperature aging [Leslie, 1981]. This kind of room temperature aging leads to the formation of Lüder's band (stretcher strains) which is not acceptable for exposed auto-body parts. The composition of BH steels is thus designed in such a way that the

solute nitrogen is eliminated to avoid the room temperature aging and BH effect is controlled through the amount of carbon only.

With increasing the amount of solute carbon in steel, BH response should also increase. This is because of the fact that with increasing solute carbon in steel, more solute is available to pin mobile dislocations and the formation of clusters will occur more rapidly. Van Snick *et al.* [1998] showed that an increase of carbon from 0 to 40 ppm increased the BH response from 40 to 70 MPa but further increase in solute carbon had no effect in BH response (Fig. 2.4).
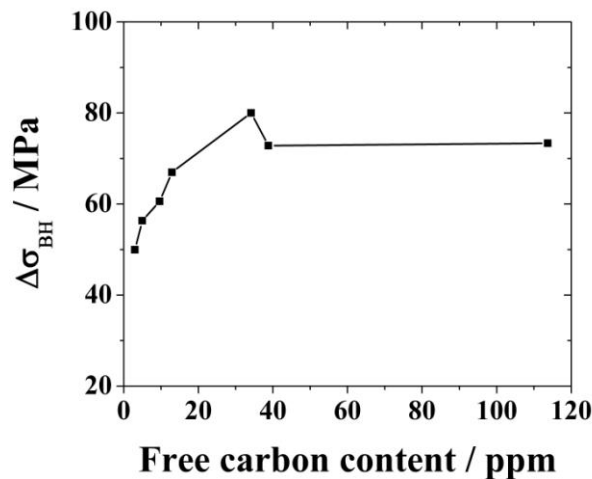
Fig. 2.4: *Influence of solute carbon content on bake hardening response ($\Delta\sigma_{BH}$) (grain size: 17μm) [Van Snick et al., 1998]*

Hanai *et al.* [1984] have carried out their work with low carbon (0.04 by wt%) Al-killed steel and varied the amount of carbon and nitrogen in solid solution by varying the annealing temperature and heating rate and bake hardened at 170 $^{\circ}$C for 20 minute. They have observed that only 5 ppm carbon is sufficient to complete the formation of atmosphere which corroborates the findings of Wilson and Russel [1960]. Finally, they [Hanai *et al.,* 1984] have concluded that the BH response reaches its maximum at 20 ppm solute carbon. When the amount of carbon becomes higher, they segregate and lock the dislocations during prestraining itself and thereby reducing the bake hardening response.

Rubianes and Zimmer [1996] divided the effect of increasing carbon content on room temperature aging and BH into three domains (Fig. 2.5). When the amount of solute carbon is 3 ppm, steels offer excellent room temperature stability but show no significant

BH. The second domain consists of steels with >7 ppm carbon in solution. In this case, the BH response is excellent (> 60 MPa) but does not vary much with carbon (Fig. 2.5) and at the same time, the tendency for room temperature aging is also high. The third region applies to those steels which have carbon in between these two i.e. >3 ppm but <7 ppm in solution. These kinds of steels show a good BH response (20 - 60 MPa) and at the same time have suitable resistance to room temperature aging. BH grade steels should be designed to fall in this region.
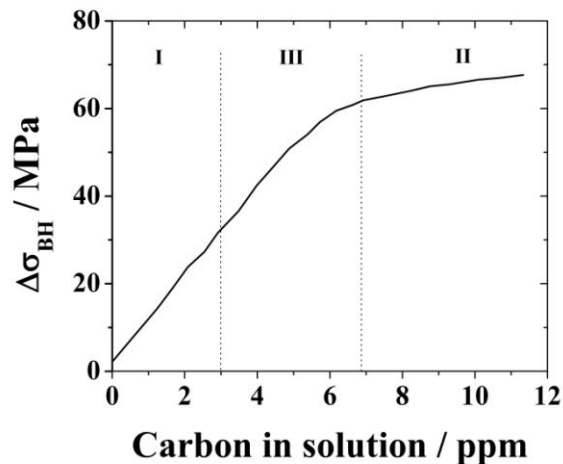
Fig. 2.5: Influence of carbon in solution on bake hardening [Rubianes and Zimmer, 1996]

The results of Rubianes and Zimmer [1996] do not appear to be consistent with those of Van Snick *et al.* [1998] and Hanai *et al.* [1984]. However, it should be noted that Rubianes and Zimmer [1996] measured the carbon contents by internal friction method which cannot detect the carbon atoms lying at grain boundaries [Massardier *et al.,* 2004]. This might explain why these results are lower than those reported by Van Snick *et al.* [1998] or Hanai *et al.* [1984].

2.4.2   Baking temperature and time

Since strain aging is directly related to diffusion of interstitial solute atoms, it is expected that baking response would depend on temperature and time of baking.

The baking response of BH grade steel is a function of both time and temperature. In a temperature range, where recovery of the cold worked structure is minimal, the strength increases at a constant temperature asymptotically with time and at a constant

time, exponentially with temperature [Elsen and Hougardy, 1993]. In experiments with a low carbon (~ 0.03 wt%) BH grade steel at different aging temperatures, it was found that the beginning of the second stage at 180 ^{o}C occurred 20 minutes earlier compared to the results at 150 ^{o}C [Elsen and Hougardy, 1993]. At lower baking temperature (50-120 ^{o}C), the first step of hardening had a dependence on aging time. However, at higher temperatures (> 120 ^{o}C), the first step gets completed within a very short period of time. Other researchers also found similar results during their experiments with Ti stabilised Ultra Low Carbon (ULC) grade steels [De *et al.,* 1999; Zhao *et al.,* 2000 and Zhao *et al.* 2001].

De *et al.* [1999] have proposed that there exists an *'incubation time'* of about 30 minutes before any appreciable change in YS is observed at lower baking temperature. The maximum increase in YS in the second stage at a constant prestrain level was found to be independent of the aging temperature provided the aging treatment was sufficiently long (Fig. 2.6). However, according to Baker *et al.* [2002*a*; 2002 *b*], though the first stage of BH is independent of prestrain, the second stage showed a deterioration in strength increment with increasing pre-strain.

Dehghani and Jonas [2000] obtained some interesting results in their experiments with BH. They performed the prestraining at elevated temperatures and then baked the material at different temperatures. They found that when the baking temperature is higher than the prestraining temperature, the bake hardening response is quite significant; but when the baking temperature is lower than the prestraining temperature, the corresponding BH response is very low. They argued that when the aging temperature (170 ^{o}C) is lower than the prestraining temperatures (200 ^{o}C or 250 ^{o}C), the relatively high temperature of prestraining lead to overaging caused by coalescence of the precipitates.

Himmel *et al.* [1981] had found that a rapid plateau can be achieved in case of BH grade steel after aging at low temperature (50-100 ^{o}C) whereas in case of DP steels, some researchers concluded that an improvement of YS was obtained by increasing the aging temperature to around 200 ^{o}C from at 170 ^{o}C [Terao and Baugnet, 1990].
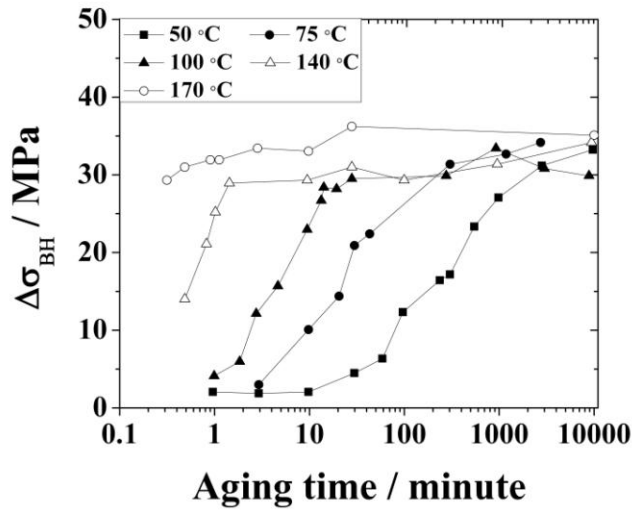
Fig. 2.6: *BH response at different aging temperature for a 5% prestrained sample [De et al., 1999]*

2.4.3 Prestrain

Many auto components undergo a small amount of straining during the final forming operation before the baking process. The BH experiments are, therefore, carried out by subjecting the samples to a small amount of prestrain at room temperature. A tensile prestrain of 2% has been found reasonable for this purpose [Elsen and Hougardy, 1993; Jeong, 1998]. The application of prestrain to the specimens increases the dislocation density. Additional dislocations generated during prestraining are pinned by free solute atoms that diffuse to the dislocation core during baking and as a result YS increases [Fig. 2.2].

Berbenni *et al.* [2004] predicted the dislocation density as a function of amount of prestrain and concluded that for a prestrain range of $1 - 10\%$, the dislocation density would be in the range of $10^9 - 10^{10}$ cm^{-2}. Kalish and Cohen [1970] calculated the average number of carbon atoms per iron atom plane normal to an intersecting dislocation as a function of dislocation density for various weight percentages of interstitial carbon. The work shows that for steel with 0.001 wt% C, if the dislocation density changes from 10^9 cm^{-2} to 10^{10} cm^{-2}, the number of carbon atoms which might be trapped in those dislocations per iron atom plane normal to the dislocations could vary from 10 to 100.

Various studies have been carried out to investigate the effect of prestrain on the BH property. The maximum increase in YS due to Cottrell atmosphere formation in the first stage of BH was found to be independent of the amount of prestrains both in low and ultra low carbon (ULC) steels (Fig. 2.7) [Elsen and Hougardy, 1993; De *et al.,* 1999]. Higher amount of solute atoms is required for complete pinning of dislocations at higher prestrains. In ULC steels, as a result, the formation of the Cottrell atmosphere in samples with higher prestrains exhausts all the solute carbon atoms and thus sufficient amount of solute carbon may not be available for carbide precipitation during the second stage [De *et al.,* 2000]. Elsen and Hougardy [1993] also found a decrease in the BH response with increasing amount of prestrain during the second stage. They concluded that most of the carbon atoms segregated to the dislocations (Cottrell atmosphere formation) in the first stage of BH. This leaves no excess carbon atoms in the bulk for precipitation to occur in the second stage as their steel contained only 5 ppm carbon by weight [Elsen and Hougardy, 1993]. Van Snick *et al.* [1998] also observed similar incident. Pereloma *et al.* [2008] found the precipitation of NbC particles along the dislocation and concluded that the high dislocation density of pre-strained material and pipe diffusion might be responsible for the observed phenomena. They are also of the view that dislocation density has a strong effect on the maximum precipitation density and can change the BH behaviour in the DP and TRIP assisted steels [Pereloma *et al.,* 2008 *a* and *b*]. It should be remembered here that the work by Kalish and Cohen [1970] showed that a dislocation density of the order of 10^{10} cm^{-2} can trap all the carbon atoms and prevent the formation of ε-carbide in a steel containing 0.001 wt% carbon.

Dehghani and Jonas [2000] have carried out a study with ULC steel (23 ppm carbon by weight) and found that at low prestrains, the amount of BH increases with the prestrain until it reaches a maximum and then with further increase in prestrain, BH response decreases. This happens because with increasing prestrain, the carbon concentration to dislocation density ratio decreases and they found no pronounced increase in BH beyond 4% prestrain [Fig. 2.8]. Al-Shalfan *et al.* [2006] found that BH in the outer door panel decreased as work hardening increased which indicated that the BH steel must be applied to shallow drawn parts in order to maximise the BH effect for improving the dent resistance.
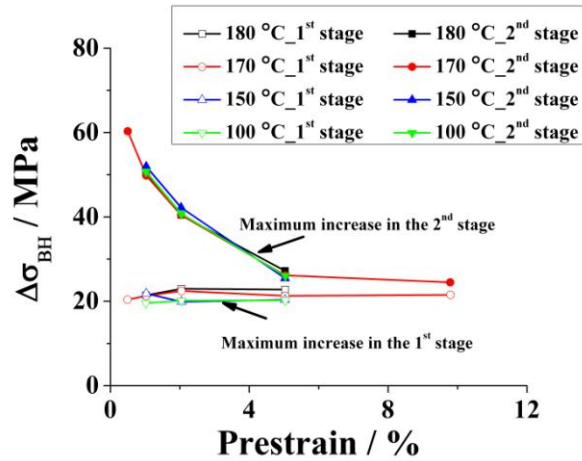
Fig. 2.7: *BH response due to Cottrell atmosphere and precipitate formation as a function of different prestraining and aging at different temperatures [Elsen and Hougardy, 1993]*
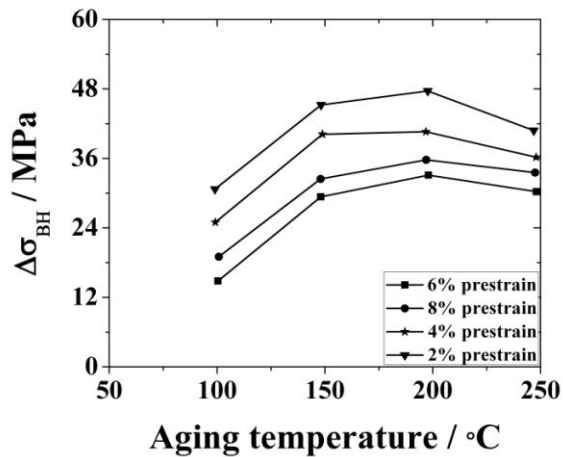
Fig. 2.8: *Effect of temperature and strain on the bake hardening values [Dehghani and Jonas, 2000]*

2.4.4 Effect of grain size

The effect of grain size on the final BH response is not clear in the existing literature. Some researchers have concluded that decreasing the grain size positively influences the BH response [Obara *et al.,* 1985; Van Snick, 1998; Sakata *et al.,* 1994 and Matlock *et al.,* 1998] whereas some others [Takahashi *et al.,* 2005] did not find any dependency on grain size.

According to Obara *et al.* [1985], supersaturation of carbon in ferrite is the most important factor governing the cementite nucleation rate in the grain. In a low carbon steel (0.035 wt%), they first have soaked the material at 1000 ^{o}C for a short time, brought down the temperature closer to the corresponding A_1 temperature, rapidly cooled it up to about 400°C where they held the material and then finally cooled it to room temperature. Thus the amount of carbon in ferrite also changes and they estimated this change in solute carbon content in the ferrite grain during rapid cooling from austenite condition and found that the amount of carbon in solution increases with increasing grain size (grain size range of 10 μm to 30 μm) for increasing degree of rapid cooling (from 10 ^{o}C s$^-$^{1} to 150 ^{o}C s^{-1}). They [Obara *et al.,* 1985] found supersaturation of carbon inside the grain is higher for larger grain size and cementite precipitation takes place inside these larger grains at a medium cooling rate. With increasing cooling rate, cementite particles precipitate even inside the smaller grains. After the precipitation of cementite particles, the yield stress of the material increased and the precipitation did not leave any solute carbon atoms for Cottrell atmosphere formation. Thus, the bake hardening response decreased. From these observations, Obara *et al.* [1985] have concluded that the bake hardening response would decrease with increasing grain size, assuming that bake hardening is determined by the amount of intragranular carbon.

Like Obara *et al.* [1985]*,* Van Snick and his co-workers [Van Snick *et al.,* 1998] also found many cementite particles inside the larger grains when they varied the ferrite grain size from 8 μm to 32 μm by varying the cold rolling reduction from 90% to 25%. They found higher number of cementite particles in the interior of larger grains than the smaller grains. After performing bake hardening treatment, they found that the fine ferrite grains give higher bake hardening response. From this observation, Van Snick *et al.* [1998] concluded that if the carbides are present in the grains during the baking process, the available free carbon should move to these carbides (further precipitation due to supersaturation of carbon) and to the dislocations as well. Consequently the dislocation pinning effect is less in coarse grains resulting in a lower value of bake hardening. Matlock *et al.* [1998] also mentioned that for a given carbon content, the bake hardenability increases with decrease in grain size and the dependence on grain size increases with increasing carbon.

In a study with a low carbon steel, Hanai *et al.* [1984] varied the grain size by changing the annealing conditions and found that decreasing the grain size increases the BH response and Kinoshita and Nishimoto [1988] also found similar behaviour but did not offer any metallurgical explanation. Meissen and Leroy [1989] concluded that BH might involve a combination of carbon in solution and carbon segregated at grain boundaries. Sakata *et al.* [1994] accepted the above explanation and suggested that small amount of solute carbon that cannot be measured by internal friction method segregate to grain boundaries during cooling. Grain boundaries offer low energy positions for solute atoms, making them more stable and therefore these grain boundary atoms do not contribute to aging at room temperature. It has been argued that at the paint baking temperature (170 ^{o}C), it would be possible for carbon atoms to diffuse   to the grain interior and contribute to bake hardening [Sakata *et al.,* 1994]. Van Snick *et al.* [998] also reported that during heating to the paint baking temperature, carbon atoms present at the grain boundaries diffuse back to the grain interior resulting in an increase of the yield stress (BH effect) through pinning of the dislocations.

Takahashi *et al.* [2005] have measured the amount of carbon segregating to the grain boundaries by 3-D Atom Probe technique and found that only $2 - 3$ ppm of carbon by weight can reside in the grain boundary regions. Judging by the fact that this value is considerably smaller than the total amount of solute carbon which is estimated to be $10 - 20$ ppm by weight, they argued that the direct influence of the grain boundary segregation of carbon on the BH properties is small. They also argued that the binding energy for the segregation of carbon atom at grain boundary is sufficiently large and it is therefore difficult to suppose that the atoms are freed from grain boundaries at the paint baking temperature of 170 ^{o}C.

De *et al.* [2004] have extensively studied the strain aging behavior in ultra low carbon (ULC) bake-hardenable steel as a function of grain size. They found that the variation in the grain size influences the distribution of carbon in grain interior and in the grain boundary and more importantly it affects the dislocation distribution in the grains which strongly influences the strain aging behavior. Their modelling calculations and experimental observations show that a decrease in grain size decreases the matrix carbon content in the ULC-BH steels after continuous annealing and hence the bake hardening

response decreases. However, they also found that for a specific amount of tensile prestrain, there appears to be a critical grain size when the carbon atoms at the grain boundaries can contribute to aging process and increases the bake hardening response [De *et al.,* 2004]. From this observation, it was concluded that the bake hardening effect increases with decreasing grain size only in the case of ULC-BH steels with a critical fine grain size and specific prestrain.

2.5   Summary

From the above discussion, it is evident that though a great deal of understanding has been developed, further work is needed to understand the effect of different controlling parameters. Further understanding of the influence of aging condition, free carbon content, total carbon content, prestraining and prestarining condition, alloying elements on BH would be useful since it would then allow BH to be increased without compromising room temperature stability.

Chapter 3

Bake Hardening in Some Common Steels

Chapter 3

Bake Hardening in Some Common Steels

3.1   Introduction

Bake hardening is an important phenomenon which needs to be understood clearly. To appreciate various aspects of bake hardening, four different steels were chosen. The steels which were chosen for this work are: Interstitial Free (IF), Bake Hardening (BH), Extra Deep Drawing (EDD) and Dual Phase (DP) steel. It will be appropriate to give a brief description of these steels before going further into the actual experiments.

3.1.1   Interstitial Free (IF) steel

"Interstitial Free" steels refer to ultra low carbon steels where the bcc ferrite is free from interstitial solutes. The interstitial elements are "fixed" by suitable alloying additions (Nb and/or Ti). The absence of the interstitials (carbon and/or nitrogen) from ferrite leads to a significant increase in the drawability of IF steel. Such steels typically contain 5-20 ppm (by weight) of total carbon [Hoile, 2000]. If higher strength is desired, these steels can be strengthened by the solid solution hardening effect of the substitutional elements like P, Si and Mn. Figure 3.1 depicts a typical production route of such steels.
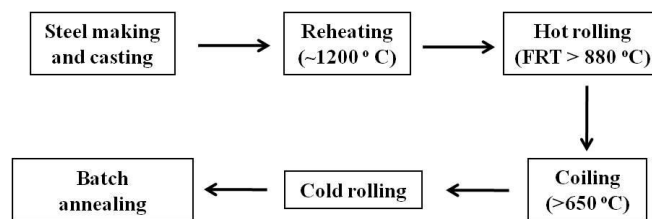
Fig. 3.1: Typical production cycle of the IF steel used in the current study

3.1.2   Bake Hardening (BH) steel

BH steels were discussed in the last chapter. Such steels typically contain 20-30 ppm (by weight) of total solute carbon and some amount of this solute is intentionally kept in solution in ferrite for bake hardening response [Baker *et al.,* 2002 *a*]. These steels also

show excellent ductility though they are inferior to the IF steels. Figure 3.2 represents a typical processing cycle of such steel.
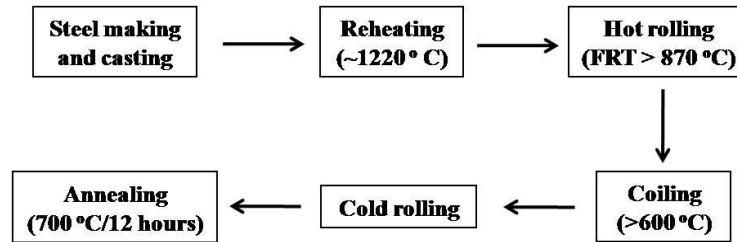
Fig. 3.2: *Typical process cycle for BH steel*

3.1.3 Extra Deep Drawing (EDD) steel

The "Extra Deep Drawing" or EDD steels are generally unalloyed mild steel sheets containing 0.03 – 0.05 wt% C used mainly for extra deep drawing applications, such as in automotive industry for both the appearance sensitive parts and structural components. These steels also possess very good ductility. A schematic process cycle for such grade of steel is shown in Fig. 3.3.
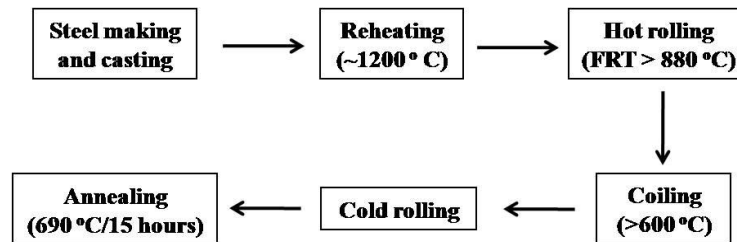
Fig. 3.3: *Schematic representation of typical process cycle for EDD steel*

3.1.4 Dual Phase (DP) steel

DP steels typically consist of ferrite as the matrix phase with dispersion of 5-30% martensite [AHSS 2006]. It is difficult to produce this steel in the *as-hot rolled* condition because formation of martensite requires very low temperature coiling. Therefore, ferrite-bainite dual phase steel has been developed in recent years. This variety can easily be produced in the as-hot rolled condition. Figure 3.4 represents the schematic of a typical

process cycle for the production of ferrite-bainite dual phase steel that was used in the current study. This family of steels is very attractive for many applications because of their excellent strength-elongation combination.

| Steel making and casting | → | Reheating (~1200 °C) | → | Hot rolling (FRT > 840 °C) | → | Coiling (<500 °C) |
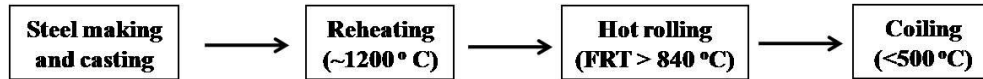
Fig. 3.4: Schematic process flow chart for the production of ferrite-bainite DP steel

3.2 Objective of the experiments

Depending on the availability of these steels, three different experimental schemes were designed with three different objectives. The ***First objective*** was to explore the effect of baking temperature on the final bake hardening response for BH, EDD and DP steels. This set of experiments was carried out with hot rolled (HR) samples. The ***Second objective*** was to investigate the effect of different annealing temperatures on the BH property for IF, BH and EDD grades of steels. These experiments were carried out with cold rolled (CR) samples. And finally the ***Third objective*** was to study the effect of different aging temperatures on precipitation behavior of IF steel. Typically, IF steels are processed in such a way no interstitials are left in solution in ferrite in the final product. Therefore, these steels are not expected to show any BH effect. However, in the present work, processing cycle was altered to leave some interstitials in solution so that they could be measured and their effect on BH could be observed. The experiments for this third objective were carried out with cold rolled (CR) sample. The significance of each of these sets of experiment is briefly described below.

Scheme 1: Effect of baking temperature on the BH property

Automotive body parts are painted and baked at an elevated temperature (170 ^{o}C for 20 minutes) after the forming operations. This is the stage when bake hardening takes place. Consequently, from the industrial point of view, the baking temperature plays a very crucial role in increasing the strength of the material due to baking. Researchers have previously developed mathematical models and indicated that BH response increases

with increasing baking temperature [Das *et al.,* 2008; Das *et al.,* 2011]. Many different grades of steels are used to manufacture the car body [Fig. 1.2] and all these steels go through the paint baking cycle as the final step of the production cycle. Keeping this in mind and also to investigate the extent of BH response as a function of baking temperature, an effort in the current work was made to study the effect of the baking condition on three different grades of steels (DP, EDD and BH grade) having different total carbon.

Scheme 2: Effect of annealing temperature on the BH property

It is very important for the automotive manufacturers to carry out the forming operations with ease for which "annealing" of cold rolled material is a must for the steel producers. The main purpose of annealing the cold rolled materials is to recrystallise the material so that it becomes soft and formable.

There are contradictory reports in the literature about the possible influence of annealing condition on the BH response. While some researchers found that increasing the annealing temperature affects the corresponding strength increment due to BH in a negative way [Hanai *et al.,* 1984; Meissen and Leroy, 1989], others found that an increase in the annealing temperature effectively increases the BH response [Al-Shalfan *et al.,* 2006]. An investigation in the current work was carried out with IF, BH and EDD grade of steel to study the effect of increasing the annealing temperatures on the final bake hardening response of these three steel grades. Different annealing conditions (temperature and time) were applied for different steels and the details are described later in the chapter.

Scheme 3: Effect of aging temperature on precipitation

In IF steels, all the interstitial atoms are "*fixed*" by suitable alloying elements and as the name suggests, there are no free interstitials available in the solid solution in IF steels because of their prior precipitation as different carbides and/or carbonitrides and carbosulphides. The general sequence of precipitation in Ti-stabilised IF steel could be as follows [Bhattacharya, 2009]: TiN, TiS, $Ti_4C_2S_2$ and TiC. In order to study the

precipitation of an interstitial element, it should be in solution in austenite (γ) so that it is available for precipitation in ferrite (α) during aging at a lower temperature.

The experiments were therefore designed in such a way that only carbon atoms were allowed to go into the solution so that only carbides would precipitate out during the subsequent aging treatment and the amount of carbon could be measured by Thermo-Electric Power technique described later in the chapter.

3.3   Experimental procedure

3.3.1   Materials selection and processing

As already mentioned, four different grades of steels in different initial conditions (HR or CR) were chosen for the experimental work. The chemical compositions of these four steels are given in Table 3.1 whereas Table 3.2 enlists some typical properties of each of these steels.

Table 3.1   Chemical composition of the steels studied in wt%.

Sample	State	C	Mn	S	P	Al	N	Nb	Ti
IF	CR	0.002	0.1	0.006	0.007	0.007	0.0025		0.065
BH	CR, HR	0.0035	0.45	0.007	0.035	0.045	0.003	-	-
EDD	CR, HR	0.04	0.15	0.007	0.012	0.045	0.003	-	-
DP	HR	0.07	1.4	0.01	0.012	0.045	0.004	0.045	-

Table 3.2   Mechanical properties of as-received steels.

Sample	Condition	Thickness /mm	YS / MPa	UTS / MPa	Elongation/ %
BH	HR	3.2	265	300	42
EDD	HR	3.0	275	350	44
DP	HR	3.0	540	610	26

The *as-received* material was first cut into tensile specimen of 25 mm gauge length following ASTM specification [ASTM E8]. Fig. 3.5 and Table 3.3 give the drawing of

the tensile specimen and the dimensions, respectively. These tensile specimens were further processed following the three experimental schemes described above.
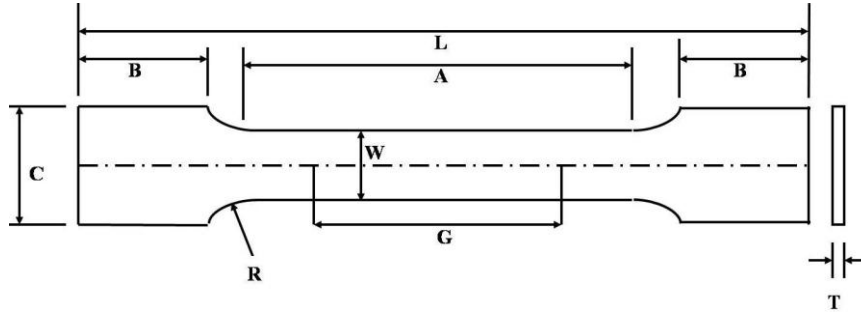
Fig. 3.5: *Schematic representation of the tensile sample used in the study as described in Section 3.3.1. The dimensions are given in Table 3.3.*

Table 3.3 Dimensions of the tensile specimen

Symbol	Explanation	Dimension / mm
G	Gauge length	25.0 ± 0.1
W	Width	6.0 ± 0.1
T	Thickness	Thickness of material
R	Radius of fillet	6
L	Overall length	130
A	Length of reduced section	32
B	Length of grip section	30
C	Width of grip section	10

3.3.2 Design of experiments

Three different objectives of the work were discussed earlier (Section 3.2); the corresponding experimental procedures are now described here.

Scheme 1: Effect of baking temperature on BH property

Since the available ferrite-bainite dual phase steel was produced through the hot rolling route, the other two steels for this study, namely BH and EDD, were also taken from the hot rolling stage in order to maintain the identical nature and enable a like-to-like comparison. Moreover, as bake hardening is chiefly governed by the amount of free carbon, prestrain and aging condition [Matlock *et al.,* 1998], it was expected the

metallurgical difference between hot rolled and cold rolled-annealed steel will not play a role as far as the present objective is concerned.

To simulate the steps during the production of a part used in automobile industries, the tensile samples were given a prestrain of 2% in tension with the rolling direction parallel to the tensile axis followed by a baking treatment for 20 minutes at different temperatures in a hot air oven. Finally, the BH response was measured as specified in Fig. 2.3. Two sets of tensile tests were carried out for each condition and the results were averaged. After the tensile tests, hardness measurement was also carried out for each sample. The time gap between the baking treatment and the final property evaluation was minimal (2-3 days) and the samples were kept in refrigerator (1-5 ^{o}C) during this period. Fig. 3.6 schematically describes the experimental steps followed for this scheme.
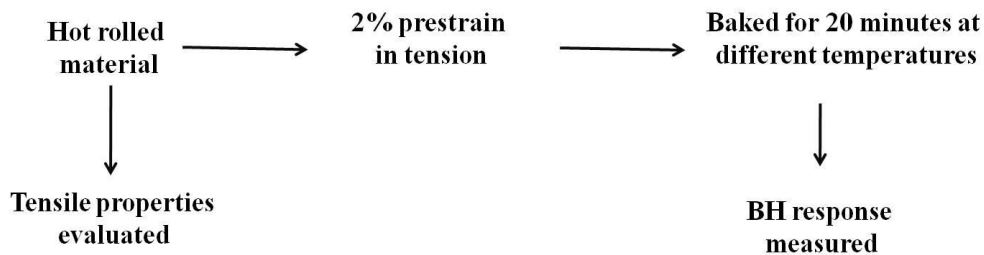
Fig. 3.6: *Schematic representation of the experimental procedure to investigate the effect of baking temperature on the final bake hardening response (Scheme 1)*

Scheme 2: Effect of annealing temperature on BH response

Cold rolled (CR) IF, BH and EDD steels were chosen for this experimental scheme. In industrial practice, the annealing temperature for IF steels is kept between 750-850°C. Thus, in the current study, annealing temperature for cold rolled IF steel was varied between 750 – 850 ^{o}C only and the annealing time was 5 minute. However, the annealing temperatures for BH and EDD grade steels were kept between 510-750 ^{o}C only and the annealing time was 20 minute.

Four samples were used for each annealing condition. After the annealing operation, two samples for each annealing temperatures were used for obtaining the tensile properties and the average values were taken. The other two samples were first given 2% prestrain in tension followed by baking at 170 °C for 20 minutes and then

finally tensile tested. The bake hardening response was estimated as described in Fig. 2.2, following Elsen and Hougardy [1993]. Schematic representation of the experimental steps is given in Fig. 3.7 in the form of a flow chart.
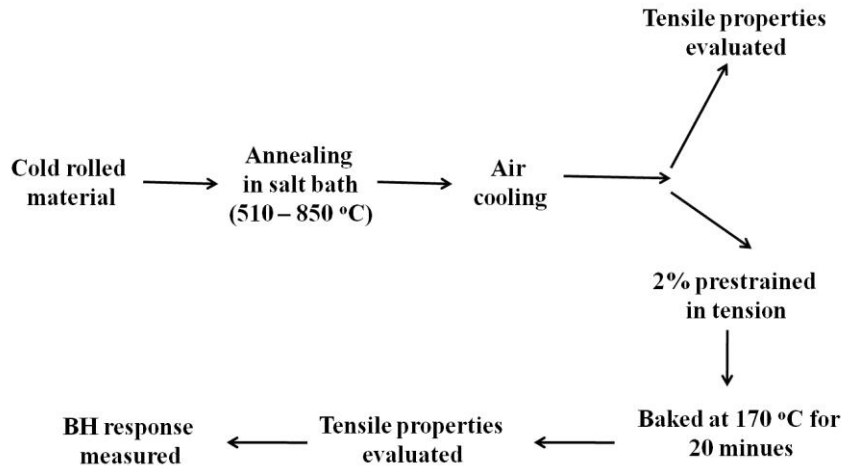
Fig. 3.7: *Flow chart of the experimental procedure for investigating the effect of annealing temperature on the final bake hardening response (Scheme 2)*

Scheme 3: Effect of aging temperature on precipitation

Cold rolled IF steel sheet was chosen for this study. It is known that, in Ti-stabilised IF steels, TiN, TiS and $Ti_4C_2S_2$ precipitates are already present in the parent matrix when the precipitation of TiC occurs [Bhattacharya, 2009]. Consequently, to take all the carbon atoms in solid solution, it was desirable to perform a solutionising treatment followed by rapid quenching. Dissolution temperatures of the carbides, carbosulphides and nitrides in austenite were calculated using the solubility product relationships proposed by Gladman [1997]. According to Bhattacharya [2009], the dissolution of $Ti_4C_2S_2$ takes place at 1050-1100 °C and can be expressed as follows:

$$0.5 Ti_4 C_2 S_2 \underset{\text{Cooling}}{\overset{\text{Heating}}{\rightleftharpoons}} TiS + [Ti] + [C]$$

.……………..3.1
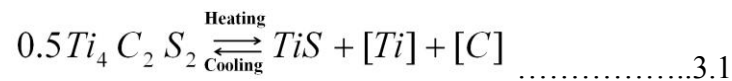
Accordingly, the cold rolled sheet of steel was heat treated in an atmosphere controlled (with 99.9% pure Argon gas) furnace at 1100 °C for 30 minutes. This treatment would result in solutionising of the carbides but would leave titanium nitride (TiN) in the matrix as the calculated solutionising temperature of TiN is still higher (>1390 °C). Next, this

steel was aged at 500°C and 700°C for different time intervals. Figure 3.8 schematically represents the steps followed during these experiments.

CR steel $\longrightarrow$ **Solutionised at 1100 ^{0}C for 30 minute** $\longrightarrow$ **Water quench** $\longrightarrow$ **Aging at 500/700 ^{o}C for different time**
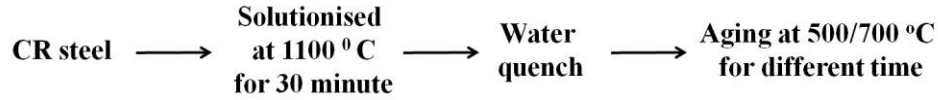
Fig.3.8: *Schematic of the experiments to study the effect of aging temperature on precipitation in IF steel (Scheme 3)*

3.3.3 Heat treatment (annealing, baking and solutionising)

Different furnaces were used for different kinds of heat treatments. A salt bath furnace with an accurate temperature controller that can control the temperature of the salt-bath within ± 3 ^{o}C was used for the annealing and aging experiments. A salt mixture, comprising of 30% $BaCl_2$ + 20% NaCl + 50% $CaCl_2$ (by volume) was used for the temperature range of 500-650 °C and another salt mixture consisting of 55% $BaCl_2$ + 20% NaCl + 25% KCl (by volume) was used for the temperature range of 650-850 °C. Annealing of the IF steel samples was carried out for 5 minutes in the temperature range of 750-850 °C and the annealing of BH and the EDD steel samples was carried out for 20 minutes in the temperature range of 510-750 °C. After the heat treatment, all the samples were cooled in still air.

For baking experiments, an oven type furnace, which was controlled by a temperature controller of accuracy of ± 1 ^{o}C, was used. After the baking experiments, the samples were cooled in still air.

The solutionising heat treatment was carried out in a tube furnace with continuous purging of 99.9% pure Argon for the entire duration of experiments which was only 30 minutes. Argon gas was used to minimise the scale formation at high temperature. The accuracy of the temperature controller was within ± 1 ^{o}C. After the heat treatment, cold water was used as the quenching medium to quench the samples quickly. After the high temperature heat treatments (in the salt baths and in the atmosphere controlled tubular furnace), the samples were pickled with HCl acid to remove the surface scale.

3.3.4 Thermo-Electric Power (TEP) measurements

Thermo-Electric Power (TEP) measurement is a special characterization technique that has been used to study the metallurgical changes that take place during recrystallisation, aging, transformation, *etc* [Borrelly and Benkirat, 1985; Benkirat *et al.,* 1988]. In the context of the present work, it was used to study the effect of higher annealing temperature in IF steel (*Scheme 2*) and precipitation of carbides during aging of IF steel (*Scheme 3*) and thereby to qualitatively estimate the amount of carbon left in the solution in ferrite as a function of the aging conditions. An in-depth review of this technique can be found in a recent thesis [Rana, 2007]. All the TEP experiments were carried out in a set-up which was designed and fabricated in the Indian Institute of Technology, Kharagpur, India. The detailed description of this set-up can be found elsewhere [Rana, 2007]. The equipment was calibrated from time to time.

A particular advantage of TEP technique is that the measurements are independent of sample dimensions and therefore there is no need to make specific samples for this experiment. The heat treated samples were directly used for the measurement after removing the surface scale. The TEP of the strip samples was measured with pure copper as the reference material considering its good thermal conductivity and specific heat [Rana *et al.,* 2006; Rana *et al.,* 2008]. The cold junction was kept at 20 °C by partially dipping the copper block in normal tap water inside a beaker and the hot junction at 25 °C by electrically heating a copper block dipped in water. Water was used to maintain the temperature at a constant value considering its high specific heat [Rana *et al.,* 2006; Rana *et al.,* 2008]. The measurement temperature was selected as 20 °C for ease of measurement and more importantly due to the fact that at this temperature, the sensitivity of the measurement in case of iron is still 75% of the peak value [Benkirat *et al.,* 1988].

3.3.5 Mechanical testing

The tensile testing (prestraining and the final tensile testing) experiments were carried out in 100 kN Instron 5582 machine attached with computer for test control and data collection. This machine has an online video unit for accurately monitoring and measuring the strain. Tests were done at room temperature at a cross-head velocity of

0.003 mm/sec and approximately 1500 data points (stress and strain) were collected for analyzing the results. Some tests were also carried out using a 100 kN Instron 8862 Servo-Electric system having side entry type 25 mm gauge length extensometer to confirm the results obtained from Instron 5582. The dimensions of the sample for the tensile test are given in Fig. 3.5 and Table 3.3.

Since, many of the experiments were carried out with very thin cold rolled material (~ 0.7 mm thickness), only microhardness measurements were suitable for hardness evaluation. Microhardness measurements on the heat treated samples were carried out using a Reicherter make Universal Hardness Tester Model UH3 (Version A) which can test in accordance with Rockwell, Brinell, Vickers and Knoop scales. In the current study, Vickers hardness was measured using the standard 136° diamond pyramid indenter with 500 gm load. Each reported hardness value represents an average of 8 – 10 readings.

3.3.6   Thermodynamic calculations

All the thermodynamic calculations were carried out with commercially available Thermo-Calc (version "S") software with TCFE-6 database allowing austenite, ferrite, cementite phases for all the grades of steels. The presence of other phases were considered judiciously; for IF steel, TiC, TiN and AlN were allowed, for BH and EDD steels, only the formation of AlN was allowed and for DP steel, the presence of NbC and AlN were allowed.

3.4   Results and discussion

3.4.1   Effect of baking temperature on BH property

The prime importance of bake hardening effect is in the automobile industry where a continuous production line has to be maintained. To meet this demand, it is not possible for the car manufacturer to keep the finished components at the paint baking shop for a very long period of time. In other words, it is not practical for the steel makers to make steel which gets fully bake hardened only at a very long baking time. Keeping this restriction in mind, the baking conditions were maintained at a level that is industrially

feasible. Figure 3.9 summarises the effect of different aging temperature for 20 minutes on the BH response for three different grades of steels.
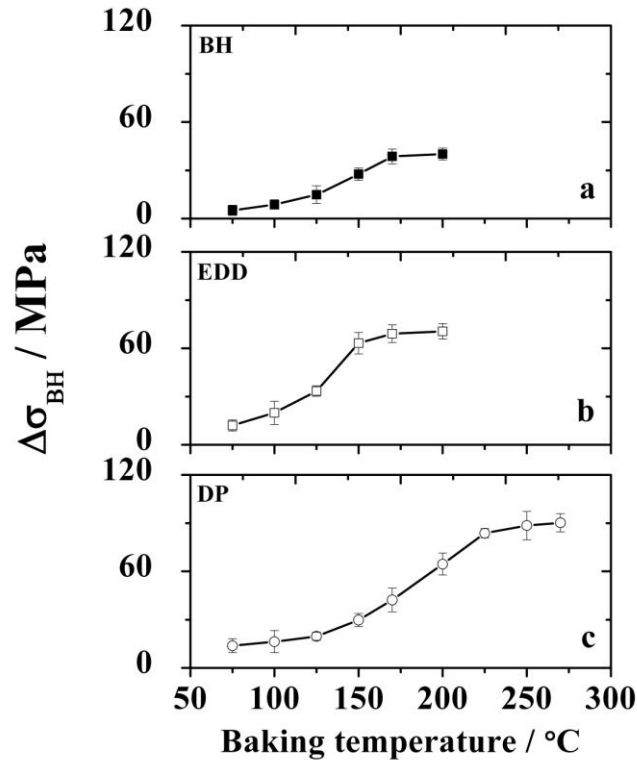
Fig.3.9: *Effect of baking temperature for 20 minutes on the final BH property for different grades of steels. (a) BH, (b) EDD and (c) DP steel*

From a metallurgical point of view, bake hardening is a strain aging phenomenon where the prestrained material is aged at the paint baking temperature. It is a well known fact that during strain aging, strength increases with the aging temperature [Das *et al.,* 2008; Das *et al.,* 2011; Elsen and Hougardy., 1993; De *et al.,* 1999; Baker *et al.,* 2002 *b*]. This fact is once again obvious from the Fig. 3.9. It can be seen from the figure that in general, with increasing the aging temperature, the corresponding BH response increases initially and then it reaches a plateau after which the aging temperature did not affect the BH response significantly in the steels studied in the work. The BH effect arises due to the migration of the interstitial atoms to the dislocation sites to form the Cottrell atmosphere in the first stage and due to the formation precipitates in the second [Elsen and Hougardy, 1993; De *et al.,* 1999]. Since nitrogen is *"fixed"* by suitable alloying elements in most of

the modern steels, BH effect is essentially due to carbon atoms only. The solubility of carbon in ferrite is limited and it is expected that the starting HR material for the BH tests had only a small amount of carbon in solution in ferrite. So, when all solute carbon atoms form the Cottrell atmosphere in the first stage and then they precipitate out, it can be expected that no further change will occur to the final BH response even if the aging temperature is increased.

For DP steel, it was found that the bake hardening does not come to a saturation point even at 200 °C. To determine the plateau temperature for this grade of steel, the baking temperature was increased up to 270 °C and the saturation temperature for BH was observed at 225 ^{o}C. The general trend of the BH behavior for DP steel is similar to that of BH and EDD grades of steel. Bleck and Bruhl [2008] and Timokhina *et al.* [2010] also found similar behavior for DP steel.

One interesting point which could be observed from Fig. 3.9 is that with the increasing total carbon in steel (Total C_{BH} < Total C_{EDD} < Total C_{DP}), maximum BH response also increases significantly. This also may be due to higher amount of free carbon in these steels (Free C_{BH} < Free C_{EDD} < Free C_{DP}). Das *et al.* [2011] also found out similar trend of BH response with increasing free carbon content. Another observation from Fig. 3.9 is that the plateau temperature for the DP steel is higher than that for the BH and EDD grade steels. This may due to be the fact that DP steel contains higher amount of carbon atoms which need to migrate to the dislocations sites to lock them and subsequently form the precipitates.

3.4.2   Effect of annealing temperature on BH property

The effect of increasing annealing temperature on strength increment due to bake hardening treatment in IF steel is shown in Fig. 3.10 from which it can be seen that the BH response increases with the increasing annealing temperature. The BH response can increase if the annealing treatment increases the amount of solute carbon in ferrite. To examine this, thermodynamic calculations using Thermo-Calc were carried out over a wide temperature range and no significant change in the ferrite carbon content for the temperature range studied here was observed.
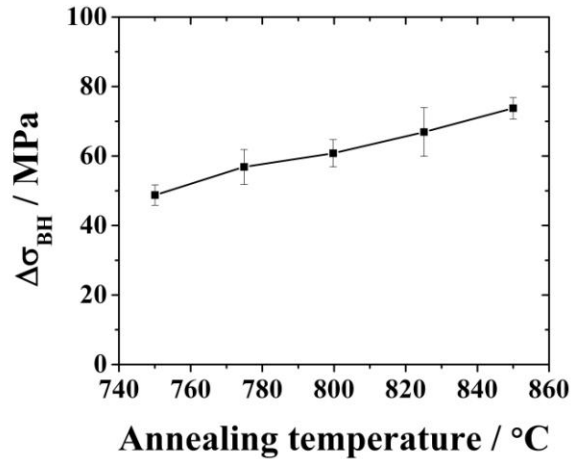
Fig. 3.10: *Effect of heating at different annealing temperature for 5 minute on the BH response of IF steel*

To investigate the possible changes in solute content in ferrite at different annealing temperatures, TEP experiments were also carried out and the results are shown in Fig. 3.11. From Fig. 3.11, it can be seen that the TEP value decreases with increase in annealing temperature. Several metallurgical factors can cause a change in TEP value. It has been shown that it decreases if recrystallisation takes place [Borrelly and Benkirat, 1985; Benkirat *et al.,* 1988]. The recrystallisation of such steel can be completed within 200-500 seconds at 720 °C as was demonstrated in literatures [Bhattacharya, 2009; Eloot *et al.,* 1998; Urabe and Jonas, 1994]. Thus the results in Fig. 3.11 essentially reveal that the decrease in TEP is not due to recrystallisation because the effect of recrystallisation on TEP will be identical for all the instances considered here.

It was pointed out by earlier researchers that grain boundaries can change the carbon concentration profile from grain interior to the grain boundary significantly and the corresponding BH response may change [De *et al.,* 2004]. It is well known that higher annealing temperature increases the grain size [Bhattacharya, 2009; Osawa *et al.,* 1989] as is clearly demonstrated in Fig. 3.12 for IF steel studied in this work. Thus the carbon atoms which were previously residing in grain boundary regions in the fine grain material may come inside the grain interiors when grains coarsen leading to a decrease in TEP value because the effect of carbon in solid solution on TEP is negative [Carabajar *et al.,*

2000; Caballero *et al.,* 2004]. TEP measurements showed similar trend when low carbon steels were annealed above 650°C after rolling [Ferrer *et al.,* 2007]. On the other hand, as higher amount of carbon is present in the solid solution, higher amount of free carbon would be available for bake hardening effect and the resultant bake hardening effect would be expected to increase with increasing annealing temperature as seen in Fig. 3.10.
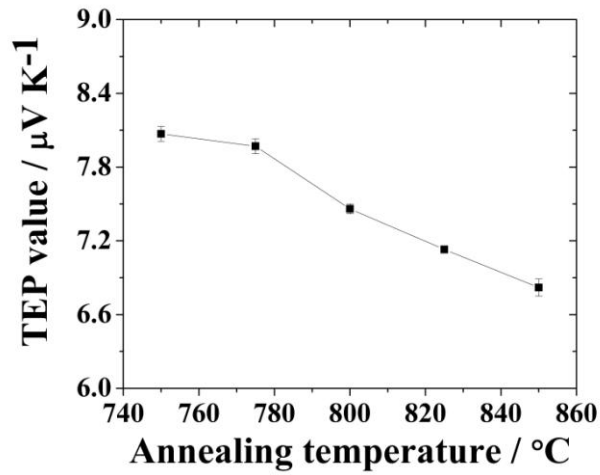
Fig. 3.11: *Evolution of TEP in IF steel due to heating at different annealing temperature for 5 minute*
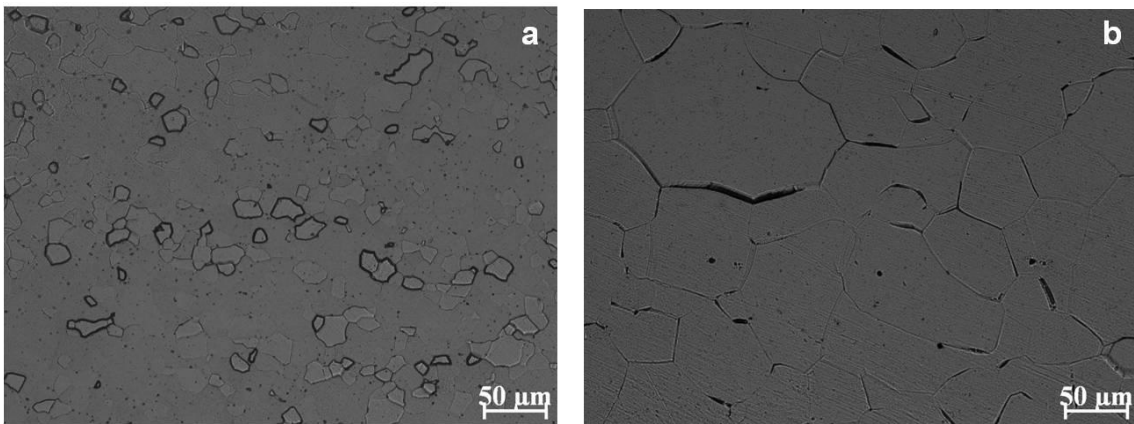
Fig. 3.12: *Optical microstructure for the IF steel samples annealed for 5 minute at (a) 750 °C and (b) at 850 °C.*

The effect of increasing the annealing temperature on the final BH property for BH and EDD grade of steel is demonstrated in Fig. 3.13. It can be seen that with increasing the annealing temperature, final bake hardening response initially increases and then reaches

a saturation point. At higher annealing temperatures, more number of carbon atoms go into the solid solution, and this increased number of carbon atoms in solid solution ultimately contributes to the final bake hardening property and therefore, the general trend in Fig. 3.13 is expected. To explain that the increased number of carbon atoms in solid solution is actually responsible for this kind of increment in strength due to baking treatment, thermodynamic calculations were carried out using Thermo-Calc with TCFE-6 database allowing ferrite, austenite, cementite, and AlN to form and the results are shown in Fig. 3.14 *a* and *b* for BH and EDD grade steel, respectively.

It is clear from Fig. 3.14 that with increasing annealing temperature, solute carbon concentration in the solid solution of ferrite in both BH and EDD steels increases initially and then when austenite starts forming, it suddenly drops to a lower value as most of the solute carbon atoms go to the austenite phase. As a consequence of the enrichment of ferrite with increasingly higher amount of carbon atoms with increasing annealing temperature, these carbon atoms can contribute to the final bake hardening property either by locking the dislocations and creating the Cottrell's atmosphere or by precipitating out or by both as both these mechanisms ultimately increase the strength of the material. Increase in bake hardening response with increasing annealing temperature was also inferred from data-driven neural network analysis reported later in Chapter 6. Similar kind of behaviour was also reported by the other researchers [Shalfan, 2001].
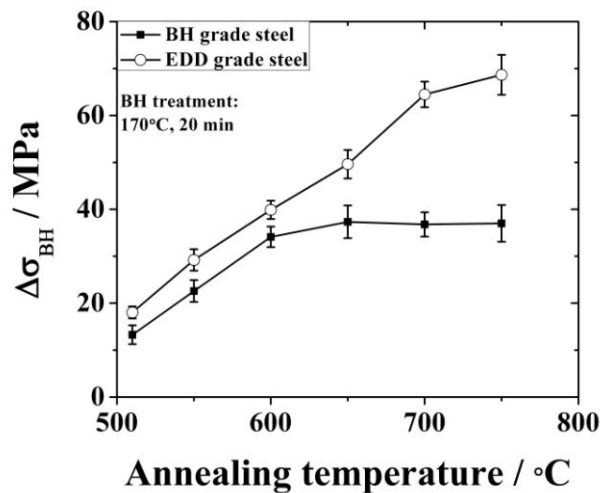
Fig.3.13: *Effect of heating at different annealing temperature for 20 minute on the final bake hardening property of the BH and EDD grades of steel*
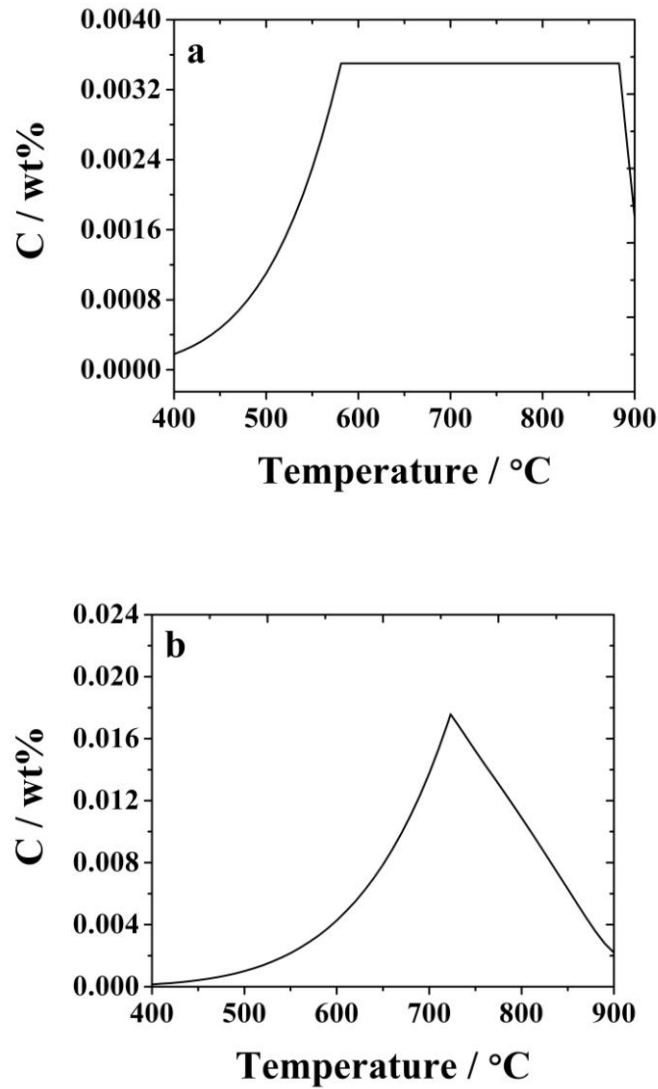
Fig. 3.14: *Calculated amount of carbon in ferrite as a function of increasing annealing temperature obtained using Thermo-Calc software with TCFE-6 database allowing ferrite, austenite, cementite and AlN to exist, a. BH steel and b. EDD steel*

3.4.3 Effect of aging temperature on the precipitation

The effect of aging temperature and time on the evolution of TEP in IF steel is shown in Fig. 3.16. The figures reveal that with ageing time, the TEP values increase sharply in the early hours and then reach a saturation value.

When the concentration of the element is low ($<10^{-1}$wt%), Nordheim and Gorter [1935] have suggested the following relationship for the contribution of the elements present in solid solution on the TEP of pure iron:

$$S_{ss} = \sum K_i \, [i]_{ss} \quad \text{…………………………………………………...………3.2}$$

where, S_{ss} is the TEP of solid solution, i_{ss} is the content of the element i in the solid solution, and K_i is a proportionality constant that reflects the effect of solute i on the TEP value of pure iron. All the common alloying elements which are generally present in the solid solution in ferrite (C, Al, N, Mn *etc*) have a negative effect on the TEP value when they are there in the solid solution [Carabajar *et al.,* 2000; Ferrer *et al.,* 2007; Caballero *et al.,* 2004, Rana *et al.,* 2006]. Thus, their precipitation should lead to an increase in the TEP value as observed in Fig. 3.15. The two stage increase in TEP for the sample aged at 500 °C indicates that precipitation occurs at two stages (Fig. 3.15*a*). On the contrary, for aging at 700°C (Fig. 3.15*b*), the TEP increases with increasing time and then reaches a saturation value when the carbon content in solution in ferrite reaches the solubility limit at the aging temperature and precipitation stops.
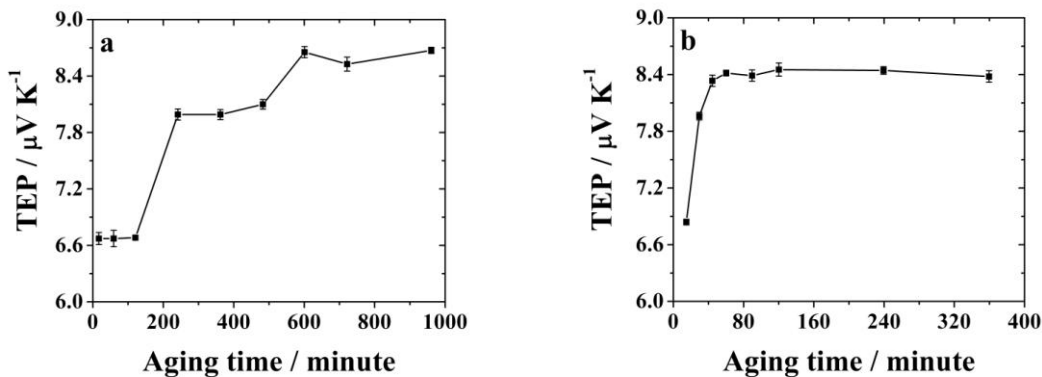
Fig.3.15: *Evolution of TEP in IF steel due to aging for different time intervals at: (a) at 500 °C and (b) 700 °C. The samples were solutionised at 1100 C for 30 minute followed by quenching prior to aging.*

Unfortunately, it would not be possible to quantify the amount of carbon precipitated out during the aging treatment using the Nordheim-Gorter [1935] relationship due to mainly two reasons. Firstly, the steel was quenched from 1100 °C which may lead to introduction

of dislocation which might have annihilated during aging process leading to an increase in TEP [Carabajar *et al.,* 2000] and secondly, the value of the proportionality constant, K_i for carbon may be different for different steel [Carabajar *et al.,* 2000; Caballero *et al.,* 2004].
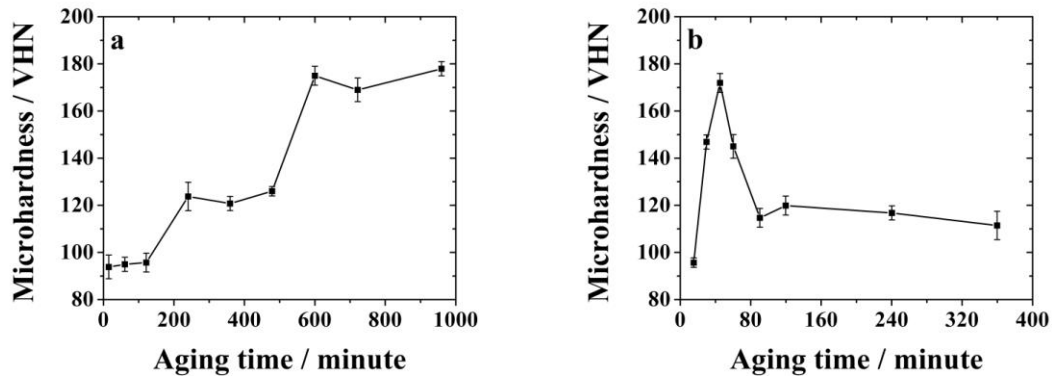
Fig. 3.16: *Change in hardness of IF steel due to aging for different time at (a) 500 ^{o}C and (b) 700 ^{o}C. The samples were solutionised at 1100 C for 30 minute followed by quenching prior to aging.*

3.5   Summary

In this chapter, some experimental studies were conducted to investigate the effect of annealing and aging temperature on the final bake hardening response of different steels (IF, BH, EDD and DP). Following interesting conclusions can be drawn from the above discussion:

   i.   Increasing the annealing temperature increases the solute carbon content in ferrite. This higher solute carbon can then participate in locking the dislocation by forming Cottrell's atmosphere and in extreme case may form precipitates during the baking treatment and this leads to an increase in strength.

   ii.   Bake hardening response can be induced even in IF steel by increasing the annealing temperature. With increasing the annealing temperature, ferrite grains becomes richer with free carbon atoms which can take part in subsequent BH response.

iii.   Once properly annealed to enrich the ferrite matrix with free carbon, both EDD and DP steel can provide a bake hardening response as high as approximately 80 MPa.

iv.   In the current study, precipitation of carbides was qualitatively analysed with the help of TEP. However, in a properly designed experiment, TEP can be used to quantify the amount of free carbon available in the matrix.

Chapter 4

New Model for Bake Hardening

Chapter 4

New Model for Bake Hardening

4.1 Introduction

Bake hardening is essentially a strain aging phenomena where the migration of interstitial carbon atoms to dislocation core results in locking up of the dislocations and their immobilisation. The formal theory of strain aging was developed during 1948 - 1949 by Cottrell and co-workers [Cottrell, 1948; Cottrell and Bilby, 1949] and several studies have been carried out during the subsequent sixty years [Harper, 1951; Bullough and Newman, 1959; Elsen and Hougardy, 1993; Berbenni *et al.,* 2004]. However, our understanding of the bake hardening phenomena is not complete. None of the known studies gives an accurate prediction of the bake hardening response. In this work, an effort has been made to bridge this gap and develop a simple, easy to use theoretical model from basic understanding of diffusion of carbon to the dislocations under aging condition and subsequent precipitate formation.

4.2 Previous works

Several theoretical models for the phenomena of bake hardening have been proposed by different researchers [Elsen and Hougardy, 1993; Elsen, 93; Zhao *et al.,* 2001; Soenen *et al.,* 2004; Berbenni *et al.,* 2004]. Amongst these, the models proposed by Zhao *et al.* [2001] and Soenen *et al.* [2004] will not be discussed as they are based on *Monte-Carlo Simulation* which is beyond the scope of the current work. To begin with, the advantages and the limitations of other available models are described. For simplicity, the model developed by Elsen and Hougardy [1993] and Elsen [1993] will be referred here as "Elsen model" and the one developed by Berbenni *et al.* [2004] as "Berbenni model".

4.2.1 Elsen model

Though the BH grade of steel was developed in the 1980s [Irie *et al.,* 1981; Kurosawa *et al.,* 1988], probably the work by Elsen and Hougardy [1993] was the first one to develop a theory to understand and predict the final BH effect. According to them, the final BH response is the summation of two effects which occur due to the BH treatment, namely the Cottrell atmosphere formation and precipitation of very fine particles. The strength increment due to the formation of Cottrell atmosphere can be calculated from the following equation.

$$\Delta\sigma_{Cottrell} = \Delta\sigma_{Max\_C} \cdot \left(\frac{\left(t/k_C \right)^{n_C}}{1 + \left(t/k_C \right)^{n_C}} \right) \quad\text{..4.1}$$

where $\Delta\sigma_{Max\_C}$ is the largest possible increase in strength in the first stage of bake hardening, k_C is Arrhenius type temperature dependent parameter, t is the aging time and n_C is a constant (≈ 0.9). For the second stage or the precipitation stage, they developed another equation which is given as:

$$\Delta\sigma_{ppt} = \Delta\sigma_{Max\_P} \cdot \left(\frac{\left(t/k_P \right)^{n_p}}{1 + \left(t/k_p \right)^{n_p}} \right) \quad\text{..4.2}$$

where $\Delta\sigma_{Max\_P}$ is the largest possible increase in strength in the second stage of bake hardening, k_p is a temperature dependent Arrhenius parameter and n_p is a constant. The total increase in strength due to bake hardening treatment can then be expressed as

$$\Delta\sigma_{BH} = \Delta\sigma_{Cottrell} + \Delta\sigma_{ppt} = \Delta\sigma_{Max\_C} \cdot \left(\frac{\left(t/k_C \right)^{n_C}}{1 + \left(t/k_C \right)^{n_C}} \right) + \Delta\sigma_{Max\_P} \cdot \left(\frac{\left(t/k_P \right)^{n_p}}{1 + \left(t/k_p \right)^{n_p}} \right) \quad\text{...4.3}$$

Elsen and Hougardy [1993] have reported the values of the different constants for three different temperatures in their work and the predicted $\Delta\sigma_{BH}$ due to BH treatment for

these three cases were shown to be very close to the experimental results. However, it was not possible to use this particular model to calculate $\Delta\sigma_{BH}$ for other temperatures or for different prestrain level for which the values of the different model parameters were not reported. In a parallel report, these parameters were shown to be related to either the aging temperature or to the prestrain level [Elsen, 1993]. The values and the expressions for each of these parameters are given in the following equations (equations 4.4 - 4.9):

i. $\quad \Delta\sigma_{Max\_C} \quad = \quad 21\pm1 \; Nmm^{-2}$ ……………………..…………………………4.4

ii. $\quad \Delta\sigma_{Max\_P} \quad = \quad 50.\varepsilon^{-0.35} \; Nmm^{-2}$ ……………………………………………………4.5

iii. $\quad k_C \quad = \quad 6.918\times10^{-15} \times \exp\left(\dfrac{103.4}{RT}\right)$ ……………………………………………4.6

iv. $\quad k_p \quad = \quad 5.495\times10^{-16} \; \exp\left(\dfrac{141.2}{RT}+0.6\varepsilon\right)$ ………………………………………..4.7

iv. $\quad n_C \quad = \quad 0.9$ …………………………………………………………….4.8

v. $\quad n_p \quad = \quad 0.0026\times(T-273)+0.927$ …………………………………...4.9

where the aging temperature (T) is in K and the amount of prestrain (ε) is expressed in percent. It is expected that with the knowledge of the dependence of the different parameters, which were considered *"constant"* before (*e.g.* n_p, k_p, k_C *etc*), it would be possible to predict the final $\Delta\sigma_{BH}$ for different aging time, temperature and prestrain.

A comparison of the $\Delta\sigma_{BH}$ predicted by this method with the experimental value given in Table 4.1 indicates that the model is not adequate to predict the BH response of steels having different carbon content and given different BH treatment. It should be pointed out here that one of the major drawbacks of this particular model is that it did not take into account the effect of solute carbon (as nitrogen is already fixed by suitable alloy addition) though it is believed that the carbon (or any interstitial) atoms play a very important role in any strain aging process. Another major drawback of the model is to assume a certain level of maximum strength increment due to Cottrell atmosphere as well as precipitate formation and it appears from the work that the values are applicable only for a fixed level of solute carbon.

Table 4.1

Comparison of the prediction of $\Delta\sigma_{BH}$ using the model developed by Elsen [1993] with the original experimental results obtained from different sources. The amount of free carbon was calculated using Thermo-Calc at the corresponding annealing temperatures allowing ferrite, austenite, cementite, TiC, TiCN, VC and NbC phases to exist with TCFE-6 database.

Calculated free C / wt%	ε / %	Aging temp. / K	Aging time / s	Predicted BH / MPa	Experimental BH / MPa	Reference for experimental results
0.00149	2	373	294	60.2	20.2	Baker *et al.*, 2002*b*
0.00149	1	473	29574	71	40.1	Baker *et al.*, 2002*b*
0.00193	1	348	532020	71	29.4	De *et al.*, 1999
0.00193	5	373	2292	49.4	23.6	De *et al.*, 1999
0.00052	2	423	1200	60.2	5.0	Dehghani and Jonas, 2000
0.00052	4	373	1200	51.7	6.0	Dehghani and Jonas, 2000
0.00321	2	443	1200	60.2	52.0	Al-Shalfan, 2001
0.00232	5	329	3582	49.4	26.4	De *et al.*, 2001
0.00232	5	350	408	49.4	27.8	De *et al.*, 2001
0.00193	5	323	30678	49.4	17.2	Zhao *et al.*, 2001
0.00308	2	423	173148	60.2	57.4	Elsen and Hougardy, 1993
0.00308	1	453	714	71	44.2	Elsen and Hougardy, 1993

4.2.2 Berbenni's model

Berbenni and co-workers [2004] have developed a model to predict the final BH response for low carbon steels. According to this model also, the BH response is the resultant of

two additive components, named the Cottrell atmosphere formation and subsequent precipitation of fine carbides [Berbenni *et al.,* 2004] and therefore the BH response, expressed in terms of shear stress, is given by:

$$\tau_{BH} = \tau_1 + \tau_2 \qquad\qquad\qquad\qquad\qquad\qquad\qquad\qquad\qquad\qquad 4.10$$

where τ_1 is the shear stress required for unpinning the dislocations from their Cottrell atmosphere and τ_2 is the shear stress needed for shearing of clusters and precipitates. According to Berbenni and co-workers [Berbenni *et al.,* 2004], the reference shear stress required to unpin the dislocations from their atmosphere is, for each slip system s, a linear function of the atmosphere saturation state. The term τ_1 can be expressed as follows:

$$\tau_1 = \eta \frac{C_\perp}{C_{sat}} \qquad\qquad\qquad\qquad\qquad\qquad\qquad\qquad\qquad 4.11$$

where η is an adjustable parameter. The expressions for $C_\perp$, C_{sat} and τ_2 are given in the following equations:

$$C_{sat} = 10^6 \times \left(\frac{\rho_p M_C}{a N_A d} \right) \qquad\qquad\qquad\qquad\qquad\qquad 4.12$$

$$C_\perp = 3 C_{ss}^0 \times \left(\frac{\pi}{2} \right)^{1/3} \left(\frac{AD}{kT} \right)^{2/3} \rho_p t^{2/3} \qquad\qquad\qquad\qquad 4.13$$

$$\tau_2 = \xi . \frac{f_V^{3/4}}{\sum \rho^{1/4}} \qquad\qquad\qquad\qquad\qquad\qquad\qquad 4.14$$

where d is the density of steel ($\sim$ 7800 kg m^{-3}), C_{ss}^0 is the initial content of solute C atoms (in ppm), N_A is the Avogadro constant, M_C is the molar mass of carbon (0.012 kg), k is the Boltzmann constant, ρ_p is the dislocation density for a given slip system resulting from the prestraining stage and A is the constant used by Cottrell and Bilby [1949]. The effect of the formation of clusters or very fine precipitates was dealt with in terms of the right hand side of the equation 4.14 where ξ is a constant that can be evaluated by comparison with the experimental data and f_V is the volume fraction of the

precipitates. The volume fraction of precipitates f_v was calculated using Avrami type relation [Berbenni *et al.,* 2004] given by:

$$f_v = f_v^{\infty} \times \left[1 - \exp\left(-\frac{Dt}{\delta} \right)^q \right] \quad \dots\dots\dots\dots\dots\dots\dots\dots\dots\dots\dots\dots\dots\dots\dots\dots \; 4.15$$

$$\text{and } D = D_0 \exp\left(-\frac{E_a}{RT} \right) \quad \dots\dots\dots\dots\dots\dots\dots\dots\dots\dots\dots\dots\dots\dots\dots\dots \; 4.16$$

where q is a parameter related to the diffusion process (~0.5); f_v^{∞} is the maximum volume fraction of precipitates; δ is a constant (5×10^{-13} m^2); D is the diffusion co-efficient of C atoms in α-iron; R is the universal gas constant (8.314 J mol^{-1} K), D_0 is a constant (2×10^{-6} m^2 s^{-1}) and E_a is the activation energy for the diffusion process (84 kJ mol^{-1}). f_v^{∞} was calculated following equation 4.17 considering that the precipitation results exclusively from the initial content of solute C atoms [Berbenni, 2009].

$$f_v^{\infty} = \frac{c_0 M_{Cementite}}{10^6 M_C} \quad \dots\dots\dots\dots\dots\dots\dots\dots\dots\dots\dots\dots\dots\dots\dots\dots\dots\dots \; 4.17$$

where $M_{Cementite}$ is the molar mass of cementite (0.1795 kg).

The structure of the model proposed by Berbenni *et al.* [2004] appears better than that proposed by Elsen and Hougardy [1993] because Berbenni *et al* considered the effect of the free interstitial solute atoms. The model proposed by Berbenni *et al.* [2004], unlike the model developed by Elsen and Hougardy [1993], did not assume any maximum strength increment due to Cottrell atmosphere and precipitate formation also. Thus, it was expected that this model would make better prediction than the model proposed by Elsen [1993]. However, when the predictions of Berbenni model are compared with the experimental results (Table 4.2), it is found that the predictions are far away from the experimental results possibly because equation 4.11 assumes a linear relationship between strength increment and carbon concentration at dislocation.

Above discussion makes it clear that even though the basic mechanism of strain aging is well understood, the existing models are not general and they fail to predict the bake hardening response effectively. Therefore, an effort was made in the current study to propose a model which can be efficiently used to predict the final BH responses from

the very basic understanding of diffusion of carbon atoms to the dislocation stress field, the locking of dislocations, the volume fraction of precipitates and the stress required to overcome those. The model can then be used to predict the final BH response.

Table 4.2

Comparison of results obtained using the model developed by Berbenni *et al.* [2004] with of the original experimental results collected from different sources. Amount of free carbon was calculated at the corresponding annealing temperatures with Thermo-Calc software allowing ferrite, austenite, cementite, TiC, TiCN, VC and NbC to exist with TCFE-6 database.

Calculated free C / wt%	ε / %	Aging temp. / K	Aging time / s	Predicted BH / MPa	Experimental BH / MPa	Reference for experimental results
0.00149	2	373	294	374.7	20.2	Baker *et al.*, 2002*b*
0.00149	1	473	29574	24573.2	40.1	Baker *et al.*, 2002*b*
0.00193	1	348	532020	3164.03	29.4	De *et al.*, 1999
0.00193	5	373	2292	647.6	23.6	De *et al.*, 1999
0.00052	2	423	1200	1020.2	5.0	Dehghani and Jonas, 2000
0.00052	4	373	1200	358.01	6.0	Dehghani and Jonas, 2000
0.00321	2	443	1200	3941.4	52.0	Al-Shalfan, 2001
0.00232	5	329	3582	264.09	26.4	De *et al.*, 2001
0.00232	5	350	408	240.02	27.8	De *et al.*, 2001
0.00193	5	323	30678	395.11	17.2	Zhao *et al.*, 20*0*1
0.00308	2	423	173148	32249	57.4	Elsen and Hougardy, 1993
0.00308		453	714	4077.2	44.2	Elsen and Hougardy, 1993

4.3   Development of new model

As discussed earlier, the strength increment after the bake hardening treatment occurs in two stage; first due to the formation of Cottrell atmosphere around the mobile dislocations and then due to the precipitation of fine carbides [De *et al.,* 1999; Baker *et*

al., 2002*b*; Elsen and Hougardy, 1993]. Consequently, the final bake hardening response can be expressed as a combination of these two effects as follows:

$$\Delta\sigma_{BH} = \Delta\sigma_{Cottrell} + \Delta\sigma_{ppt} \quad \dots\dots\dots\dots\dots\dots\dots\dots\dots\dots\dots\dots\dots\dots\dots\dots\dots\dots\dots\dots \quad 4.18$$

where, $\Delta\sigma_{Cottrell}$ and $\Delta\sigma_{ppt}$ are the strength increment due to the formation of Cottrell atmosphere and precipitates, respectively. In the current analysis, a model will be developed combining these two effects to predict the final bake hardening response in low carbon steels. As nitrogen is always "*fixed*" with suitable alloying addition, the model here will be restricted to carbon atoms only.

4.3.1   Formation of Cottrell atmosphere

Cottrell and Bilby [1949] analysed the formation of "*atmosphere*" of interstitial atoms around the dislocations. They assumed that the "drift force", pulling interstitial atoms towards the dislocation core, is the most important factor. Neglecting the effect of the variation of the concentration of interstitial atoms and the saturation of dislocations, Cottrell and Bilby [1949] calculated, for unit length of dislocation, the number of interstitial atoms that arrive at dislocation core within a time '*t*' [$N(t)$] as

$$N(t) = 3n_0 \left(\frac{\pi}{2}\right)^{1/3} \left(\frac{ADt}{kT}\right)^{2/3} \quad \dots\dots\dots\dots\dots\dots\dots\dots\dots\dots\dots\dots\dots\dots\dots \quad 4.19$$

where, n_0 is the initial interstitial content. They also have argued that, N_s, the total number of interstitial atoms per unit length of the dislocation required to form an atmosphere of one carbon atom per atom plane is $1/\lambda$, so that the extent of formation of the atmosphere at time '*t*' is

$$\frac{N(t)}{N_s} = 3.n_0.\lambda.\left(\frac{\pi}{2}\right)^{1/3} .\left(\frac{ADt}{kT}\right)^{2/3} \quad \dots\dots\dots\dots\dots\dots\dots\dots\dots\dots\dots\dots\dots\dots \quad 4.20$$

In the above equation, λ is the slip distance of the dislocation, T is the temperature in Kelvin, k is the Boltzmann's constant, D is the diffusion co-efficient, A is a constant (3

x 10^{-29} dyne.cm^2) as suggested by Cottrell and Bilby [1949]. To validate their model, Cottrell and Bilby [1949] analysed the results obtained experimentally by other researchers by introducing a term "*degree of strain aging*". The degree of strain aging, H, is defined as

$$H = \frac{H_t - H_0}{H_m - H_0} \quad \text{...} 4.21$$

where, H_t is the hardness after aging for time t, H_0 is the value before aging and H_m is the maximum hardness produced by long aging. Cottrell and Bilby [1949] assumed that

H should be proportional to $\dfrac{N(t)}{N_s}$ $\left(i.e.\, H \propto \dfrac{N(t)}{N_s} \right)$ and found out that the equation

4.19 represents the observed aging behavior fairly well up to $\dfrac{N(t)}{N_s} = 0.3$ only and

beyond this range it gives a rate of aging which is too high. The above discussion indicates that it is possible to predict the strength increment due to Cottrell atmosphere formation in a bake hardenable low carbon steel by using a modified version of equation 4.20.

For macroscopic yielding and plastic flow at relatively low plastic strain (less than 10%), the following relation is assumed to hold at constant temperature [Cottrell, 1963; Cocks, 196; Hartley, 1966]

$$\dot{\gamma} = b.L.\gamma_0.[\exp\{-V.\sigma / kT\}] = b.L'.\gamma_0.[\exp\{-V.\sigma_{aged} / kT\}] \quad \text{...............………}4.22$$

where b is the magnitude of the Burger's vector, L and L' are the total length of dislocations before and after aging respectively, γ_0 is a factor representing the frequency of attempts at an elementary yielding (or flow) event per unit length, V is the activation volume as defined by Conrad [1964], σ and σ_{aged} are the yield stress before and after aging respectively, k is the Boltzmann constant, T is the temperature in absolute scale and $\dot{\gamma}$ is the strain rate. So, from equation 4.22, following Hartley [1966], it can be written,

$$\frac{L'}{L} = \exp[V(\sigma_{aged} - \sigma)/kT] \quad \dots\dots\dots\dots\dots\dots\dots\dots\dots\dots\dots\dots\dots\dots 4.23$$

Hartley [1966] has also shown that

$$\frac{L'}{L} = (1-q)^{1+\frac{l_c}{b}} \cdot \left(1 + \frac{l_c}{b} \cdot q\right) \dots\dots\dots\dots\dots\dots\dots\dots\dots\dots\dots 4.24$$

where $\dfrac{L'}{L}$ is the ratio of the length of mobile dislocations after aging to that before aging,

l_c is the length of free dislocation line due to free segments longer than or equal to some

critical length, q is the concentration of impurities on a dislocation. Furthermore, q was

expressed as [Hartley 1966]:

$$q = 1 - \exp\left[-3n_0 b \left(\frac{\pi}{2}\right)^{1/3} \left(\frac{ADt}{kT}\right)^{2/3}\right] \dots\dots\dots\dots\dots\dots\dots\dots 4.25$$

Now, equating equations 4.23 and 4.24, we can write

$$\exp\left[V \cdot \frac{\sigma_{aged} - \sigma}{kT}\right] = (1-q)^{1+\frac{l_c}{b}} \cdot \left(1 + \frac{l_c}{b} \cdot q\right) \dots\dots\dots\dots\dots\dots\dots\dots 4.26$$

Some amount of energy has to be spent to bring about plastic deformation and on

removal of the load, some of the invested energy remains stored in the material [Krausz

and Krausz, 1996]. With increasing the amount of plastic deformation, the free length of

mobile dislocation decreases as the dislocation density increases [Harper, 1951]. Thus, it

is expected that l_c/b is effectively a function of the stored energy due to the plastic

deformation. Honeycombe [1984] has argued that approximately 5% of the plastic work

is stored in the material so that the amount of the stored energy is $0.05\sigma\varepsilon$ where ε is the

total strain due to plastic deformation. It can then be argued that the term l_c/b is

inversely proportional to the stored energy and thus equation 4.26 can be re-written as

$$\exp\left[V \cdot \frac{\sigma_{aged} - \sigma}{kT}\right] = (1-q)^{1+\frac{S}{0.05\sigma\varepsilon}} \cdot \left[1 + \frac{S}{0.05\sigma\varepsilon} \cdot q\right] \dots\dots\dots\dots\dots\dots 4.27$$

In the above expression, the value of S is an empirical constant that relates the term l_c / b to the stored energy. After rearranging, the equation 4.22 can be rewritten as:

$$\Delta \sigma_{cottrell} = \sigma_{aged} - \sigma = \frac{kT}{V} . \ln \left[(1-q)^{1 + \frac{S}{0.05 \sigma \varepsilon}} . \left(1 + \frac{S}{0.05 \sigma \varepsilon} . q \right) \right] \dots\dots\dots\dots 4.28$$

Equation 4.28 is the generalised representation of the strength increment due to Cottrell atmosphere formation ($\Delta \sigma_{cottrell}$) during strain aging.

4.3.2 Strengthening from precipitation

If solute C atoms are still present after the formation of Cottrell atmosphere, they tend to form the precipitates of ε-carbide. These precipitates present further obstacles to dislocation motion. The strengthening obtained in this way is dependent upon the metallic system involved, the volume fraction and size of the precipitate particles, and the nature of the interaction of these particles with dislocations. Various mechanisms have been proposed which involve particle shearing or bypassing the precipitate particles by forming Orwan loops *etc*. Theoretical treatment of these different mechanisms are available and can be used to predict the degree of strengthening that can be expected in case of a bake hardening grade of steel from the possible precipitation of ε-carbides. Following Gladman [1997; 1999], the increase in the yield stress in shear because of the presence of precipitation ($\Delta \tau_y$) can be represented as

$$\Delta \tau_{ppt} = 0.85 \left(\frac{1.2Gb}{2\pi \overline{L}} \right) . \ln \left(\frac{X}{2b} \right) \dots\dots\dots\dots\dots\dots\dots\dots\dots\dots\dots\dots\dots\dots\dots 4.29$$

where G is the shear modulus of the matrix, b is the Burger's vector of the dislocation, $\overline{L}$ is the inter-particle spacing, X is the mean linear intercept diameter of precipitate particles. Assuming in the usual manner that tensile stress is twice the shear stress (*i.e.* $2\tau = \sigma$) [Leslie, 1981], the above expression in equation 4.29 becomes

$$\Delta \sigma_{ppt} = 1.7 \left(\frac{1.2Gb}{2\pi L} \right) . \ln \left(\frac{X}{2b} \right) \dots\dots\dots\dots\dots\dots\dots\dots\dots\dots\dots\dots\dots\dots 4.30$$

Using the appropriate values of G and b and considering the spherical shape of the precipitate, Leslie [1981] obtained the following simplified relationship,

$$\Delta\sigma_{ppt} = \frac{0.59 V_{ppt}^{1/2}}{X} . \ln\left(\frac{X}{2.5 \times 10^{-4}}\right) \dots\dots\dots\dots\dots\dots\dots\dots\dots\dots\dots\dots\dots\dots 4.31$$

where V_{ppt} is the volume fraction of the precipitates. The volume fraction of this ε-carbide precipitates (V_{ppt}) can be calculated as a function of aging time and temperature using the formula given by Wert [1949].

$$V_{ppt} = \left(\frac{4\pi}{3}\right). \alpha^3 .(Dt)^{3/2} \dots\dots\dots\dots\dots\dots\dots\dots\dots\dots\dots\dots\dots\dots\dots 4.32$$

where D is the diffusion coefficient and α is a growth coefficient that depends on certain constants as defined by Zener [1949]. Zener [1949] has classified the precipitation into mainly two types: the first one is the *"Positive precipitation"* where the solute atoms diffuse *into* the moving interface (*e.g.* precipitation of iron carbide in α iron) and the second one is the *"Negative precipitation"* where the solute atoms must diffuse *away* from the moving interface (*e.g.* growth of ferrite in austenite). Zener [1949] has proposed an equation which is given in equation 4.33 for a spherical precipitates. The equation was used here to calculate the value of α for the precipitation of ε-carbide.

$$\alpha = 2^{1/2} \{(n_\alpha - n_1)/(n_0 - n_1)\}^{1/2} \dots\dots\dots\dots\dots\dots\dots\dots\dots\dots\dots\dots 4.33$$

In the above expression, n_0 is the concentration of the solute atoms in the precipitate, n_1 is the solute concentration in the matrix which is in equilibrium with the precipitate and n_α is the concentration in the matrix far away from the precipitate [Fig. 4.1]. The growth coefficient α depends only on the degree of supersaturation with respect to n_0 and n_1. The amount of solute C atoms in the matrix which is in equilibrium with this carbide at any given temperature, T, can be calculated using the following equation suggested by Leslie [1981].

$$Log[C]_{ppm} \quad = \quad 4.06 - \frac{1335}{T} \quad \ldots\ldots\ldots\ldots\ldots\ldots\ldots\ldots\ldots\ldots\ldots\ldots\ldots\ldots\ldots\ldots\ldots\ldots 4.34$$

where $[C]$ is the concentration of solute C in matrix expressed in ppm by weight and T is in absolute scale.

The value of n_1 can be computed from equation 4.34. Considering the chemical formula of ε-carbide as $Fe_{2.4}C$, n_0 can be obtained from stoichiometric calculation. Instead of considering the total amount of C as the solute concentration far away from the growing interface, *i.e.* n_α, the C concentration in each case was calculated at the corresponding annealing temperatures using commercially available thermodynamic software Thermo-Calc with TCFE-6 database allowing ferrite, austenite, cementite, TiC, TiCN, VC and NbC to exist.
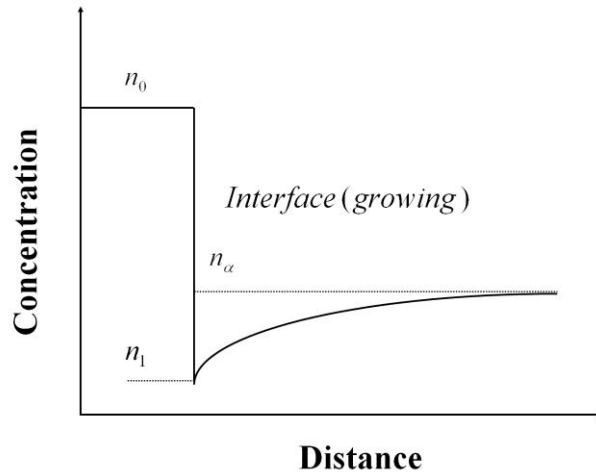
Fig.4.1: *Example of advancing interface with positive precipitation as discussed in Section 4.3.2 [Zener, 1949]*

4.4   Analysis of the model

The effectiveness of the model in predicting the BH response over a number of different steels for a range of BH treatments was examined with the help of published data collected from different sources [Baker *et al.,* 2002 *b*; Elsen and Hougardy, 1993; Dehghani and Jonas, 2000; Al-Shalfan, 2001; De *et* al., 1999; De *et al.,* 2001]. The "*best fit value*" of the empirical constant S was found by fitting equation 4.28 and equation

4.31 to experimental data collected from published literature as mentioned above. The best fit value of S was found to be 7×10^5; with this value of S, the predicted value of the BH response ($\Delta\sigma_{BH}$) was within ± 10 MPa of the experimental value for most of the cases considered here (279 out of 282 data points) and the correlation coefficient (R^2) value was also quite satisfactory (0.795). The constant "S" is termed as "*Bake hardening constant*".

Figure 4.2 compares the predictions using the new model over the entire data range consisting of 282 data points. It can be seen from the figure that in most of the cases (~80%), the predicted values fall within ± 7 MPa of the original experimental results. In some cases (~20%), the deviation is greater than ± 7 but less than ± 10 MPa and only for a very few cases (~1%), the predicted values deviate by more than ± 10 MPa. Thus, it is evident that the equations developed in the current work, can effectively predict the final BH response for a wide variety of steels having different level of interstitial content (C only) and processed at different prestraining and aging conditions. So, this model can now be used to study the effects of different parameters like prestrain level, free carbon and aging condition on the final BH response. An attempt will also be made to calculate individual contribution of Cottrell atmosphere formation and carbide precipitation to the total BH response.
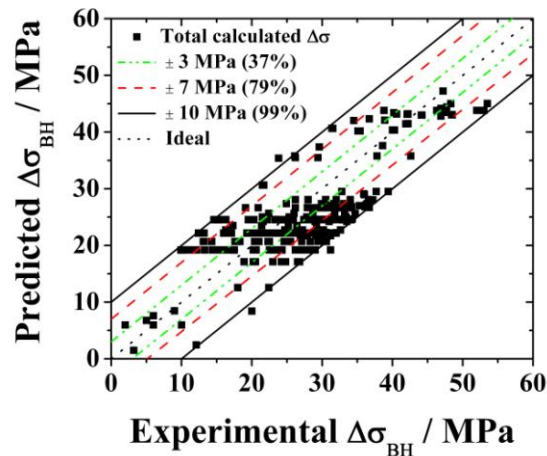
Fig.4.2: *Actual vs. predicted BH response. The predictions were made using the model developed in Section 4.3.*

4.4.1 Effect of aging time and temperature on final BH

It is well established in literature that aging temperature and time, both play a very crucial role in determining the final BH response [De *et al.,* 1999; Elsen and Hougardy, 1993]. Higher the aging temperature and/or the aging time, larger will be the strength increment due to the bake hardening effect for a given concentration of free carbon atoms in bake-hardenable steel. Aging time and temperature have similar kind of influence on final BH response; since these parameters effectively control the diffusion distance of the carbon atoms, it is appropriate to represent the aging time (t) and temperature (T) with one single parameter "Dt" where "D" is as described in equation 4.16. Preferring Dt over individual consideration of aging time and temperature has another advantage that it can represent the aging kinetics as well. The Dt values for each experimental condition were calculated from the corresponding aging conditions and the model was run for making the predictions for all those cases.

It is not usually possible to quantify the individual contributions from Cottrell atmosphere formation and that from subsequent precipitations for a given aging treatment. In the current study, using the model developed here, an effort was made to predict these contributions for different steels. Two typical steel compositions studied in literature were chosen for this purpose. The details of these two steels are given in Table 4.3 from which it can be seen that they are completely different in respect of the total C content, calculated amount of free C and prestrain level. The amount of free carbon at the corresponding annealing temperatures (850 ^{o}C for Steel 1 and 900 ^{o}C for Steel 2) were calculated using commercially available thermodynamic software (Thermo-Calc) with TCFE-6 database allowing ferrite, austenite, cementite, TiC, TiCN, VC and NbC to form.

Table 4.3 Examples of the steels studied using the model. Calculated amount of free C was obtained from Thermo-Calc software with TCFE-6 database at the corresponding annealing temperatures allowing ferrite, austenite, cementite, TiC, TiCN, VC and NbC to exist.

Serial No.	Total C / wt%	Annealing temp./ ^{o}C	Prestrain / %	Calculated free C / wt%	Reference
Steel 1	0.002	850	1	0.00193	De *et al.,* 1999
Steel 2	0.03	900	2	0.00308	Elsen and Hougardy,1993

The results are plotted in Fig. 4.3 where Fig. 4.*3a* shows the comparison of the experimental values with those obtained using the model. It can be seen from the Fig. 4.*3a* that the model predictions are in close agreement (within ±7 MPa) with the experimentally observed values of bake hardening for both the cases. Fig. 4.*3b* and 4.*3c* reveal the contributions to the final BH response from Cottrell atmosphere and precipitate formation, respectively. The contribution from the Cottrell atmosphere formation constitutes only a part of the total BH response in both the steels. The remaining contribution arises from precipitate formation. It can also be observed from Fig. 4.*3b* and 4.*3c* that the strength increment due to Cottrell atmosphere formation is essentially independent of Dt whereas the strengthening contribution from the precipitate particles increases with increasing Dt. It is worth mentioning here that the major part of the strain aging is completed at low values of Dt and the final BH response reaches a saturation value at higher Dt. This behavior is expected as each steel, at the beginning, has a particular amount of free carbon atoms that are consumed gradually due to the formation of Cottrell atmosphere and then by the precipitate particles. Once the free C atoms are exhausted they are simply not available to contribute to BH response at higher Dt. The finding is consistent with the results given in Chapter 5 and 6 and the works published by Das *et al.* [2008; 2011].

4.4.2   Effect of carbon

There is no general agreement in the literature on the amount of C that is necessary to give a high bake hardening response [Van Snick *et al.,* 1998; Rubianes and Zimmer, 1996; and Hanai *et al.,* 1984]. This aspect was discussed in detail in Section 2.4.1 of the thesis. To rationalise this, effort was made in the current study to analyse the data in the published literature and to compare them with the model predictions. It was expected that such an endeavour would lead to the prediction on the amount of free C necessary to provide good BH response. The data were taken from various sources as mentioned earlier in Section 4.4. The total initial C content in the experimental dataset varied between 0.0020 wt% and 0.03 wt% and the steels were prestrained to the same extent (2%) but were aged for different time and temperature combinations (Dt). The amount of free carbon was calculated as described earlier and the BH response was calculated

from the present model. The results are shown in Fig. 4.4 where BH response was calculated for varying free C and aging condition (Dt).

Figure 4.4*a* shows the match between the model calculated results and the experimental results. Though the experimental data points are spread over the entire bake hardening range and the steels studied have different range of carbon concentration and aging condition, the model is accurate enough to predict the final property within a maximum error level of ±7 MPa.

(a)

(b)   *(c)*
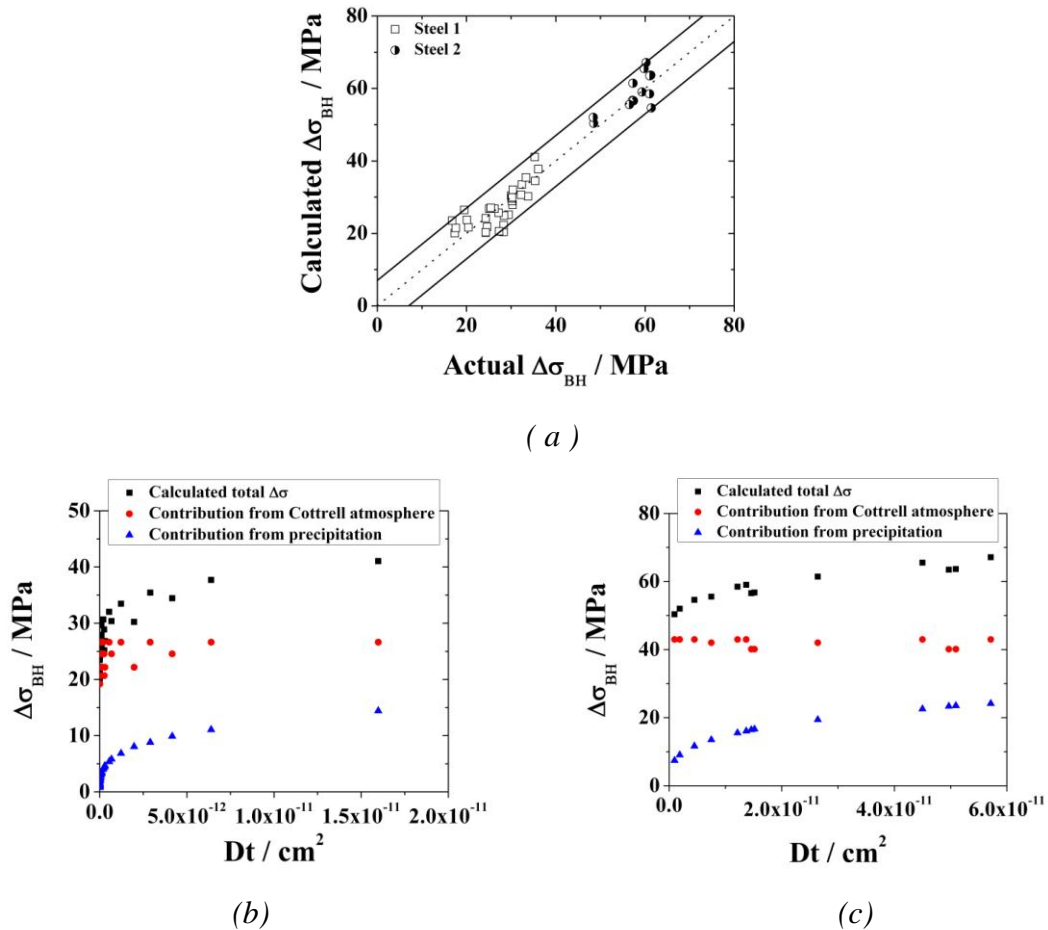
Fig.4.3: *Effect of aging time and temperature, represented by" Dt ", on the final bake hardening response. (a) Comparison of the experimental BH response with that obtained from the model for Steel 1(represented as square points) and Steel 2 (represented as circular points) given in Table 4.3; the dotted line indicates ideal 1:1 performance of the model whereas two solid black lines designate the boundary of ±7 MPa deviation from the ideal behavior. Contribution of different phenomena (Cottrell atmosphere and precipitate formation) towards the final BH response for (b) Steel 1 (c) and Steel 2*

The calculated hardening effects from the Cottrell atmosphere formation and that from the subsequent precipitation are shown as contour plots as a function of Dt and free carbon in Fig. 4.4*b* and 4.4*c*. The numbers mentioned on each iso-contour line represent respective component of the bake hardening response in MPa due to that particular combination of free carbon and Dt. Figure 4.4*b* shows that bake hardening due to Cottrell atmosphere formation increases with the increase in free carbon content for any given Dt. The bake hardening response initially increases with increasing Dt at a fixed free carbon content due to dislocation locking but the effect of increasing Dt on BH response becomes less sensitive with increasing free C content. Eventually, at higher free C content (~ 0.003 wt%), effect of increasing Dt on strength increment due to Cottrell atmosphere formation becomes negligible. In case of the contribution from precipitate particles, strengthening always increases with increasing Dt as is evident from Fig. 4.4 c, however the trend reduces with higher Dt and free carbon combination. This nature is expected considering the fact that precipitation is essentially a diffusion controlled phenomena and with higher particle size, the strengthening effect is reduced. It can also be said that approximately 0.003 wt% free carbon is required in order to achieve a good BH response.

It is very interesting to note that though the amount of free carbon calculated in this work for each of these cases is much larger than that measured experimentally by the original researchers, the present model can be used for predicting the final strength increment due to bake hardening treatment and the predictions are very much close to the experimental results. In all the reported experimental results, the amount of free carbon was determined with the help of "*Internal Friction*" measurement which cannot detect the carbon atoms at the grain boundaries [Massardier *et al.,* 2004]. It is likely that due to this inherent limitation of the technique, it was not possible to quantify the amount of free carbon precisely.

4.4.3   Effect of prestrain

The effect of increasing the prestrain on the final BH response is not very clear and there is no general agreement among the researchers [Elsen and Hougardy, 1993; Van Snick *et al.,* 1998; De *et a.,l* 2000]. In order to analyse the effect of the amount of prestrain, a steel

with 0.002 wt% total initial carbon was considered which was aged at different time/temperature combinations after different prestrain level [De *et al.*, 1999]. The amount of free carbon in this case was calculated to be 0.00193 wt%.
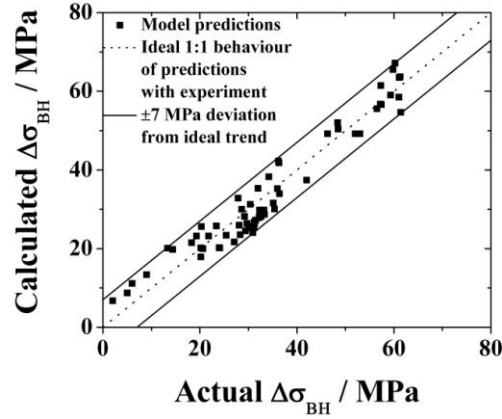
(a)
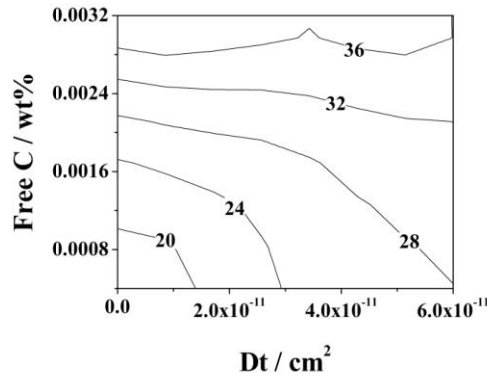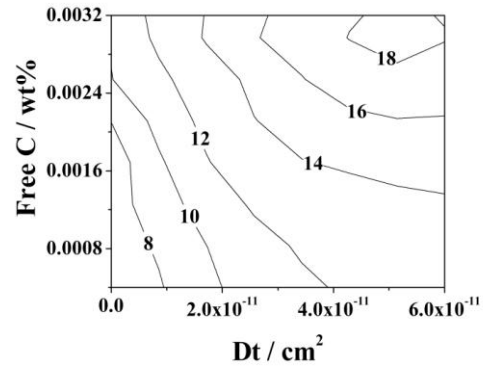
(b)   *(c)*

Fig.4.4: *Combined effect of free carbon and aging condition represented by " Dt " on the final bake hardening behavior for a prestrain level of 2%. (a) Comparison of the experimental bake hardening effect with that obtained from the model. The dotted line and the two solid lines represent the ideal 1:1 and ± 7 MPa deviations from the ideal behavior, respectively. (b – c) Contributions of Cottrell atmosphere formation (b) and precipitate formation (c) to the final bake hardening effect as a function of Dt and calculated free carbon. The numbers on the iso-contour lines are the respective components of the BH response in MPa*

The predictions of the model are compared with the experimental values in Fig. 4.5*a* where the squares show the model predictions, the dotted line represents the ideal

matching of the predictions with the experimental results and the solid lines represent a ±7 MPa deviation from the ideal nature. It is evident from the figure that the model is capable enough in predicting the final bake hardening response to a good level of accuracy (±7 MPa). Figures 4.5*b*, 4.5*c* and 4.5*d* depict the calculated total bake hardening response, contributions from Cottrell atmosphere and precipitation formation, respectively as a function of the aging condition represented by *Dt* and the amount of prestrain. The calculated total BH response, as can be seen from Fig. 4.5*b,* decreases with increasing prestrain for a fixed *Dt* and increases with *Dt* if the prestrain remains constant. This signifies that if the aging temperature and time are not sufficient for completing the dislocation pinning and subsequent precipitation process, then a decrease in BH response would be expected with higher prestrain. Similar conclusion can be drawn from empirical neural network analysis over a large dataset; the details are discussed in Chapters 5 and 6 and in Das *et al.* [2008; 2011].

Figure 4.5*c* reveals that the strengthening due to dislocation locking by the Cottrell atmosphere formation is completed at small values of *Dt* and does not change much with higher prestrain or with higher aging time and temperature combination. On the other hand, Fig. 4.5*d* reveals that at lower prestrain, the contribution from precipitate formation increases with increasing *Dt* level but if the amount of prestrain is high (~ 8-10%), then the bake hardening responses becomes negligible. At higher prestrain level, the amount of dislocations generated is also high but the total amount of free carbon remains constant for a given processing. Consequently, the number of precipitate particles that are formed around these dislocations are also higher but due to the unavailability of sufficient carbon atoms and insufficient aging conditions considered here, they may not reach the critical size [Elsen and Hougardy, 1993; De *et al,* 1999; Wilson and Russel, 1960] when they can contribute to the strength increment. Similar conclusion was drawn in Chapters 5 and 6 and in the work by Das *et al.* [2008; 2011].
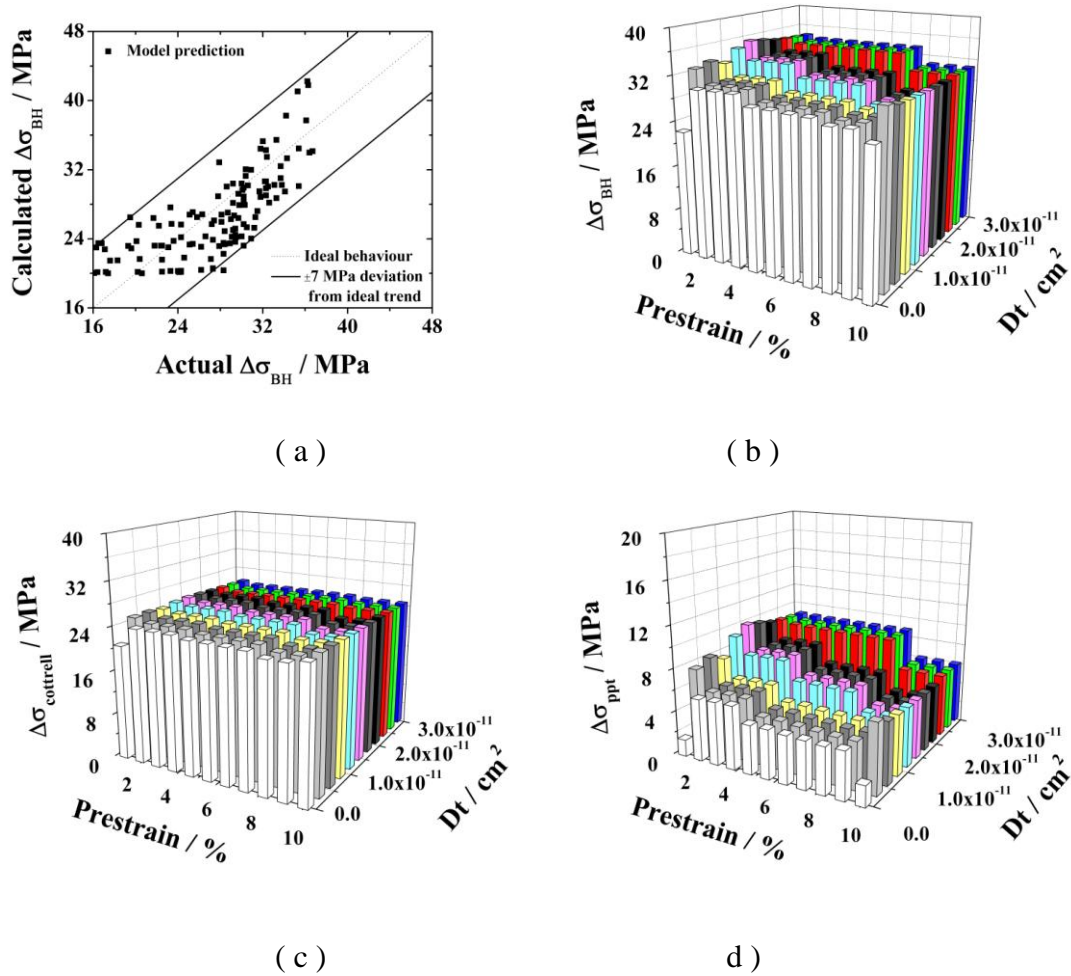
Fig.4.5: *Combined effect of prestrain and Dt on bake hardening. (a) Comparison between experimental and calculated BH;(b) variation of total calculated BH as a function of prestrain and Dt; (c – d) calculated contribution from (c) Cottrell atmosphere and (d) precipitate formation*

4.5 Comparison with other available models

In a previous section (4.2), some existing models were analysed and used to make the predictions which were compared with the experimental results. There is still another model, based on neural network analysis, where all the major contributing parameters (*e.g.* chemical composition, annealing condition, prestraining condition, and baking conditions) for BH are considered to predict the final BH response [Chapter 6, Das *et al.,* 2008]. Though the current model is very effective and precise in predicting the increase in strength due to bake hardening, it would be interesting to compare the results of this new model with those ones discussed above in Section 4.2. The comparison is given in Table 4.4.

Table: 4.4 Comparison among the existing models (including the present one) and the experimental result

Calculated free C / wt%	Prestrain / %	Aging temperature / K	Aging time / s	Experimental BH / MPa	Predictions of BH from different models / MPa					References for experimental results
					Berbenni et al 2004	Elsen 93	Elsen and Hougardy 1993	Das et al 2008 and Chapter 6	New model (Chapter 4)	
0.00149	5	373	30024	*28.7*	1482.2	49.4	-	28.8±2.7	**20.2**	Baker et al., 2002b
0.00149	1	473	294	*32.1*	2690.1	71	-	31.4±2.1	**25.8**	Baker et al., 2002 b
0.00193	2	323	9012	*14.4*	328.9	60.2	-	11.6±0.9	**19.7**	De et al., 1999
0.00193	1	348	16152	*28.3*	876.5	71	-	25±0.9	**22.7**	De et al., 1999
0.00193	10	348	25650	*27.1*	703.4	43.3	-	29.7±1.7	**22.5**	De et al., 1999
0.00193	1	413	558	*25.1*	1273.2	71	-	27.6±0.9	**26.7**	De et al., 1999
0.00193	5	373	34044	*30.2*	1808.1	49.4	-	28.9±1.3	**25.6**	De et al., 1999
0.00193	10	448	192	*34.1*	1224.3	43.3	-	30.1	**29.4**	De et al., 1999
0.00232	5	318	5736	*24.7*	224.1	49.4	-	23.1±1	**23.2**	De et al., 2001
0.00232	5	350	456	*31.7*	247.5	49.4	-	27.0±0.9	**25.6**	De et al., 2001
0.00232	5	373	144	*33*	294.6	49.4	-	30.4±0.8	**27.3**	De et al., 2001
0.00193	5	323	42900	*23.3*	437.9	49.6	-	22.3±0.9	**20.2**	Zhao et al., 2001
0.00308	2	453	139374	*60.2*	73328.3	60.2	60.8	57.6±1.4	**67.1**	Elsen and Hougardy, 1993
0.00308	1	373	2988168	*42.6*	28454.1	71	-	46.7±1.4	**50.3**	Elsen and Hougardy, 1993
0.00052	4	373	1200	*06*	358.0	51.7	-	8.8±2.2	**6.7**	Dehghani and Jonas, 2000
0.00052	2	373	1200	*02*	403.8	60.2	-	4.8±2.7	**6.7**	Dehghani and Jonas, 2000

It is evident from this Table that the only model which can be reliably used to predict the final BH response other than the present one is the neural network model discussed in Chapter 6. It is to be kept in mind that neural network is a data-driven technique whereas the current model is more fundamental and based on the physical phenomena. It is also to be remembered here that the neural network model is not able to distinguish clearly the contribution of strengthening from different sources (Cottrell atmosphere and precipitation) which is possible from the current study.

4.6   Limitations of the current model

It is interesting to note the behavior of the current model developed in the preceding sections over a range of experimental conditions. However, in the current model, it has not been possible to include the effect of some other parameters, *e.g.,* grain size, which depends on prior processing during cold rolling and annealing. The absence of these parameters might be reflected in the deviation in the predicted BH values from those obtained from actual experiments. It is also to be kept in mind that the current model can be applied to only those steels where BH treatment does not lead to any softening due to tempering.

4.7   Conclusion

A new theoretical model has been developed here to predict the final bake hardening response of low carbon steel. The main findings of this chapter are summarised below:

1. The model predictions are compared with experimental observations. It was found that the model can very effectively predict the BH response with a satisfactory level of accuracy of ± 10 MPa for more than 98% of the experimental conditions.

2. Individual contributions of Cottrell atmosphere formation and precipitation towards final strength increment have been estimated. It was found out that the Cottrell atmosphere formation contributes much more than the precipitates to the final BH response. It was also found out that the kinetics of Cottrell atmosphere formation is much faster and completes very quickly. Similar observations were also made in a later chapter.

3. The model predicts no improvement in BH response can be obtained by increasing the amount of prestrain. Rather, if the aging condition is not sufficient at higher prestrain, the contribution from precipitation would be less.

4. Effect of free C on the BH response was also estimated. It has been inferred that a steel with approximately 0.003 wt% free carbon is the most suitable one for good BH response.

Chapter 5

BH Response: An Empirical Model

Chapter 5

BH Response: An Empirical Model

5.1   Introduction

In the previous chapter, a new theoretical model was developed to predict the BH response in low carbon automotive grade steels. Although the predictions of that model were quite good and consistent with prior metallurgical knowledge, the value of the *Correlation co-efficient (R^2)* was about 0.79. If the R^2 value can be improved, the quality of the model prediction would be much more accurate. The R^2 value can be improved if the interactions between different input parameters with the output parameter can be properly represented by mathematical equation. *Artificial Neural Network (ANN)* is probably the best method, as described by many researchers [Bhadeshia, 1999; Bhadeshia *et al.,* 2009], to find out the underlying trends in a large database. The technique is well established and widely used in solving different variety of problems in materials science [Bhadeshia, 1999; Bhadeshia *et al.,* 2009; Mukherjee, 2006; Chatterjee, 2006]. Thus, it was felt to utilise *ANN* technique in order to improve the quality of BH response prediction.

As the BH response occurs due to the migration of the free carbon atoms to the mobile dislocations, *amount of free carbon* was considered as one of the input variable to the model. Mobile dislocations are generated during prestraining of the sample; thus *amount of prestrain* was considered as another input variable to the model. Migration of C atoms to the mobile dislocations takes place due to the aging treatment. Consequently, aging condition, represented by *Dt,* was also taken into consideration as input variable to the model. Details of these input parameters are described in Section 5.3 of the current Chapter. For all the above mentioned conditions, BH response ($\Delta\sigma_{BH}$) was considered as the "*output*" parameter. The current chapter describes in detail the development of *ANN* models and its use in making predictions for BH response. The model predictions were compared with prior metallurgical knowledge and with published results which were not included in the formulation of the model.

5.2   The technique

Neural networks are non-linear models which can be used for empirical regression and classification modeling [Bhadeshia, 1999]. In comparison with the traditional linear or non-linear statistical models, these neural networks are so much flexible that it becomes much easier to discover more complex relationships in dataset. Another disadvantage of statistical models is that they make an *apriori* assumption regarding the relationship between the input and output variables. The *ANN* models, on the other hand, make no *apriori* assumptions regarding the relationship between the input and the output parameters; they "*discover*" such relationships through the data only. Thus, at the beginning, a set of examples of input and output data is fed to the model for *"training"*. The outcome of such training is a set of coefficients which are called *"weights"*. Training of the model also generates the functions which in combination with the weights relate the input parameters to the output. The *training* process involves a search for the optimum non-linear relationship between the inputs and the output [Singh *et al.,* 1998].

Since the *training* of the model depends heavily on the quality of the input data, model will try to capture the trend with any spurious noise in the data also and thus gives rise to a problem called *"overfitting"*. *Overfitting* makes the relationship between input and output variables poor to generalise. In order to avoid such problem, the example dataset which is fed to the model for *training*, is first divided into two parts, named the *"training data"* and *"test data"*. *Training* is first completed with the *training data* only and subsequently the model is verified with the help of *test data* before using for prediction with unknown dataset.

MacKay has developed [Mackay, 1992 a; Mackay, 1992 b; Mackay, 1994] a Bayesian framework for neural networks in which the appropriate model complexity is inferred from the data. The Bayesian framework has got two more advantages. First, the *significance* of the input variables is automatically quantified. Consequently, the model-perceived *significance* of each input variable can be compared against metallurgical theories. The second advantage is that the predictions of the network are accompanied by error bars which depend on the specific position in the input space. These quantify the model's certainty about its predictions.

5.3   The data

The raw data for the model were collected from the results published in journal papers and Ph.D thesis [Elsen and Hougardy, 1993; Baker *et al.,* 2002 b; De *et al.,* 1999; Dehghani and Jonas, 2000; De *et al.,* 2000; Al-Shalfan, 2001; Zhao *et al.,* 2001; De Meyer *et al.,* 2000]. Bake hardening effect is the result of the migration of the interstitial solute atoms during the paint baking cycle to the dislocations sites. One way of obtaining the interstitial solute concentration is to calculate the phase composition at the corresponding annealing temperatures as was done at Chapter 4. However, the amount of freely available solute carbon at room temperature may be greatly influenced by the processing after annealing treatment (*e.g.* cooling rate). Thus, the experimentally obtained values of free solute carbon, mentioned in the respective reports (papers and thesis), were considered for the analysis. It may be important to note here that any error in measuring the amount of carbon in ferrite at room temperature should be reflected as *noise* in the model.

Bake hardening is essentially a strain aging phenomena governed by the diffusion of interstitial atoms (carbon in this case) to dislocations. Therefore, the diffusion distance of carbon atoms during the course of baking treatment is an important parameter; the diffusion distance is related to the parameter Dt where "D" is the diffusion coefficient of C in ferrite at the baking temperature and is given by $D = 5.2 \times 10^{-4} \exp\left(\dfrac{-9000}{T}\right)$ [Wert, 1950] and "t" is the aging time. Using *Dt* over aging time and temperature has got two fold advantages: *firstly*, it gives a kinetic view of the aging process and *secondly*, it helps to reduce the number of process variables in the model. For simplicity, natural logarithm of *Dt i.e. Ln (Dt)* was used instead of *Dt*.

Presence of mobile dislocations is a very important aspect of BH. Such fresh dislocations are generated during prestraining prior to the aging treatment. Thus the amount of prestraining was also considered as one of the inputs. In Table 5.1, a list of the input variables with their maximum, minimum and average values and the standard deviation is provided.

Table 5.1: Properties of data used in creating the model

Variables	Maximum	Minimum	Average	Standard deviation
Free C / ppm	21	0.69	8.8102	6.2268
Prestrain / %	10	1	3.9041	2.4879
Ln (Dt)	-14.1347	-31.4365	-23.1327	3.7992
Bake hardening / MPa	72	0.1	27.7724	14.2345

5.4   Artificial Neural Network model

The model first normalises both the input and the output variables within the range ±0.5 as follows

$$x_N = \frac{x - x_{min}}{x_{max} - x_{min}} - 0.5 \quad\text{...5.1}$$

where x_N is the normalised value of the variable x which has maximum and minimum values given by x_{max} and x_{min}, respectively. The network consisted of the variables which were chosen previously (*free carbon, prestrain, Dt and BH response*) and used as the input nodes in the analysis, a number of hidden nodes and an output node representing the bake hardening response (Fig. 5. 1). The network was trained with a randomly chosen 291 of the examples from a total of 582 datasets available; the remaining 291 sets of examples were kept aside at first to be used as '*new*' experiments to test the behaviour of the trained network. This procedure helps avoid over-complex and overfitting models. Linear functions of the normalized inputs, x_N^j, are operated on by a hyperbolic tangent transfer function

$$h_i = \tanh\left[\sum w_{ij}^{(1)}.x_N^j + \theta_i^{(1)}\right] \quad\text{..5.2}$$

so that each input contributes to every hidden units (Fig. 5. 1). The term $\theta_i^{(1)}$ in the above expression (equation 5.2) represents the *bias* which is analogous to the constant that appears in linear regression analysis and the term $w_{ij}^{(1)}$, which is called the *weight,*

determines the strength of the transfer function in each case. These weights are determined by training the network; the details are described elsewhere [Mackay 1992 a, Mackay 1992 b, Mackay 1994, Fuji *et al* 1996]. The *training* of the model is carried out by adjusting these weights ($w_{ij}^{(1)}$) to minimise the error function which is the regularised sum of square errors. The transfer function from the hidden unit nodes to the output y is linear:

$$y = \sum w_{ij}^{(2)} h_i + \theta^{(2)} \quad \ldots\ldots\ldots\ldots\ldots\ldots\ldots\ldots\ldots\ldots\ldots\ldots\ldots\ldots\ldots.5.3$$
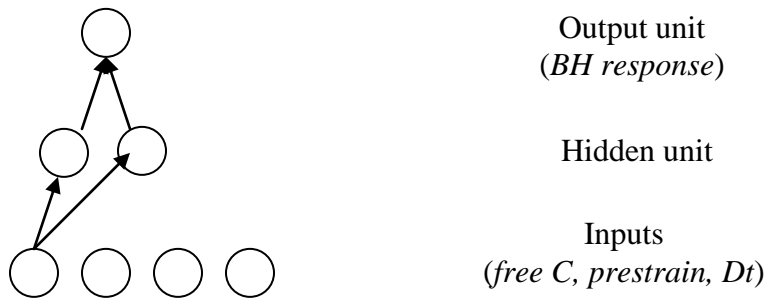
Fig. 5.1: *Typical network used in neural network analysis described in Section 5.4; only connections originating from one input are shown and two hidden units are shown [Bhadeshia, 1999]*

The complexity during *training* of the model can be controlled by varying the number of *hidden units*. However, a high degree of complexity may not be justified and in an extreme case, the model may in a meaningless way attempt to fit the noise in the experimental data. The number of hidden units was set by examining the performance of the model on the "*unseen*" test data by using two different error estimation namely *Test Error* (or TE) and *Log Predictive Error* (or LPE). *Test error* (TE), which is a measure of the deviation of the predicted value from the experimental one in the test data, is given by equation 5.4 where y_n is the predicted BH response and t_n is its measured value. Figure 5.2*a* represents the variation of *TE* with the number of hidden units. Another useful measure is the '*Log Predictive Error* (LPE)' [Mackay, 1992 a; Mackay, 1992 b; Mackay, 1994] for which the penalty for making a wild prediction is much less if the wild prediction is accompanied by an appropriately large error bar. If for each input dataset n, the model gives a prediction y_n with an error σ_n^2, the log predictive error (LPE) is given

by equation. 5.5 and its variation with the number of hidden units is shown in Fig. 5.2*b*. Figure 5.2*c* shows the framework estimate of the noise level of the data as represented by σ_v. A combination of TE, LPE and σ_v finally determines the model complexity.

$$TE = 0.5 \sum_n (y_n - t_n)^2 \quad \ldots\ldots\ldots\ldots\ldots\ldots\ldots\ldots\ldots\ldots\ldots\ldots\ldots\ldots\ldots\ldots\ldots\ldots\ldots\ldots\ldots\ldots \quad 5.4$$

$$LPE = \sum_n \left[\frac{\frac{1}{2}(t_n - y_n)^2}{\sigma_n^2} + \log\left\{ (2\pi)^{\frac{1}{2}} \sigma_n \right\} \right] \quad \ldots\ldots\ldots\ldots\ldots..\ldots\ldots\ldots\ldots\ldots \quad 5.5$$
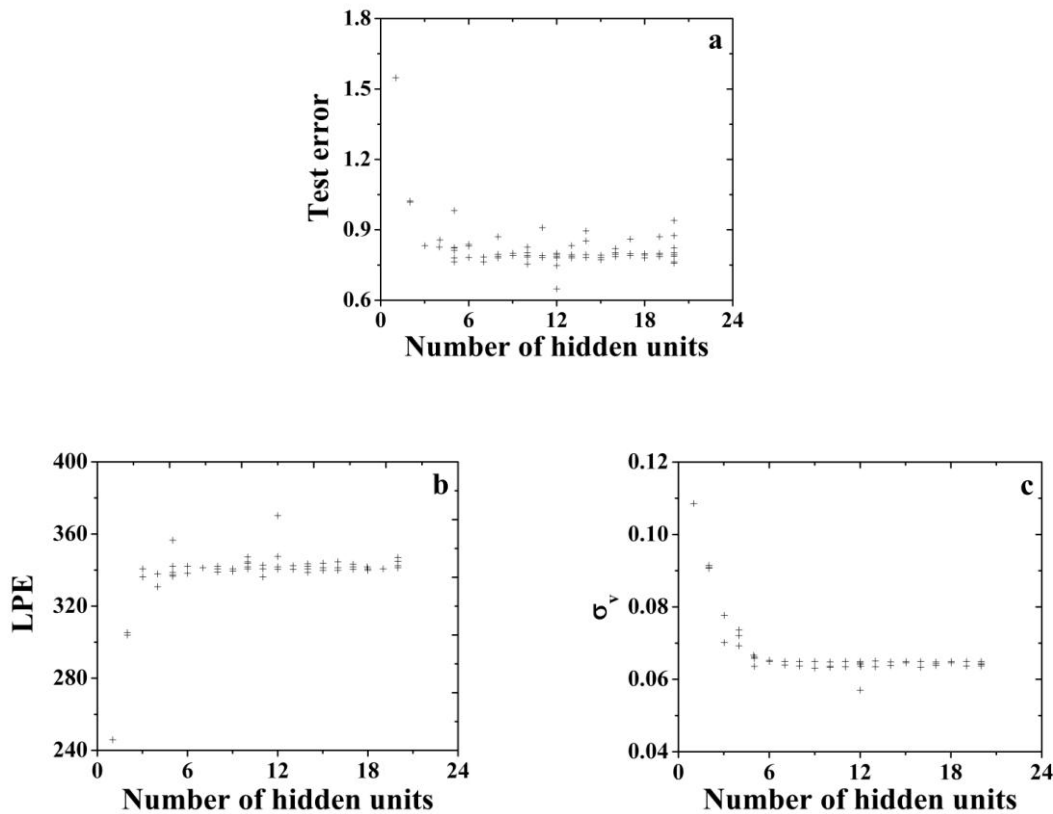
Fig. 5.2: *Performance of the ANN model of bake hardening developed in Section 5.4 (several values are presented for each set of hidden units because training for each network was started with a variety of random seeds) a. Test error (TE) for each model, b. Log Predictive Error (LPE) for each model and c. framework estimate of the noise level of the data as represented by σ_v*

It is seen that a model with twelve hidden units gives an adequate representation of the data with a minimum in the test error (Fig. 5.2*a*). The behaviour of the training and

testing data set for the best model is shown in Fig. 5.3 which shows a similar degree of scatter in both the plots, indicating that the complexity of this particular model is optimum. The error bars in Fig. 5.3 include the error bars on the underlying functions and the inferred noise level in the dataset σ_v. In all other subsequent predictions discussed below, the error bars include the former component only.
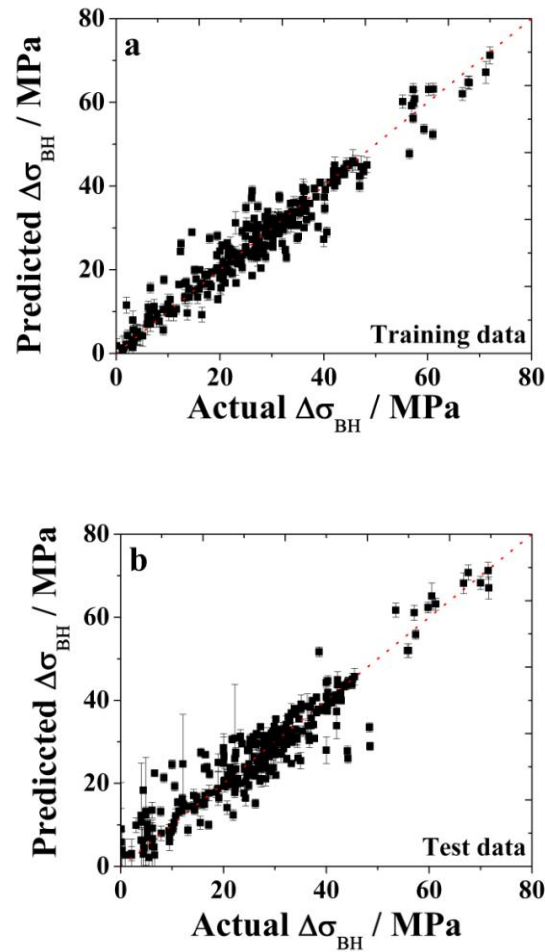
Fig. 5.3: *Performance of the best ANN model developed in Section 5.4. (a). Training and (b) testing data. Error bars represent ±1 σ*

When making predictions, MacKay has recommended the use of multiple good models instead of just one best model [Mackay, 1992 a; Mackay, 1992 b; Mackay, 1994]. This is called *'forming a committee'* [Mackay, 1992 a; Mackay, 1992 b; Mackay, 1994]. The

constituent models inside a *Committee model* are called as *sub-models*. The committee prediction $\bar{y}$ is obtained using the following expression:

$$\bar{y} = \frac{1}{N_m} \sum_i y_i \qquad\qquad\qquad 5.6$$

where N_m is the number of models in the committee and y_i is the prediction made by a particular *sub-model i*. The optimum size (*i.e.* the number of *sub-models*) of the committee is determined from the validation error of the committee's predictions using the test data set. The *Combined Test Error* (*CTE*) of the predictions made by a committee is calculated by equation 5.7. In the present analysis, a *Committee Model* was used to make more reliable predictions. The *sub-models* were ranked according to their LPE. Committees were then formed by combining the predictions of best *M* models, where *M* gives the number of members in a given committee model. The test errors of the first 40 committees are shown in Fig. 5.4. It was found that a committee model, comprising of 3 sub-models (two with 12 hidden units and the third with 5 hidden units) produces the lowest test error.

$$CTE \ = \ 0.5 \sum_n (\bar{y} - t_n)^2 \qquad\qquad\qquad 5.7$$
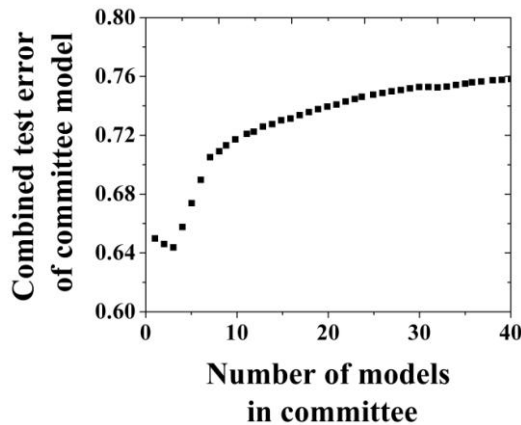
Fig 5.4: *Combined test error of the ANN model as a function of the number of models in the committee developed in Section 5.4.*

Once the best committee is formed, each constituent *sub-models* of the best committee was retrained over the entire dataset beginning with the *weights* determined by the

previous training and the the extent of agreement between the predicted and the measured values of bake hardening is illustrated in Fig. 5.5. The plot represents the entire available dataset of 582 experiments with the calculations done using the optimised committee of models as described elsewhere [MacKay, 1992b; Bhadeshia, 1999; MacKay, 2003; Singh *et al.,* 1998]. The error bars represent $\pm 1\sigma$ modelling uncertainty and the value of the *Correlation coefficient* (R^2) is 0.89.
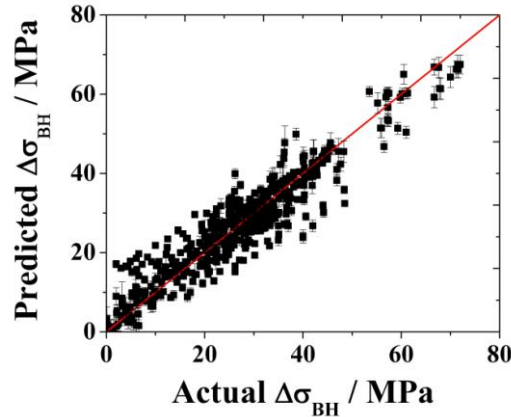
Fig. 5.5: *Training data for best bake hardening committee model developed in Section 5.4; modelling uncertainties illustrated correspond to $\pm 1\sigma$*

5.5   Application of the model

After the development of the model, it was subjected to extensive testing to explore the behaviour of the model. Four different cases were selected for the purpose. The input parameters (*free carbon in ferrite, amount of prestrain and Dt*) for each of the four steels are listed in Table 5.2. The data listed in Table 5.2 form the basis for studying the trends described below. It may henceforth be assumed that when a plot of $\Delta\sigma_{BH}$ is presented against a particular variable (say, *prestrain*), then the values of all the other variables correspond to those listed in Table 5.2 for that particular steel.

Table 5.2: Examples of steels studied using the model

Variable	Steel 1	Steel 2	Steel3	Steel 4
Free carbon / ppm	8	6	4	5.4
Prestrain / %	1	5	4	2
Ln(Dt)	-18.62	-22.15	-20.79	-20.79

5.5.1   The aging condition

As discussed earlier, the bake hardening effect in steel is effectively an accelerated strain aging which depends both on the aging time and temperature. In the present analysis, the parameter Dt was used to study the effect of aging time and temperature. The effect of Dt on $\Delta\sigma_{BH}$ is shown in Fig. 5.6. Two distinct stages of strength increment can be observed from all the plots. The first stage is due to the formation of Cottrell atmosphere and the second increment is due to the precipitation of extremely fine carbides [Elsen and Hougardy, 1993; Baker *et al.,* 2002 b; De *et al.,* 1999; Al-Shalfan, 2001]. The higher bake hardening response at higher Dt values is possibly due to the formation of ε-carbide on the existing dislocations [Bhadeshia and Honeycombe, 2006]. Initially, with increasing Dt, more and more carbon atoms migrate to the dislocation sites. As a result, strength increases due to the formation of Cottrell atmosphere. With further increase in Dt, continuous pipe diffusion along the dislocation lines lead to the formation of clusters of carbon atoms on the dislocation sites [De *et al.,* 2001]. Eventually, nucleation of very fine precipitates occurs from these clusters [Al-Shalfan, 2001; Bhadeshia and Honeycombe, 2006]. Although the existence of this kind of precipitates was not observed using TEM, the work by De *et al.* [1999] confirmed the formation of low temperature carbides during late stages of bake hardening.

It can be seen from Fig. 5.6 that bake hardening effect does not increase continuously with increasing Dt, rather, it reaches a certain plateau. This behaviour is expected because, each steel has a fixed amount of free carbon which gets consumed firstly due to the Cottrell atmosphere formation and secondly due to the precipitation. So, after a certain time, no free carbon atoms are available in the steel to contribute to the bake hardening response and it becomes insensitive to increasing Dt.

5.5.2   Free Carbon

Undoubtedly, one of the most important parameters in controlling the BH response is the amount of free carbon in solution in ferrite. An effort was made in the current work to find the influence of free carbon in ferrite on the final bake hardening response. It can be seen from Fig. 5.7 that BH response increases with the amount of free carbon initially, but then it reaches a saturation point and then again increases with increasing free carbon

content. However, the error bars are too large to properly draw any final conclusion. The large error bars may originate from the scarcity of data with high free carbon in the original training and test data. However, the results indicate that at a given Dt, carbon atoms first form the Cottrell atmosphere and then with increasing free carbon content, precipitation occurs. From this figure, it can be said that effective bake hardening is obtained when the amount of free carbon remains in the range of 6 - 12 ppm which is in accordance with the previous work which was not been included in the dataset for neural network analysis [Van Snick *et al.,* 1998].

(a)   (b)

(c)   (d)
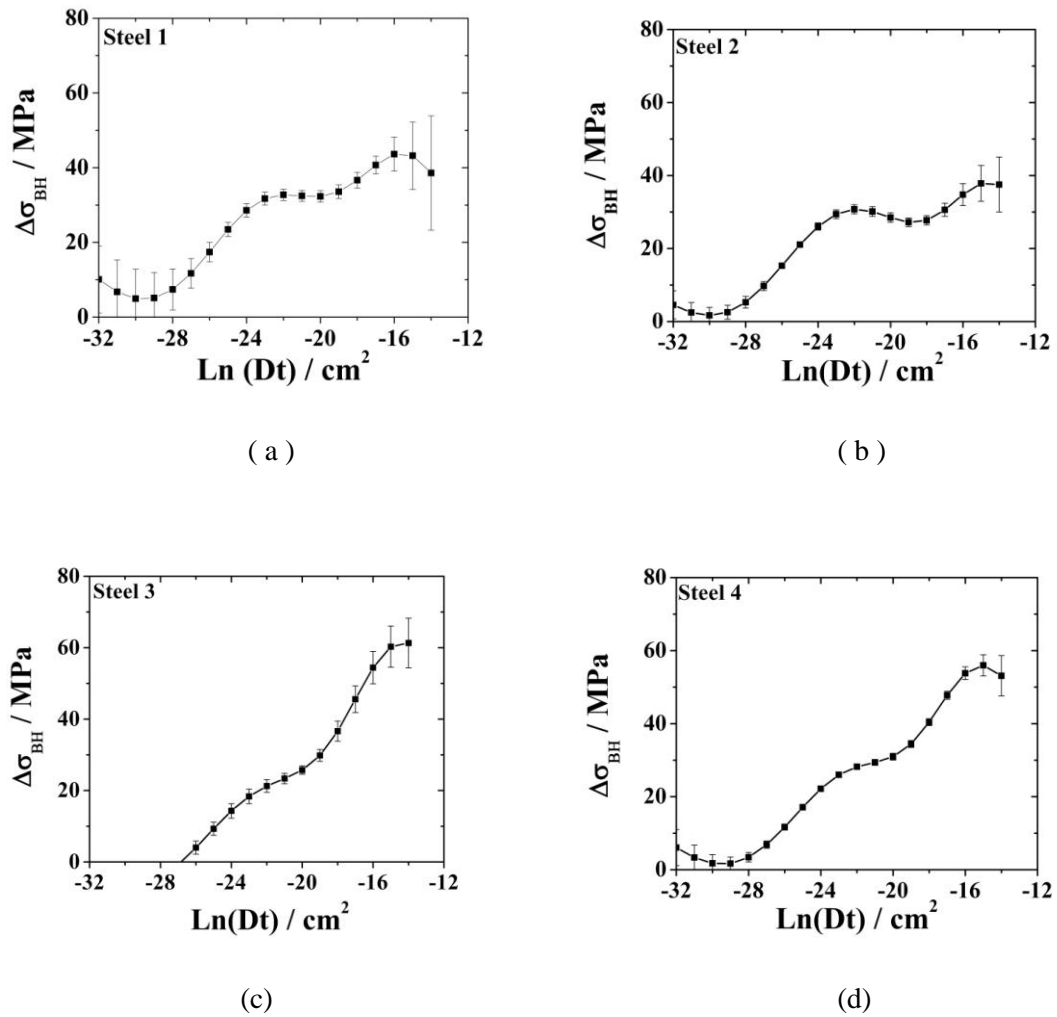
Fig. 5.6: *Calculated $\Delta\sigma_{BH}$ as a function Dt for (a) Steel 1, (b) Steel 2, (c) Steel 3 and (d) Steel 4. Details of these steels are mentioned in Table 5.2.*

An effort in the current study was also made to find out the combined effect of free carbon in ferrite and Dt on the final bake hardening property and the results in the form of contour plots are shown in Fig. 5.8 for a prestrain of 5%. The predicted BH values and the corresponding uncertainties are plotted as isocontour coloured regions and lines, respectively. From Fig. 5.8, it can be seen that a higher bake hardening effect can be obtained at a combination of high Dt with higher amount of free carbon. However, it should be noted here the predictions in this region of high free carbon and Dt have higher uncertainty suggesting that more experiments are required in this range.

For steel having around 12 ppm free carbon and high Dt, the model predicts a reasonably high degree of bake hardening response at an acceptable range of uncertainty in the prediction. This finding is also in accordance with the experimental values reported in the literatures [Van Snick *et al.,* 1998].
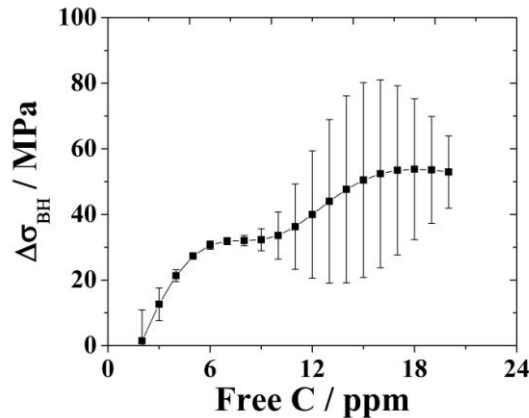
Fig. 5.7: *Calculated $\Delta\sigma_{BH}$ as a function of amount of free carbon in ferrite for steel with prestrain = 4% and Ln(Dt) = -20.79*

5.5.3 Prestrain

In most of the applications of steels that show bake hardening behaviour, the steel sheet undergoes a small amount of strain during the final forming operation that is carried out before the baking process. The bake hardening experiments are, therefore, carried out by subjecting the sample to a small amount of prestrain. However, the effect of prestrain on bake hardening response is not well established in literature. While some researchers

found an initial increase followed by decrease in strength increment due to baking with increasing prestrain [Dehghani and Jonas, 2000], other researchers found a continuous decrease in bake hardening response with increasing prestrain [Elsen and Hougardy, 1993]. A third group of researchers reported that bake hardening effect does not depend on the amount of prestrain [De *et al.,* 1999; De *et al.,* 2000].
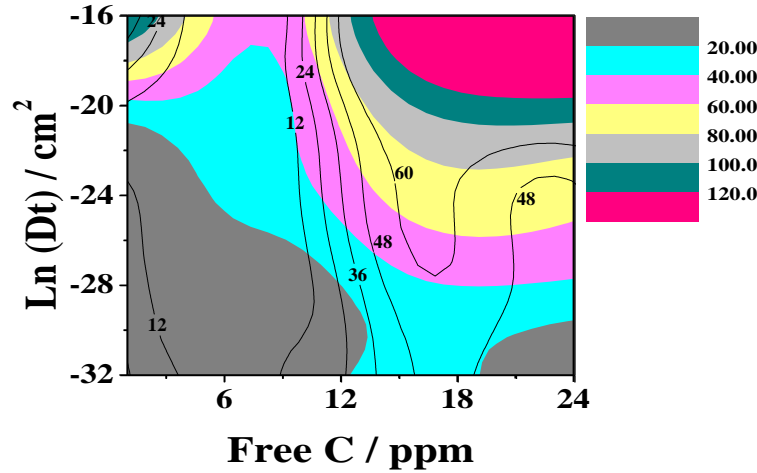
Fig.5.8: *Calculated combined effect of Dt and free carbon on* $\Delta\sigma_{BH}$ *for steels with 5% prestrain. The coloured regions represent different* $\Delta\sigma_{BH}$ *range whereas each isocontour line reflects the different levels of uncertainties. The units of the numbers mentioned on the isocontour lines and on the different colour codes are in MPa.*

The results of the present model shown in Fig. 5.9 reveal that increasing the prestrain does not affect the final bake hardening property positively, rather large prestrains may even lead to a reduction in the final BH response. For any particular steel, the amount of free carbon is fixed for a given set of processing parameters. The effect of increasing the amount of deformation is to increase the dislocation density which may not be locked by the existing amount of free carbon. It will therefore be interesting to examine the combined effect of increasing the amount of prestrain as well as the amount of free carbon simultaneously for a particular aging condition. Steel 2 was chosen for this kind of analysis and the corresponding results are shown in Fig. 5.10. Corresponding BH response in MPa is shown as colour codes and different isocontour lines indicate different levels of uncertainties (in MPa) in the prediction.

Figure 5.10 clearly shows that with increasing the prestrain, final BH response decreases for a particular aging condition. Such a reduction might be expected if not all

the dislocations introduced during prestraining, are pinned during the aging process. A higher pre-deformation would leave higher density of free dislocations and hence a diminished bake hardening response could be the outcome. This hypothesis will only be valid if the aging condition is insufficient and hence carbon atoms are not able to migrate to the dislocation sites to lock them up within the available time. If sufficient time and temperatures are given, then the carbon atoms might have been able to travel to the all possible locations of dislocation sites and lock them.
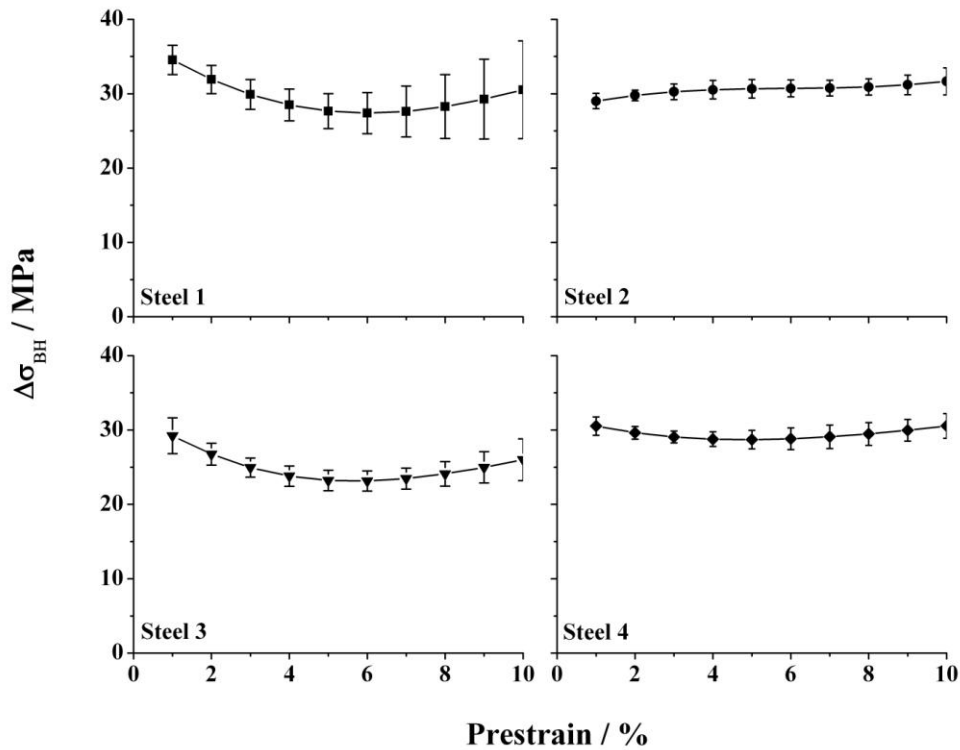
Fig.5.9 *Calculated effect of prestraining on the* $\Delta\sigma_{BH}$ *property for different steels mentioned in Table 5.2.*

To cross examine this hypothesis, another analysis was carried out where the amount of prestrain and aging condition (*i.e. Dt*) were varied keeping the initial amount of free carbon constant. The results are showed in Fig. 5.11 from which it can be seen that given sufficient time and temperature, all the dislocations may be locked and the total bake hardening response does increase with the amount of prestrain provided there are enough

carbon atoms to lock them up. This kind of behaviour was also reported elsewhere [Das *et al.,* 2008; Das *et al.,* 2011].
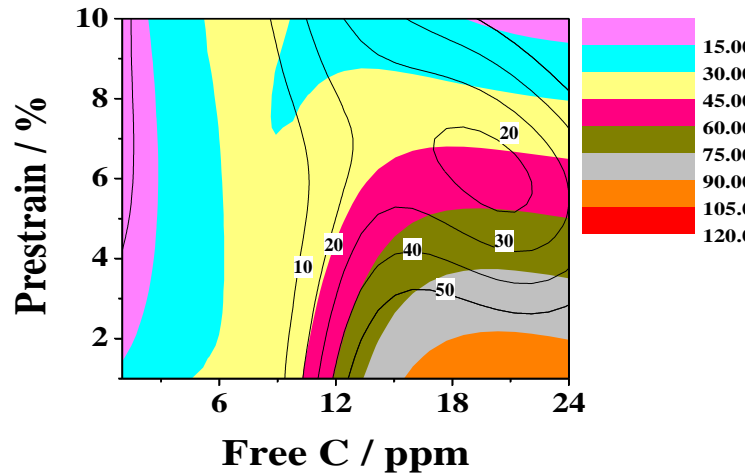
Fig.5.10: *Calculated effect of prestrain and free carbon on $\Delta\sigma_{BH}$ for Dt = -22.15. Different colours show different iso-BH profiles and different contour lines represent varying degrees of uncertainties in predictions. The units of the numbers mentioned on the isocontour lines and on the different colour codes are in MPa*
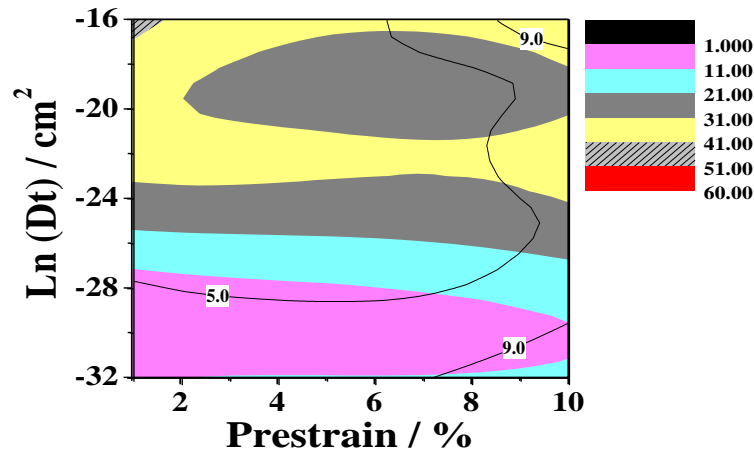
Fig.5.11: *The calculated combined effect of increasing the amount of prestrain and Dt on the final bake hardening effect for a steel with 8 ppm free carbon. Different colours show different iso-BH profiles and different contour lines represent varying degrees of uncertainties in predictions. The units of the numbers mentioned on the isocontour lines and for the different colour codes are in MPa*

5.6   Conclusion

A neural network based model had been developed to study the influence of free carbon, prestrain and aging condition on the final bake hardening response of low C steels. The

predictions are consistent with the basic understanding of the bake hardening mechanism. The predictions are meaningful and are supported by the results of other work which were not considered during the development of the model. Following conclusions can be drawn from the work presented in this chapter.

i. Aging condition and amount of free carbon are the most important parameters that influence the bake hardening response.

ii. Systematic experiments with gradual change in the free carbon content should be performed in order to better predict its effect.

iii. Approximately 10-12 ppm free carbon is sufficient to provide good BH response

iv. Effect of prestraining on the final BH response is not very significant, provided sufficient aging condition is allowed.

Chapter 6

<u>Complexities of Bake Hardening</u>

Chapter 6

Complexities of Bake Hardening

6.1   Introduction

In the previous two chapters (Chapter 4 and Chapter 5), models were described to predict the final bake hardening response on the basis of the amount of free solute carbon available during the baking operation, amount of prestrain and aging condition (represented by *Dt*). However, BH response can depend on some other parameters also *e.g.*, alloying elements other than carbon, prestrain condition *etc*. Thus, a model incorporating such parameters would be more general and can make better predictions.

In the ANN model described in Chapter 5, the measured amount of free carbon was considered as one of the input variables to the model. The measurement of free carbon in all the cases was done by employing *internal friction* technique. However, such measured value might be an underestimation because it has been shown that the internal friction technique cannot measure the grain boundary carbon [Massardier *et al.,* 2004]. For this reason, the total amount of carbon was considered instead of free carbon in the current analysis. Presence of elements like phosphorous (P), manganese (Mn) *etc* and other microalloying elements (niobium and/ titanium) can influence the amount of free carbon in ferrite and thus has the potential to affect the BH response. Hence, full chemical composition of the steels was chosen as the input to the model and estimation of the interrelationship between the input and output variable was determined by the model.

Temperature of prestrain, other than the amount of prestraining, is another important input which is considered in developing the current model as dynamic strain aging can take place during prestraining itself [Dehghani and Jonas, 2000]. Annealing temperature and time are also important in determining the available amount of free carbon available in solution. As the diffusion of carbon atoms are mainly governed by the aging temperature and time, these two variables are also included in the dataset as input parameters.

The method has been described in details in Chapter 5 of the thesis. Therefore, only the results of this new model will be explained in this chapter.

6.2   Data

The raw data for the model were collected from the results published in journal papers and Ph.D thesis [Elsen and Hougardy, 1993; Baker *et al.,* 2002 b; De *et al.,* 1999; Dehghani and Jonas, 2000; De *et al.,* 2000; Al-Shalfan, 2001; Zhao *et al.,* 2001; De Meyer *et al.,* 2000]. Some publications did not state the concentrations of Ti, Nb, Al and Si, in which case they were assumed to be zero since these usually are all deliberate additions. Similarly, the temperature of deformation before baking was assumed to be 25 ^{o}C when not stated. The cooling rate from the annealing temperature, grain size and the strain rate should influence bake hardening, but were omitted as variables given the lack of data and this should contribute to the noise in the output. The maximum, minimum, average and the standard deviation of the input database are listed in Table 6.1.

Table 6.1: Summary of the data used in the analysis.

Variables	Minimum	Maximum	Average	Standard deviation
C / wt%	0.002	0.03	0.0093	0.0122
Mn / wt%	0.09	0.53	0.1665	0.1192
S / wt%	0.003	0.023	0.0061	0.0056
Si / wt%	0	0.022	0.0044	0.0072
P / wt%	0.007	0.045	0.0312	0.0173
N / wt%	0.0016	0.0034	0.0021	0.0007
Nb / wt%	0	0.018	0.001	0.0027
Ti / wt%	0	0.06	0.0095	0.015
Al / wt%	0	0.05	0.0448	0.014
Annealing temperature / ^{o}C	720	900	857.7	20.2
Annealing time / s	1	250	98	75.9
Prestrain / %	1	10	4	2.5
Prestrain temperature / ^{o}C	25	250	33	35.5
Baking temperature / ^{o}C	25	250	112.5	50
Baking time / minute	0.1	49803	1346	5046.7
Bake hardening / MPa	0.1	72	27.9163	14.14

It is worth emphasising that the range of each of the variables stated in Table 6.1 does not define the limits beyond which extrapolation is considered to occur. This is because the data are not necessarily uniformly distributed in the variable space. The modelling uncertainty, on the other hand, is an excellent indicator of positions in the input space where knowledge is sparse.

6.3   Application of model

The optimum complexity and quality of the model were judged by different parameters *e.g. Test Error (TE), Log Predictive Error (LPE)* and noise level of data represented by σ_v. The details are described in Chapter 5 of the current thesis. Figure 6.1 represents TE, LPE and σ_v as function of the number of hidden unites in the model. It was found that a model with three hidden units gives good representation of the data with a minimum in *Test Error*. The behaviour of this best model on the *training* and *test* dataset is shown in Fig. 6.2 which represents similar scatter in both the datasets.

Subsequently, following Mackay [Mackay 1992 a, Mackay 1992 b, Mackay 1994], the *Committee* model was developed. The details of developing such *Committee model* have been described in Chapter 5. The *Combined Test Error* (*CTE*) of this committee model can be seen in Fig. 6.3. It was found that a committee of 3 models gave the best results. Finally, the agreement between the actual and predicted values of BH response of this committee model on the *known* dataset of 622 experimental conditions is shown in Fig. 6.4. The error bars represent ±1σ modelling uncertainty. Three different steels were selected in order to explore the behaviour of the model, both with respect to known and understood trends and in order to resolve some inconsistencies across published data. The parameters representing these steels are listed in Table 6.2. Steel 3 is interesting because its deformation temperature is greater than that at which it was bake hardened. The three alloys also cover a significant range of prestrain (ε). Steel 1 has a particularly high manganese concentration and there are detailed differences in the microalloying additions. The data listed in Table 6.2 form the basis for studying trends. It may henceforth be assumed that when a plot of $\Delta\sigma_{BH}$ is presented against a particular variable (such as Mn), then the values of all the other variables correspond to those listed in Table 6.2 for that particular steel.
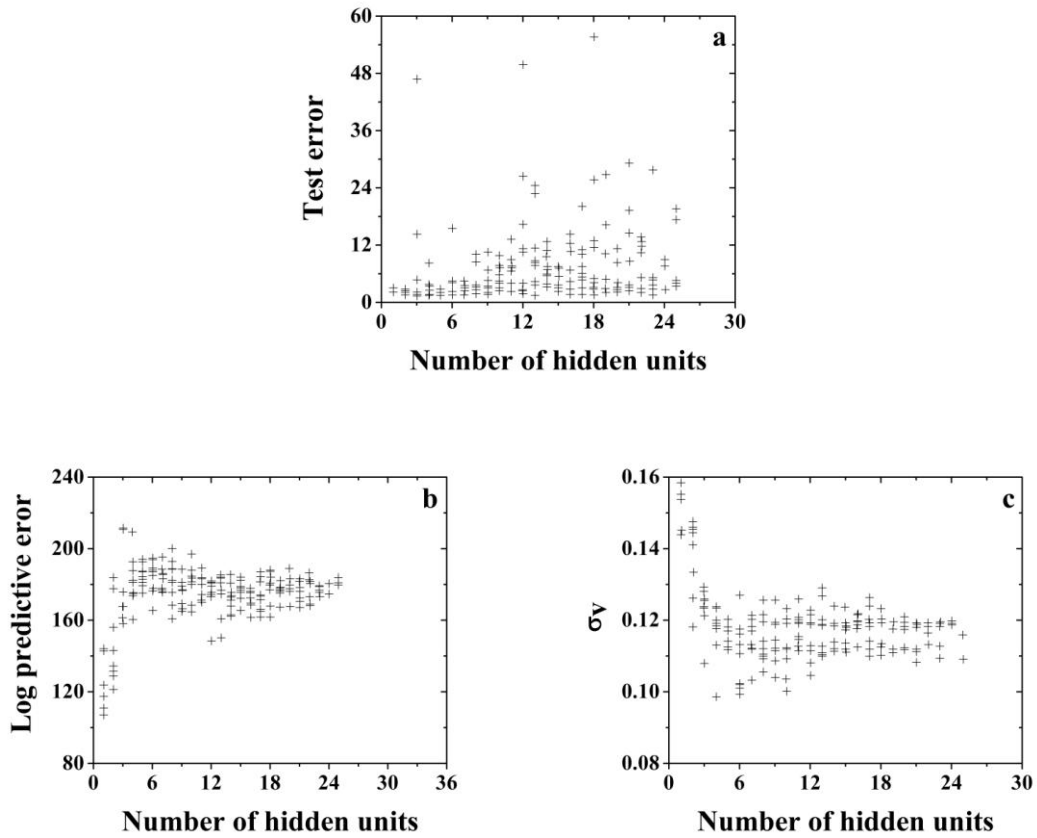
Fig. 6.1: *ANN based bake hardening model as discussed in Section 6.3 (several values are presented for each set of hidden units because training for each network was started with a variety of random seeds) a. Test error (TE) for each model, b. Log Predictive Error (LPE) for each model and c. framework estimate of the noise level of the data as represented by σ_v*
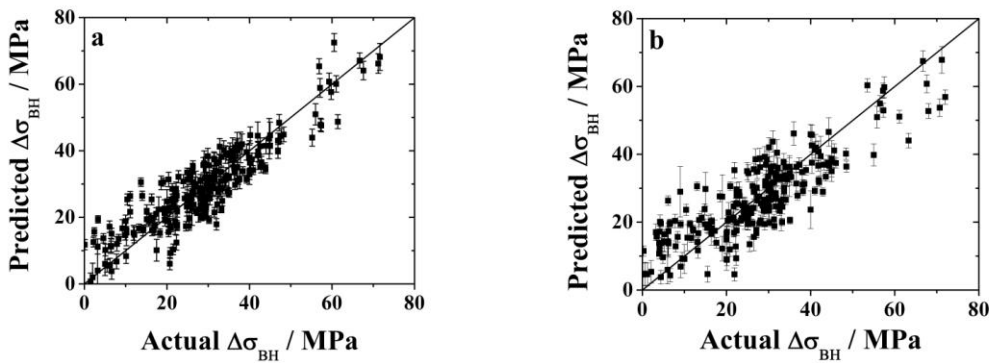
Fig. 6.2: *Performance of the best model ANN model as discussed in Section 6.3. (a) Training and (b) Testing data. Error bars represent ±1 σ*
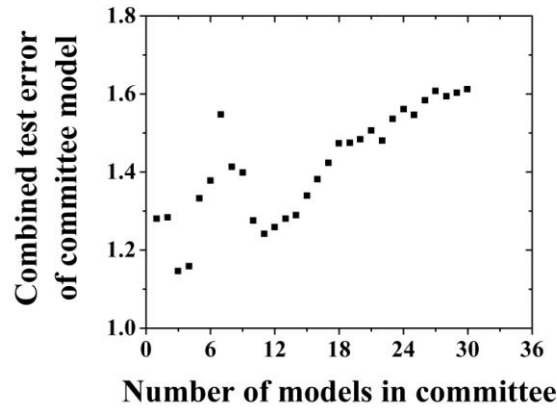
Fig. 6.3: *Combined test error of the ANN model discussed in Section 6.3 as a function of the number of models in the committee*
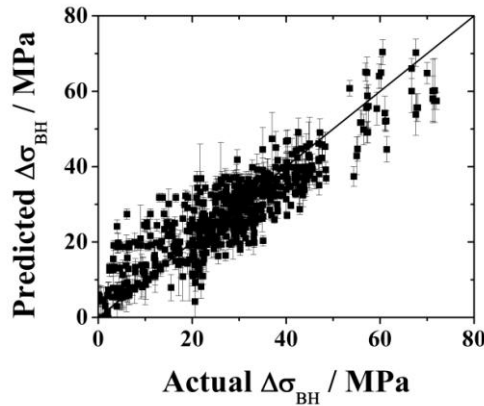
Fig. 6.4: *Training data for best bake hardening committee model discussed in Section 6.3; modelling uncertainties illustrated corresponds to ±1 standard deviation*

6.3.1   Deformation prior to aging

The prestrain refers to the plastic deformation before the aging treatment; in laboratory experiments such as those considered here, it is applied homogeneously, although in practice the state of deformation will depend on the application and shape of the component. It was pointed out earlier that $\Delta\sigma_{BH}$ decreases monotonically with prestrain (ε) [Elsen and Hougardy, 1993; Van Snick *et al.,* 1998], although others suggest $\Delta\sigma_{BH}$ should be insensitive to the prestrain [De *et al.,* 1999; De *et al.,* 2000].

Table 6.2: Alloys studied with the newly developed model.

Variables	Steel 1	Steel 2	Steel 3
C / wt%	0.0021	0.002	0.0023
Mn / wt%	0.53	0.09	0.16
S / wt%	0.012	0.003	0.023
Si / wt%	0.001	0	0
P / wt%	0.029	0.045	0.011
N / wt%	0.002	0.0016	0.0032
Nb / wt%	0.006	0	0.005
Ti / wt%	0.008	0.007	0.06
Al / wt%	0.047	0.049	0
Annealing temp / $^{\circ}$C	820	850	900
Annealing time / s	80	60	60
Prestrain / %	1	2	4
Prestrain temp. / $^{\circ}$C	25	25	200
Aging temp. / $^{\circ}$C	100	50	170
Aging time / min	98.9	283.7	20

For the conditions listed in Table 6.2, Steels 1 – 3 have ε =1, 2, 4% respectively, and all show a reduction in $\Delta\sigma_{BH}$ as a function of ε, as illustrated in Fig. 6.5a. Such a reduction might be expected if not all of the dislocations introduced by deformation become pinned during the aging period. A larger ε would leave more free dislocations and hence a diminished bake hardening response. However, this hypothesis would only be valid if the aging conditions are insufficient to ensure the pinning of all available dislocations. In their analysis, De *et al.* [2000] showed that the maximum increase in yield strength corresponding to the completion of carbon atmosphere formation on dislocations was independent of the level of prestrain. This has been simulated here for Steel 1 by increasing the aging time to 8000 minute; the results are illustrated in Fig. 6.5b and confirm that the strength increment becomes insensitive to the prestrain when the aging time is long.

It follows therefore that $\Delta\sigma_{BH}$ will only decrease as a function of ε when the aging conditions do not allow sufficient time for the dislocation–pinning process to be completed. This is entirely consistent with the classical work on strain aging by Cottrell

and Bilby, also involving steels with dissolved carbon concentrations < 0.003 wt-% [Cottrell and Bilby, 1949].
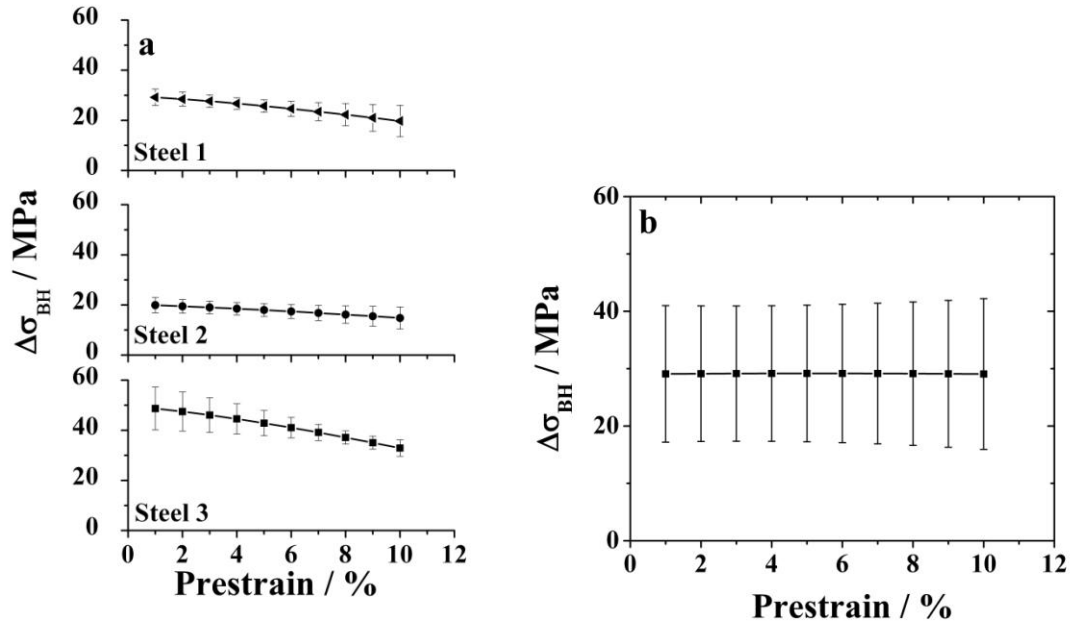
Fig.6.5: *Effect of prestrain on the corresponding BH behavior of different steels mentioned in Table 6.2. (a) Effect of prestrain on Steel 1, 2 and 3, keeping the other parameters constant as mentioned in Table 6.2; (b) Effect of prestrain on Steel 1 for aging time 8000 minute*

An interesting observation in Fig. 6.5*a* is that Steel 3 has a very high bake hardening response at low ε, and hence $\Delta\sigma_{BH}$ exhibits a larger decline as the prestrain increases. This is because the alloy was prestrained at 200 ^{o}C which is greater than the aging temperature of 170°C (Table 2). Dynamic strain aging is therefore likely at the deformation temperature [Tsuchida *et al.,* 2005]. This is also proven by the calculations presented in Fig. 6.6, where it is seen that a reduction in the deformation temperature to values less than the aging temperature leads to a dramatic decline in $\Delta\sigma_{BH}$.

6.3.2   Influence of aging condition

The effect of temperature and time on strain aging behaviour has long been understood [Cottrell and Bilby, 1949]. Figure 6.7*a* shows the calculated dependence of $\Delta\sigma_{BH}$ on the aging temperature. Also plotted is the normalised measure of strain aging, $H = (H_t - H_0)/(H_M - H_0)$ versus Dt where for a given steel, H_t, H_0 and H_M are the

instantaneous, minimum and maximum values of $\Delta\sigma_{BH}$, respectively. $D = 5.2\times10^{-4}\exp(-9000\,/T)\,\mathrm{cm^2 s^{-1}}$ is the diffusion coefficient for carbon in ferrite [Cottrell and Bilby, 1949] and t is the aging time. The calculated data from the three different steels are rationalised in this way (Fig. 6.7*b*). It is interesting that the major part of the strain aging is completed at low values of $Dt < 2 \times 10^{-9}$ cm^2. This is consistent with the substantial bake hardening apparent even from room temperature aging (Fig. 6.7*a*). It is worth mentioning here that similar trend was observed in Chapter 4 also (Fig. 4.3 and 4.4).
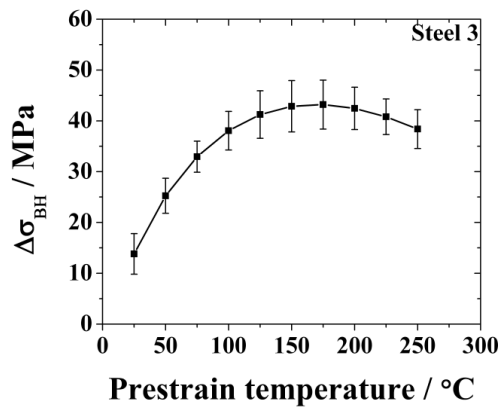
Fig.6.6: *Effect of prestraining temperature on final BH response for Steel 3. Details of Steel 3 is given in Table 6.2*
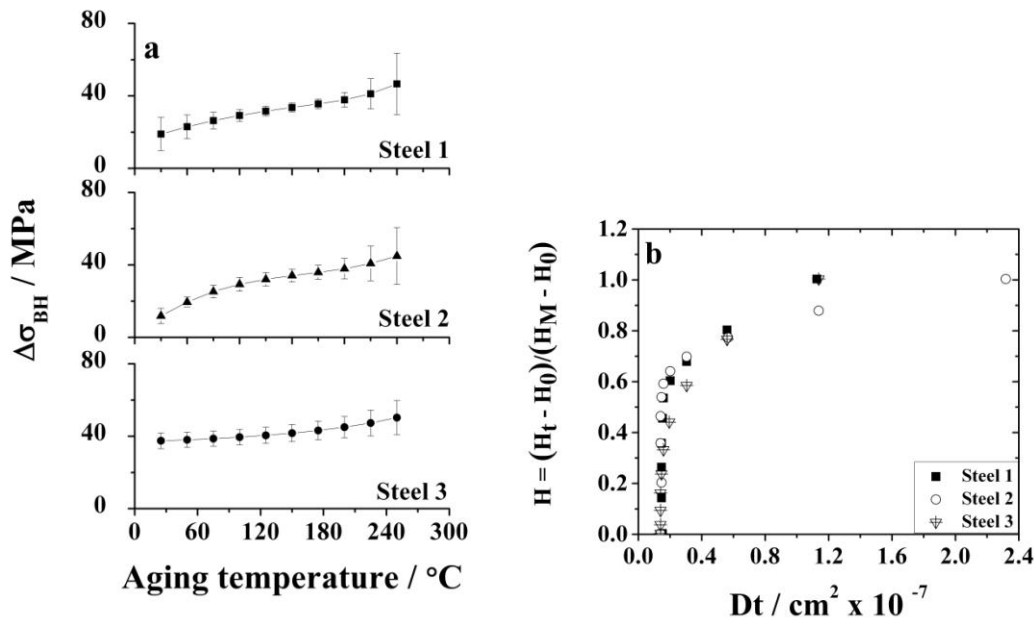
Fig. 6.7: *Influence of aging condition on final BH response. (a) Effect of aging temperature on Steel 1, 2 and 3. All other parameters are same as mentioned in Table 6.2. (b) Interpretation of data*

6.3.3 Effect of microalloying elements

There are indeed a number of reports related to the design, stabilisation and precipitation sequence of microalloying elements (Nb and/Ti) in ultra low carbon (ULC) bake hardenable steels. However, the effect of increasing the amount of such microalloying elements (Nb and/Ti) on the bake hardening response has not been systematically studied. To rationalise this issue in the current work, it was decided to predict the amount of bake hardening with increasing Nb and Ti content for a particular steel.

The influence of niobium additions on the bake hardening tendency was too uncertain to be reliably perceived on the basis of the data used to create the model (Fig. 6.8*a*). However, the situation is somewhat different for Ti. The effect of increasing Ti on BH response is shown in Fig. 6.8*b*. From a metallurgical point of view, the addition of Ti (and Nb also) is expected to reduce the BH response as it is strong carbide former and hence reduces the amount of C in ferrite which can later on take part in increasing the strength during paint baking operation. Thus the trend with Steel 1 and Steel 2 for increasing Ti is meaningful. However, the influence of increasing Ti addition in Steel 3 is too uncertain to draw any conclusion but is still shown for illustrative purpose.
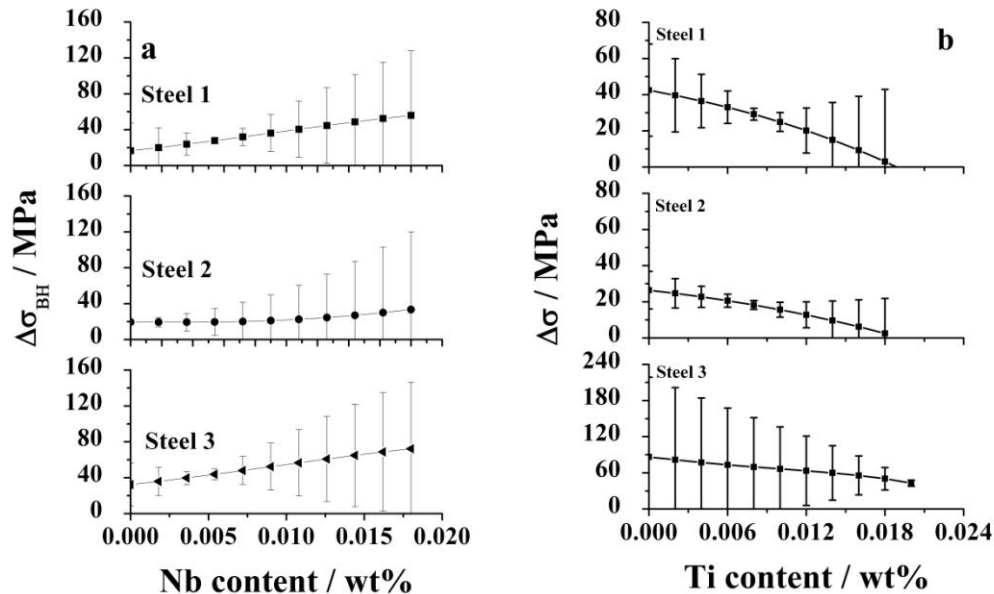
Fig.6.8: *Effect of (a) Nb in Steel 1,2 and 3 and (b) Ti in Steel 1, 2 and 3 on final BH response. Details of Steel 1, 2 and 3 can be found in Table 6.2.*

6.3.4   Effect of Mn

It has been found by earlier researchers that the addition of Mn actually deteriorates the bake hardening response [Taniguchi *et al.,* 2005; Hanai *et al.,* 1984]. Similar behavior can also be seen from Fig. 6.9 which indicates a decrease in BH response with increasing Mn content. Researchers [Cuddy and Leslie, 1972; Li and Leslie, 1978] have showed that other than the interstitial solute atoms (C and N), strain aging can also be affected by the interaction of interstitial-substitutional solute pairs (Mn-C or Mn-N) with dislocations. Using internal friction, Li and Leslie [1978] showed that interstitial atoms prefer sites next to Mn atoms rather than sites where they are surrounded by iron atoms. As a result, Mn, probably by forming Mn-C pairs, reduces the mobility of interstitial solutes to participate in bake hardening. So, it is expected that the addition of Mn leads to a reduction in the BH response.
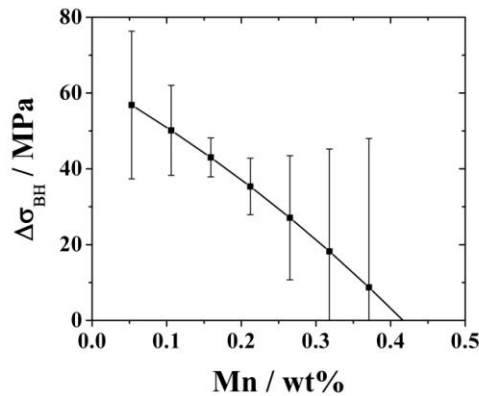
Fig.6.9: *Effect of Mn on BH response in Steel 3. Details of Steel 3 are given in Table 6.2.*

6.3.5   Effect of P

In Fig. 6.10, the calculated effect of P on the bake hardening effect is presented for steel 1. The figure shows an increase in the bake hardening response with increasing P content. Other researchers [Taniguchi *et al.,* 2005; Okamoto *et al.,* 1981] have also observed similar behaviour. Hanai *et al.* [1984] argued that not only interstitials but also P enhances the locking of dislocations and thus an increase in BH response is observed. However, such behaviour needs to be investigated further.
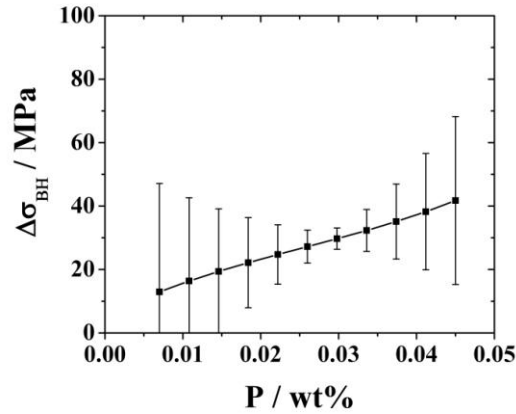
Fig. 6.10: Calculated BH response as a function of total P content for steel 1. Details of Steel 1 can be found in Table 6.2.

6.3.6 Annealing temperature

Figure 6.11 represents the effect of annealing temperatures on the corresponding BH response. It can be seen that for the conditions listed in Table 6.2, increasing annealing temperature increases the BH response for Steel 1 and 2 both. This can be expected if higher annealing temperatures increase the free C content of ferrite Thus, the ANN predictions are consistent with well established metallurgical principles. However, the associated error bars are too big for Steel 3 to perceive any meaningful trend. It should also be mentioned here that similar trend was observed in Chapter 3 (Fig. 3.10 and 3.14).
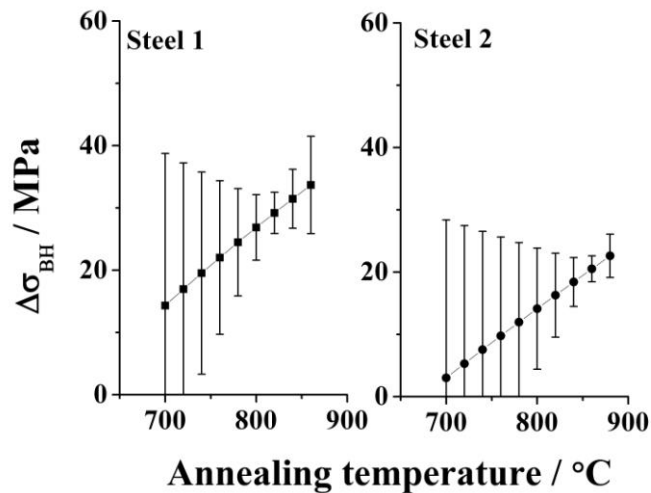
Fig. 6.11: Effect of increasing annealing temperature on subsequent BH response for Steel 1 and 2. Details of Steel 1 and 2 can be obtained from Table 6.2

6.3.7   Other parameters

In the current neural network model, effect of increasing total C content for the conditions mentioned in Table 6.2 did not show any significant change. This may possibly be due to the fact that even with increasing C, the annealing condition and the composition of these steels did not increase the free solute content in ferrite. The effect of S, Si, Al were all associated with too large error bars to perceive any meaningful trend.

In future experimental work, it would be useful to report the cooling rate from the annealing temperature. Although the equilibrium concentration of carbon in solution can be estimated as a function of temperature using phase diagram calculations, the concentration may deviate from equilibrium if the rate is sufficiently large. The attempts at correlating the amount of dissolved carbon calculated for the annealing temperature, against the bake hardening response proved unsuccessful, presumably because of the absence of information on cooling rates.

6.4   Conclusion

It is evident from this analysis that although there is a great deal understood about bake hardening steels, there are significant gaps in knowledge when the whole set of variables is considered together. In the current chapter, some inconsistencies in the published literature were addressed satisfactorily and some needs further systematic experiments to understand their behavior properly. The main findings of the current chapter are summarised below:

i.   With the neural network model it has been possible to rationalise the effects of the 'prestrain'. It can be concluded that increasing the prestrain does not increase the BH response and BH response actually becomes insensitive to prestraining if sufficient aging time is provided. However, the temperature at which prestraining is carried out has a pronounced effect on subsequent BH response.

ii. It was found that aging conditions have a great effect on the BH response. If prior prestrain operation is carried out at elevated temperature, aging temperature must be kept higher than that in order to obtain good BH response.

iii. It was also found out that a major portion of BH response can be completed within very short time.

iv. Increasing the annealing temperatures is another important parameter which improves the BH response.

v. A number of other trends, such as the influence of the solutes Mn and Ti are well defined. However, it has not been possible to extract a comprehensive understanding of the effects of all the variables, for example total C, Si, Al content of steel. System experiments should be carried out to investigate their effect properly.

Chapter 7

Bake Hardening in Delta TRIP Steel

Chapter 7

Bake Hardening in Delta TRIP Steel

7.1   Introduction

The increase in yield stress (YS) that occurs due to the thermal treatment during paint baking of already formed steel parts is known as the bake hardening effect. In industrial processing, after the forming operations, the automotive grades of steels undergo a finishing treatment, where the paints of the automotive parts are baked at a temperature of 170 °C for 20 minutes. During this baking treatment, interstitial solute atoms, such as carbon, migrate to the freshly generated dislocations to pin them. Consequently, the strength of the component increases (Fig. 2.2) [Elsen and Hougardy, 1993]. As no additional operation is required, BH could effectively result in higher strength at the same cost. The use of BH treatment has been proposed to many grades of steels, including TRansformation Induced Plasticity assisted (TRIP) steels also, to increase the strength of these steels in the final body structure [Baker *et al.,* 2002b]**.**

The microstructure of advanced automotive TRIP assisted sheet steels consists of ferrite and carbide-free bainite consisting of bainitic ferrite laths interwoven with retained austenite (RA). These steels contain enhanced Si and/or Al which suppresses precipitation of cementite during bainite formation. Consequently, carbon atoms partition to austenite and stabilise it [Edmonds and Speer, 2010].

Bainitic transformation occurs at temperatures where the shape change associated with the transformation cannot be accommodated elastically and the plastic deformation caused by the shape changes results in accumulation of dislocations both in the parent and the product phase. The measured dislocation density due to bainite transformation is typically of the order of 6×10^{15} m^{-2} [Bhadeshia and Christian, 1990; Bhadeshia, 2001]. The tendency for plastic accommodation and any recovery effects should depend largely on the transformation temperature. If the transformation is carried out at a lower temperature, it is unlikely that the dislocations, generated during the transformation, would get annihilated and hence they are retained in the material. In addition to a high

dislocation density, previous researchers have established that carbide-free bainite in these steels contain higher than equilibrium concentration of carbon [Caballero *et al.,* 2007; Bhadeshia and Waugh., 1982; Garcia-Mateo *et al.,* 2003; Caballero *et al.,* 2002; Mukherjee *et al.,* 2008].

It is thus expected that the mechanism of carbide-free bainitic transformation is such that it provides both the conditions necessary for bake hardening response (abundance of dislocations and presence of free solute carbon) and therefore it can also offer the possibility of bake hardening effect in TRIP aided steels when the steel is aged according to the paint baking condition.

Keeping this in mind, the present work was conducted to investigate the bake hardening effect due to the dislocations generated during the bainitic transformation in TRIP aided steel. In bake hardening experiments, a small amount of prestrain (typically ~ 2%) is usually given to introduce fresh dislocations in the material. These dislocations are locked by the migrating interstitial atoms during the final baking operation. The novelty of the current work is that here no extra prestrain was applied during BH experiments expecting that prior bainitic transformation would produce enough dislocations which could in turn get locked by the solute carbon atoms present in bainitic ferrite.

7.2   Material

The alloy used was made in air induction furnace in TATA Steel, India, and the chemical composition is given in Table 7.1. While the details of the design philosophy of this steel can be found elsewhere [Chatterjee, 2006], it is useful to include some details here. The intention here was to produce *carbide-free* bainite for which both Al and Si were added in optimum amounts as both of these elements are insoluble in cementite and inhibit the formation of cementite during isothermal holding [De Cooman, 2004]. The amount of Si was kept to the lowest level where it can effectively suppress the cementite formation and at the same time does not create much problem during galvanizing [Mahieu *et al.,* 2001]. Mn was added to increase the hardenability. Microstructure of the as-cast steel consist of ferrite and very fine distribution of pearlite at room temperature and this can be suitably heat treated to produce the desired TRIP microstructure [De Cooman, 2004]. Cylindrical

samples were machined from the as received cast steel for heat treatment. Separate samples were used for each transformation temperature and time combination.

Table 7.1 Chemical composition (in wt%) of the alloy studied

C	Mn	Si	Al	P	Cu
0.36	1.96	0.73	2.22	0.022	0.52

7.3   Thermodynamic calculations

Thermodynamic calculations provide equilibrium volume fraction of different phases at any temperature. Prior knowledge of volume fraction and the composition of austenite present at any temperature is important for designing the heat treatment parameters as these will ultimately determine the extent of bainitic transformation. Thermo-Calc software [Thermo-Calc] was used with TCFE-6 dataset and allowing ferrite, austenite, cementite and liquid phases were allowed to form. The change in phase fractions as a function of temperature is shown in Fig. 7.1.

In addition to the knowledge of the amount and composition of the phases, time and temperature combination used for isothermal treatment is also important in determining the degree of transformation as there will always be an incubation period during which no transformation will take place. In order to get an estimation of the minimum time for which the sample must be kept at each temperature during isothermal transformation, the time-temperature-transformation (TTT) diagram was calculated using freely available program MUCG-83 which predicts the time for the start of the transformation at a given isothermal temperature [MUCG-83] (Fig. 7.2). In carrying out this calculation, the composition of austenite at the corresponding annealing temperature was considered instead of the bulk composition.

7.4   Experimental procedure

7.4.1   Heat treatment

Presence of some amount of ferrite is necessary for obtaining adequate ductility in the material. It was, therefore, decided to have approximately 20% ferrite in the matrix. Thermodynamic calculation, as presented in Fig.7.1, predicts the evolution of phases as a

function of temperature. From this diagram, it was evident that at 900 °C, the material can possess around 17% ferrite; hence this temperature was selected for the intercritical annealing treatment.

The intercritical treatment and subsequent isothermal bainite transformation (IBT) were carried out in a Thermec Master Z simulator. The equipment utilises induction heating and the uniform temperature zone on the cylindrical samples is limited to ~ 10 mm gauge length about the center of the sample. This simulator is coupled with a LASER dilatation measuring unit which consists of a detector incorporating an optical system and an amplifier to process the photo-electric signal obtained by the detector and determines the measured dilatation. Dimensional, temperature and the time data were collected simultaneously throughout the course of the experiments.
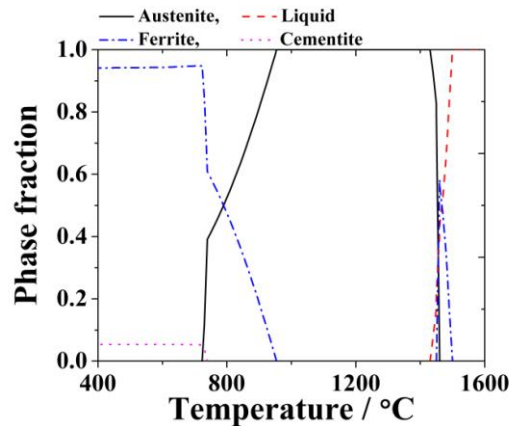
Fig.7.1: Evolution of phases in the steel discussed in Section 7.2 as a function of temperature

Cylindrical samples (8 mm diameter x 12 mm long) were used for heat treatment purpose. The samples were first heated to the intercritical temperature of 900 °C at a heating rate of 10 °C per second, held there for 15 minutes and then cooled to the isothermal bainite transformation temperature at a cooling rate of 5 °C per second using helium (He) gas as the quenching media. The applied cooling rate was sufficient to avoid the nose of diffusional transformation as can be seen from Fig. 7.2. After the isothermal transformation to bainite, the samples were cooled to room temperature and then the bake hardening experiments were carried out in a muffle type furnace at 170 °C for 20 minute with a temperature controller of ± 1°C accuracy. A schematic diagram of the heat

treatment cycle is presented in Fig. 7.3. The points "A" and "B"on the diagram indicate the start of the experiment at $t = t_0$ and the time at which isothermal bainitic transformation starts at $t = t_1$, respectively.
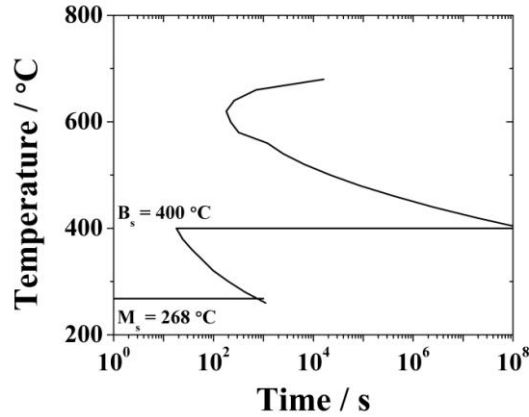
Fig.7.2: Calculated TTT diagram for the steel described in Section 7.2 considering the calculated austenite composition at 900 °C [MUCG 83]
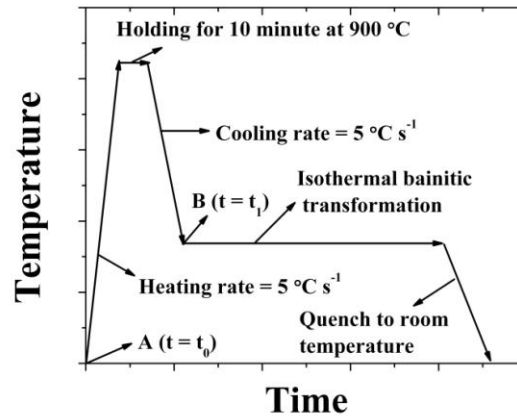
Fig.7.3: Schematic representation of the heat treatment schedule adopted in Section 7.4.1

From the TTT diagram in Fig. 7.2, it is expected that the bainitic and martensitic transformations in this steel would not start above 400 °C and 268 °C, respectively. Consequently, the isothermal treatment temperatures for bainitic transformation were chosen from 275 °C to 400 °C, at intervals of 25 °C. The holding time at each temperature except 275 °C was 120 minutes. Keeping in mind the fact that the kinetics becomes slow and sluggish at lower transformation temperature, higher holding time 360 minutes was used for the transformation temperature of 275°C.

7.4.2   Metallography

In order to examine and observe the microstructure of the samples, a Zeiss Optical Microscope was used. Quantification of different phases was carried out using an image analysis system named Axio-Vision analytical software (version 4). To cross examine the analysis, point count method was also used in some cases where a 30 x 31 grid was superimposed on the microstructure to estimate the phase fraction. The magnification of the photographs which were used for such phase analysis was intentionally kept low (typically 200X). This small magnification has been used to get a larger area under observation.

7.4.3   X-Ray Diffraction (XRD)

Knowledge of the lattice parameters of the phases and the amount of retained austenite is important in interpreting the results of dilatometric experiments. These experiments were carried out in a Philips PW 1730 X-ray diffractometer using unfiltered Cu $K\alpha_1$ radiation. Scanning was carried out with a 0.05^o step size and allowing 2 seconds for each step over a 2θ range from 35° to 145°. The machine was operated at 40 mA and 40 mV setting. The experiments were carried out on the samples which were intercritically annealed and isothermally transformed to bainite during the Thermec Master test following the thermal cycle given in Fig. 7.3. All the samples were metallographically polished to 1.0 μm finish with colloidal solution and finally etched in nital to remove any smeared surface.

The volume fraction and the lattice parameter of retained austenite were calculated from the X-ray data by Rietveld whole profile fitting method [Hill and Howard, 1987; McCusker *et al.,* 1999; Young, 2002] using commercially available X'Pert High Score Plus [X'Pert] software. The analysis was intended to utilise X'Pert High Score Plus to accurately fit the entire XRD pattern for microstructural characterisation of the constituent phases allowing the possibilities of different phases like austenite, ferrite and cementite to be there in the microstructure. A simulated diffraction pattern was obtained considering a series of parameters like unit cell, profile parameters (U, V and W), peak shape function *etc.* for each phase and background correction, zero shift *etc.* for the entire pattern. All the parameters were refined by iterative least-square procedure for the minimization of the difference between the

experimental and simulated profile [Hill and Howard, 1987]. The quality of the simulated profile fitting and the accuracy of the microstructural parameters (lattice parameters and volume fraction of different phases) were continuously monitored by evaluating various numerical "criteria of fit" parameters, namely, *weighted residual error* (R_{wp}), *expected error* (R_{exp}) and *goodness of fit* (GOF).

7.4.4　Three Dimensional Atom Probe (3-DAP)

Detailed microstructural characterization at nanoscale was done using Oxford nanoScience 3D atom probe at the Monash Centre for Electron Microscopy, Monash University, Australia. The pulse repetition rate was 20 kHz with the pulse fraction of 0.2. As the sample test temperature was 60 K (-213 °C), all the austenite retained after bainitic transformation was expected to be transformed to martensite at this temperature. Needle shaped atom probe samples were prepared using a standard two-stage electro-polishing procedure [Miller 2000]. 0.5 nm distance between the carbon atoms and 0.1 nm grid spacing was used to estimate the extent of solute enriched regions (radius of gyration) and the local solute concentrations in these regions [Miller 2000]. Only clusters containing 20 or more atoms were considered for analysis in order to minimise the error due to random solute fluctuations in the matrix. The composition of the matrix was determined based on the number of atoms present in the analysed volume. Care was taken to subtract the background noise.

7.4.5　Mechanical properties

Mechanical property was evaluated from hardness measurements after isothermal bainite treatment and also after the bake hardening treatment of each sample. Vickers hardness measurement was carried out with 30 kg load according to DIN EN ISO 6507-1 in Universal Hardness tester, Model UH3, supplied by Reicherter Stiefelmayer. The instrument was equipped with WINControl software to measure the hardness values.

7.5　Results and discussion

Figure 7.4 represents the results obtained from dilatometry experiments. The point "B" on Fig. 7.4 refers to the point "B" of Fig. 7.3 indicating the time of the start of the

isothermal treatment for bainitic transformation. The region where the dilatation curves become flat was considered as the cessation of the transformation for a particular temperature [Takahashi and Bhadeshia, 1989]. It is evident from Fig. 7.4 that the transformation at 275 °C reaches termination when it is held at that temperature for 360 minutes. The highest transformation temperature was kept at 400 °C only as the calculated B_s temperature of the austenite after forming 17% ferrite at the intercritical temperature was calculated to be 400 °C. Figure 7.4 shows that with increasing the transformation temperature, the amount of dilatation decreases indicating a lower volume fraction of bainite at higher temperature. However, dilatation data in only one direction cannot be correlated directly to the volume fraction of bainite in many cases [Bhadeshia *et al.,* 1991] and therefore these data were not analysed further to determine the fraction of bainite quantitatively.
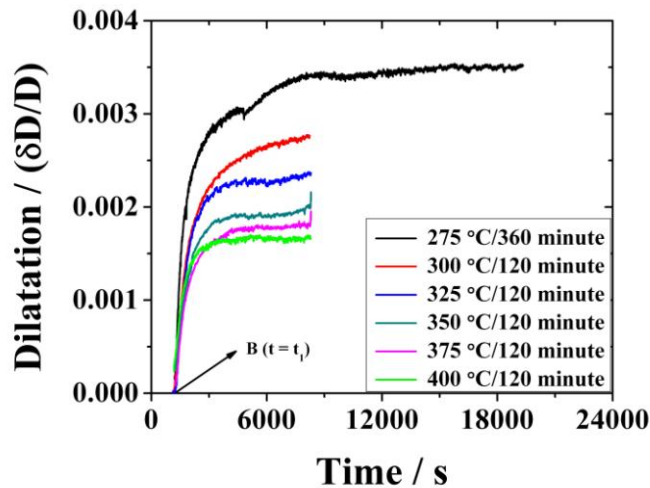
Fig.7.4: *Dilatation plots of Delta TRIP steel as discussed in Section 7.2. The figure represents isothermal transformation to bainite at different temperatures for different time periods*

The heat treated microstructures are shown in Fig. 7.5. Isothermal transformation in the temperature range of 275-400 °C led to the formation of bainite as illustrated in the optical micrographs presented in Fig. 7.5. Table 7.2 summarises the phase fractions obtained from image analysis of the heat treated samples. From the Table 7.2, it is evident that the amount of ferrite did not differ much from what was predicted using Thermo-Calc, and its variation can well be considered within the limits of experimental

error as both the multiphase analysis and point count methods are statistical tools and therefore can be associated with some error of measurement. The variation of hardness after the termination of transformation at each temperature is shown in Fig. 7.6.
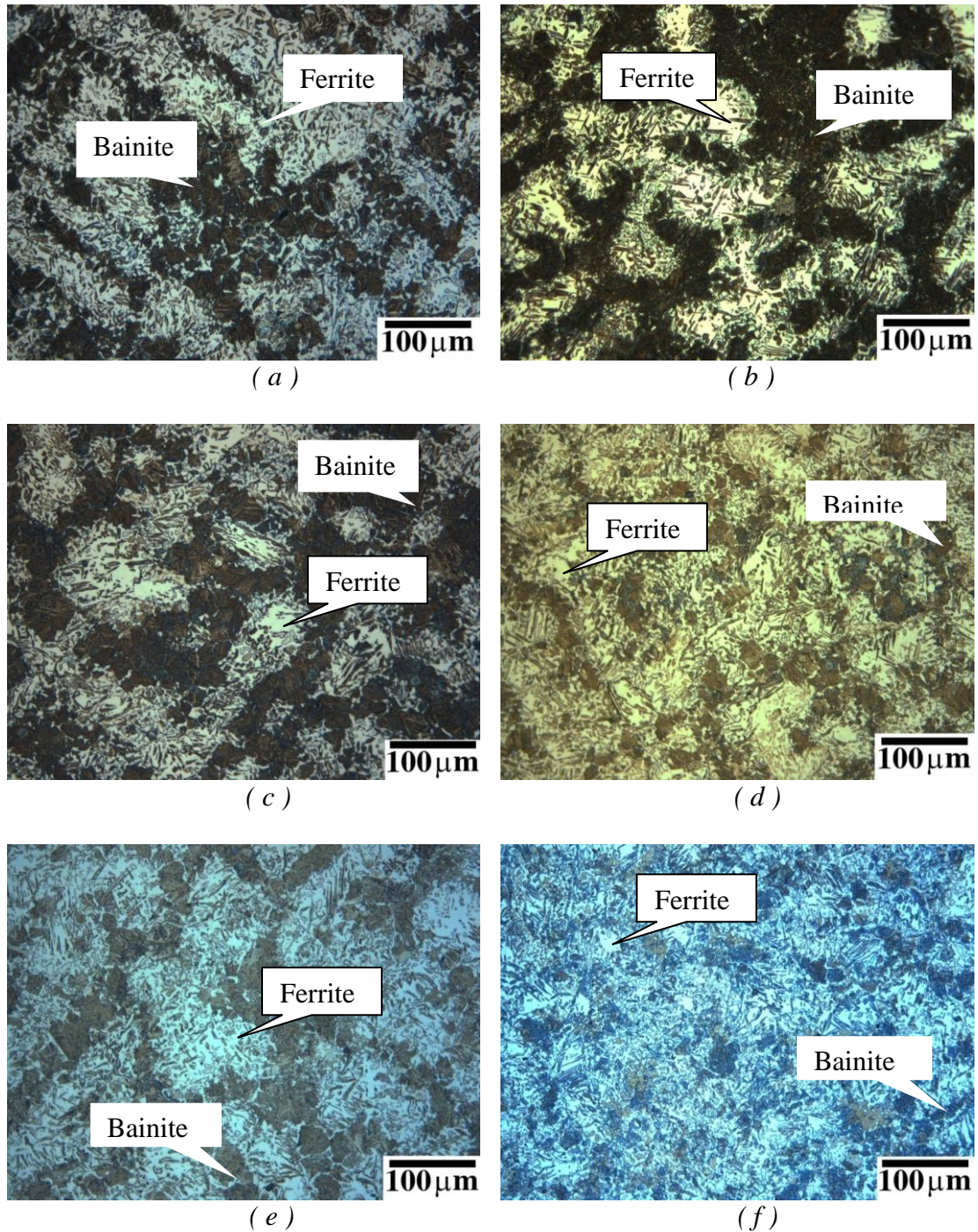
Fig. 7.5: *Optical microstructures of the Delta-TRIP steel specimens showing ferrite and bainite after the cessation of isothermal bainite transformations at different temperatures combination. a.275 °C, b. 300 °C, c. 325 °C, d. 350 °C, e.375 °C and f. 400 °C. Isothermal treatment time = 360 minute for a and 120 minute for b-f*

Table 7.2 Phase fraction from image analysis of optical microstructures. All the samples were intercritically annealed at 900 ^{o}C before isothermal transformation to bainite at indicated temperatures

Sample details	Volume fractions of phases		
	Bainite (%)	Ferrite (%)	Austenite (%)
275 °C / 360 minutes	80.5 ± 3.5	18.6 ± 2.3	1.2 ± 1.3
300 °C / 120minutes	70.9 ± 1.6	19.9 ± 2.1	8.4 ± 0.9
325 °C / 120 minutes	72.7 ± ± 2.8	17.8 ± 2.1	8.7 ± 1.7
350 °C / 120 minutes	69.3 ± 0.2	16.8 ± 0.9	10.7 ± 0.9
375 °C / 120 minutes	70.3 ± 3.6	17.4 ± 1.8	10.7 ± 1.0
400 °C / 120 minutes	78.2 ± 3.5	18.6 ± 3.4	3.1 ± 3

Enrichment of austenite with carbon atoms is the consequence of the formation of carbide-free bainite [Bhadeshia and Waugh, 1982; Garcia-Mateo *et al.,* 2003; Caballero *et al.,* 2002; Mukherjee *et al.,* 2008]. However, other substitutional solute concentration remains unaltered from that during the transformation. Three Dimensional Atom Probe (3-DAP) analysis was carried out to estimate the exact elemental compositions of austenite and ferrite in the sample transformed at 275 °C for 360 minute. The results obtained from 3-DAP experiments are summarised in Table 7.3 along with the results of Thermo-Calc calculations for the phase composition at the intercritically annealing temperature. As the results from 3-DAP experiments are normally expressed in at%, these were converted to corresponding wt% for a better comparison with the Thermo-Calc predictions. In general, the calculated values of each substitutional element in different phases match very well with those measured using atom probe. Nevertheless, it has to be mentioned here that the atom probe experiments are limited to an extremely small area where a minute change in the number of atoms can greatly influence the final values. The small differences between the calculated values and experimentally measured values can well be considered within the limits of experimental variation.

Some selected atom maps with corresponding concentration profiles are shown in Fig. 7.7 and Fig. 7.8, respectively. It is clear that the distribution of C atoms in the analysed volume is not uniform. The concentration profiles, taken at 0.15 nm step size, show enriched and depleted solute regions, which have layered arrangement as visible in

the atom maps (Fig. 7.8). Similar kind of segregation of carbon atoms was also observed by other researchers in the retained austenite of TRIP and bainitic steels after bake hardening or tempering [Caballero *et al.,* 2002; Pereloma *et al.,* 2007; Pereloma *et al.,* 2008a]. It has been speculated that carbon segregates to the regions where microtwins are present in retained austenite [Pereloma *et al.,* 2007; Pereloma *et al.,* 2008a; Pereloma *et al.,* 2008b]. It was calculated from these experiments that the retained austenite contains about 5.252 ± 0.06 at% (1.23 ± 0.007 wt%) of C. In case of Mn and Si atoms, some minute segregation was observed both from the atom map and concentration profile.
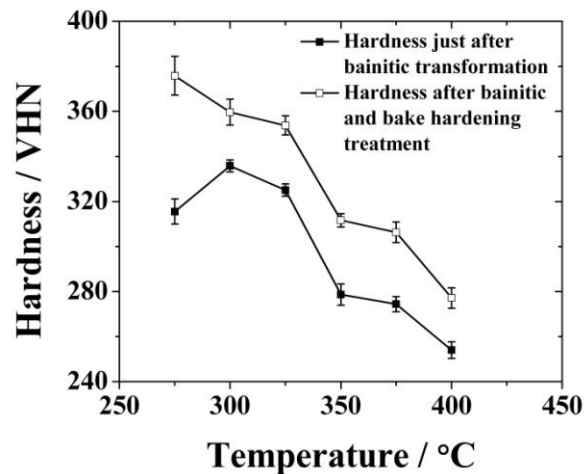
Fig.7.6: Hardness variation in Delta-TRIP steel as the function of isothermal transformation temperature

Since the XRD data were analysed following Rietveld refinement method which uses a full pattern-fitting algorithm, all the lines of each phase are explicitly taken into account. Figure 7.9*a* represents a typical XRD plot where the actual experimental results are plotted as black points, the simulated profile is plotted as continuous red line and the difference between these two (experimental and simulated profiles) is plotted as the black line and Fig. 7.9*b* shows the XRD plot for all the cases. Figure 7.9*a* shows an excellent match between the actual experimental result and the simulated profile using Rietveld refinement. Figure 7.10 represents the amount of retained austenite for each condition at the end of the transformations. The amount of retained austenite was calculated from the peak intensity of the simulated profile obtained by Rietveld refinement. The graph also shows that with increasing the transformation temperature, the amount of austenite which

remains untransformed at the corresponding temperature increases in general indicating a lesser degree of transformation. These results are consistent with the dilatation and hardness measurement results (Fig. 7.4 and 7.6). The decrease in the amount of retained austenite at higher holding temperature may be due to the formation of small amount of martensite. At higher bainitic transformation temperature, due to the formation of lower amount of bainite, austenite might not have been sufficiently enriched with carbon so that its corresponding martensite start (M_s) temperature is not suppressed below the room temperature; consequently, martensitic transformation might have occurred in this case.

Table 7.3   Comparison between the 3-DAP results with Thermo-Calc predictions. The Thermo-Calc calculations were carried out at the austenitisation temperature (900 °C) using TCFE-6 database and the 3-DAP experiments were carried out at cryogenic temperature (-213 °C).

Phase	Method	Elements		
		Si	Mn	Al
Austenite	3DAP (at%)	1.78 ± 0.03	1.94 ± 0.04	5.82 ± 0.06
	3DAP (wt%)	0.97 ± 0.01	2.07 ± 0.02	3.06 ± 0.02
	Thermo-Calc (wt%)	0.72	2.17	2.11
Ferrite	3DAP (at%)	1.54 ± 0.02	1.23 ± 0.01	4.81 ± 0.03
	3DAP (wt%)	0.79 ± 0.01	1.243 ± 0.01	2.39 ± 0.01
	Thermo-Calc (wt%)	0.76	1.16	2.65

The lattice parameter of austenite was also calculated using Rietveld refinement and the corresponding lattice parameters of austenite, for all the isothermal bainite transformation conditions, are plotted in Fig. 7.11. As the concentration of substitutional alloying elements (*e.g.* Mn, Si, Cr *etc*) in austenite does not change with bainite transformation and only carbon enrichment of austenite can occur as a result of isothermal bainitic transformation, the increment of lattice parameter observed in Fig. 7.11 can be considered as an effect of C enrichment only. Such an enrichment of austenite with C is governed by the *incomplete reaction mechanism* described elsewhere [Bhadeshia and Waugh, 1982].
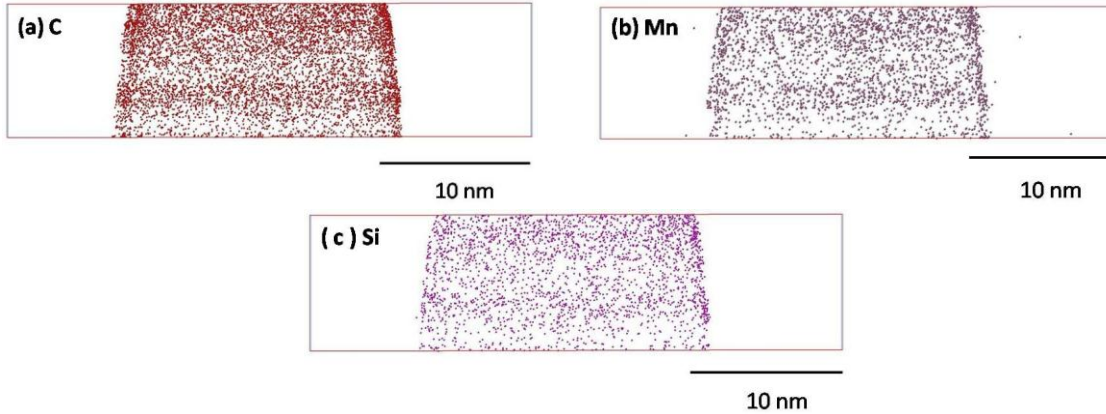
Fig.7.7: *Atom maps showing distribution of alloying elements in austenite in Delta-TRIP steel after 360 minutes holding at 275 °C. (a) C atom map, (b) Mn atom map and (c) Si atom map*
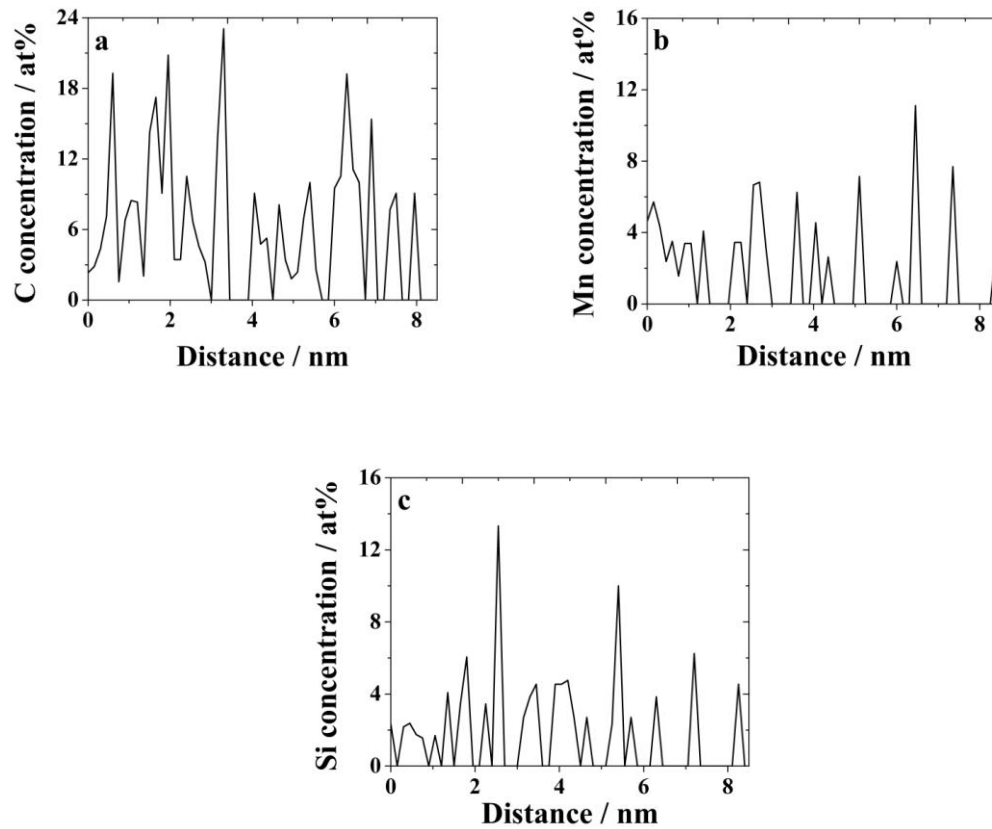
Fig.7.8*: Concentration profiles of different elements along the blue line of the boxes shown in corresponding atom maps in Fig. 7.7. (a) Carbon, (b) Mn and (c) Si.*

The locus of all the points where the austenite and ferrite of identical composition have the same free energy is called the T_o line on wt% C *vs.* temperature plot [Bhadeshia, 2001]. According to Bhadeshia and Edmonds [1983], this condition is equivalent to

stating that the carbon content of the residual austenite left untransformed after the cessation of bainitic transformation cannot not exceed the T_0 line on the phase diagram and diffusionless growth of this kind can only occur if the carbon concentration of the residual austenite is below that given by the T_0 curve [Bhadeshia, 2001]. The room temperature (298 K) lattice parameter of austenite (in nm) can be estimated using the following equation [Bhadeshia *et al.,* 1991; Dyson and Holmes, 1970].

$$a_{0,\gamma} \;=\; 0.3573 + 0.33w_C^\gamma + 0.0095w_{Mn}^\gamma + 0.056w_{Al}^\gamma + 0.015w_{Cu}^\gamma \;………..……….\,…7.1$$

where w_i^γ is the weight percent (wt%) of solute "i" in solution in γ. During calculation with equation 7.1, due to the paraequilibrium constraint, the amount of each substitutional element in austenite at the corresponding intercritical temperature (*i.e.* 900 °C) as predicted by Thermo-Calc was considered for w_i^γ. Using the equation 7.1, the amount of carbon in austenite that was left untransformed after the formation of bainite was calculated and the result is presented in Fig. 7.12 along with the T_o line computed using Thermo-Calc with TCFE-6 database. From this figure, it is evident that at higher transformation temperature, experimental data follow the T_0 line. However, at lower transformation temperatures, the actual carbon in austenite is less than the T_0 line possibly because more carbon is trapped in bainite. It is worth mentioning here that 3-DAP experiments also revealed same amount of carbon (1.23 ± 0.007 wt%) in austenite as was determined from XRD analysis (1.27 ± 0.07). Previous researchers also found similar trend in their experiments [Caballero *et al.,* 2007; Bhadeshia and Waugh., 1982; Garcia-Mateo *et al.,* 2003; Caballero *et al.,* 2002].

The present work deals with a steel containing high amount of Al which has got certain unique features including very low solubility in cementite and acceleration of the bainite formation [De Cooman, 2004]. Thus, bainite forming due to the isothermal treatment is expected to be carbide-free. Consequently, the microstructure consists of only three phases, namely ferrite, bainite and retained austenite. As the austenite carbon concentration is now measured, it is possible to calculate the amount of carbon which is trapped in the bainitic ferrite by simple mass balance equations 7.2 and 7.3.

$$C_{Total} \quad = \quad W_\alpha\,C_\alpha \; + W_\gamma\,C_\gamma \; + \; W_{bainite}\,C_{bainite} \quad \ldots\ldots\ldots\ldots\ldots\ldots\ldots\ldots\ldots\ldots\ldots\ldots\ldots\ldots\ldots 7.2$$

$$\text{and } W_\alpha + W_\gamma + W_{bainite} \quad = \quad 1 \quad \ldots\ldots\ldots\ldots\ldots\ldots\ldots\ldots\ldots\ldots\ldots\ldots\ldots\ldots\ldots\ldots\ldots 7.3$$

where W_i represents the weight fraction of each constituent phase and C_i symbolises the amount of carbon in each of these phases. The symbols "α" and "γ" stand for ferrite and austenite, respectively. In the analysis, the values obtained from XRD analysis were used for the amount of retained austenite (W_γ) and its carbon content (C_γ). The amount of ferrite obtained from image analysis matches quite well with thermodynamic prediction. Thus, the value obtained using Thermo-Calc was used for the amount of ferrite (W_α). The amount of C in ferrite (C_α) was taken as 0.00104 as was realised from 3-DAP. Since W_α and W_γ are known, $W_{bainite}$ can be calculated using equation 7.2. The results obtained using equation 7.2 and 7.3 are summarised in Table 7.4. These results are in agreement with the previous reports that the carbon content of bainite is much larger than the solubility limit of C in ferrite [Caballero *et al.,* 2007; Bhadeshia and Waugh, 1982; Garcia-Mateo *et al.,* 2003; Caballero *et al.,* 2002; Mukherjee *et al.,* 2008].
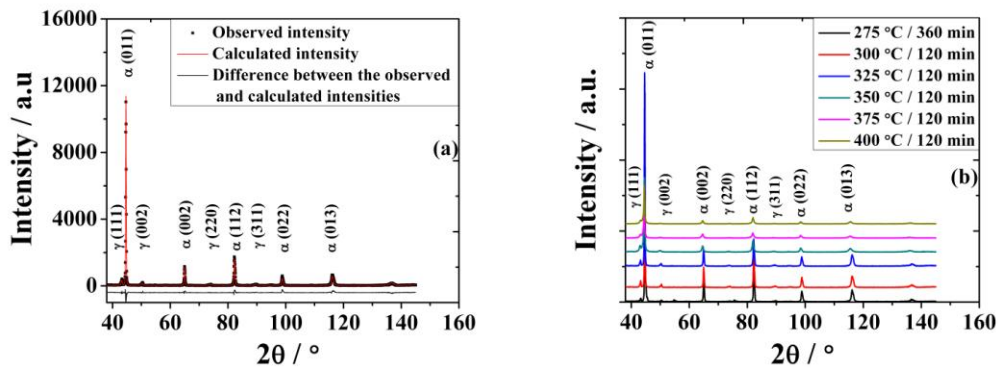
Fig.7.9: Analysis of XRD results of Delta-TRIP steel after bainitic transformation. (a) Comparision between the simulated profile using Rietveld refinement with experimentally obtained XRD result and (b) XRD profile for all the experimental cases

Bainite transformation results in a high dislocation density because the transformation is displacive [Bhadeshia, 2001]. Bhadeshia [2001] has proposed a relationship between the density of dislocations (ρ_d) generated due to bainitic transformation and the temperature

of the transformation. Using this relationship, the dislocation density (ρ_d) at each transformation temperature was calculated and the results are presented in Fig. 7.13. Berbenni *et al.* [2004] have modeled the dislocation density (ρ_d) for a prestrain range of 1-10%. From their work, the maximum ρ_d calculated for a prestrain of 10% was around 1×10^{14} m^{-2} which is significantly less than that expected from bainitic transformation as depicted in Fig. 7.13.
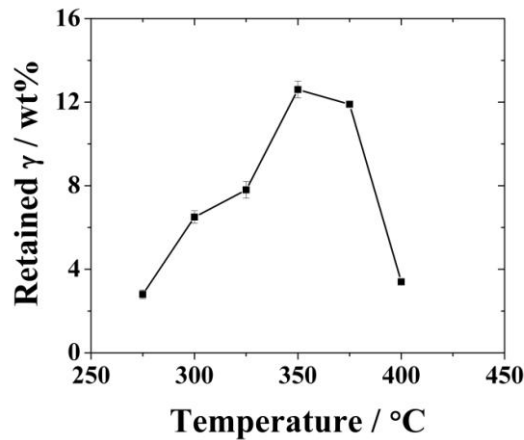
Fig.7.10: *Variation in the amount of austenite in Delta-TRIP steel after the cessation of bainitic transformation measured by XRD technique*
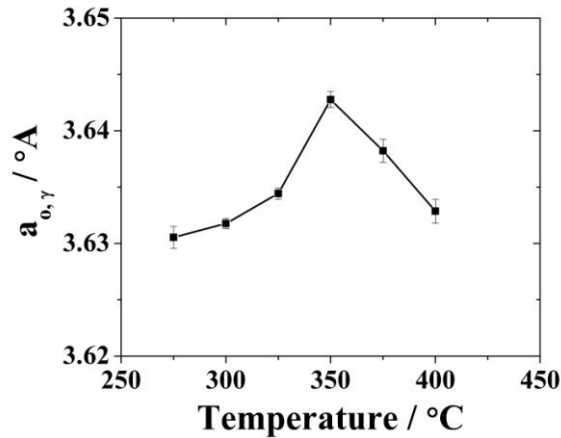
Fig.7.11: *Lattice parameters of retained austenite of Delta-TRIP steel after the cessation of bainite transformation as measured by the XRD technique*

It is evident from the above discussion that after the cessation of bainitic transformation, there will be sufficiently high density of newly generated dislocations which could be pinned down by the C atoms present in the bainitic region under suitable conditions.

Temperature increase during the paint baking stage could provide such a favourable situation where the C atoms can migrate to the dislocation to lock them up and this would result in an increase in strength or hardness.
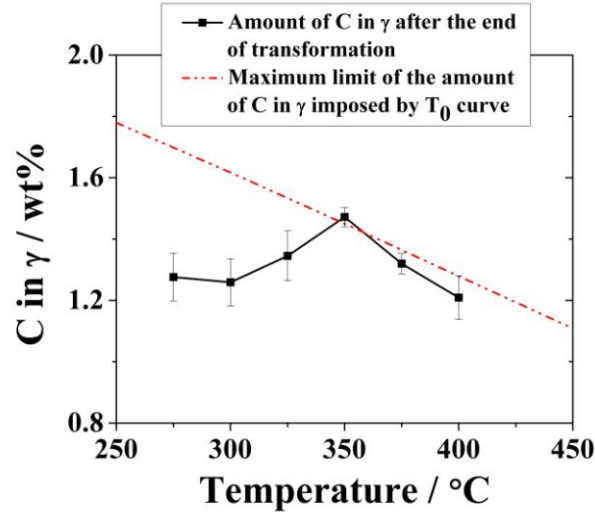
Fig.7.12: *Amount of C in retained austenite in Delta-TRIP steel as calculated from the measured austenite lattice parameter (Fig. 7.11) and equation 7.1 and the T_o calculated using Thermo-Calc is also shown after the cessation of bainitic transformation along with calculated T_0*

Table 7.4 Amount of C in bainite after the cessation of transformation at each temperature. The amount of ferrite (α / %) was calculated using Thermo-Calc software at 900 C using TCFE-6 database. Amount of C in ferrite (C_α / wt%) was realised from 3-DAP experiments. The amounts of austenite (γ / %) and C in austenite (C_γ / wt%) were calculated from XRD data. Amounts of bainite (Bainite / %) and C in bainite ($C_{Bainite}$ / wt%) was obtained from mass balance, equation 7.2 and 7.3.

Treatment temperature / ^{o}C	C_{Total} / wt% (Bulk)	α / % (Thermo -Calc)	C_α / wt% (3-DAP)	γ / % (XRD)	C_γ / wt% (XRD)	Bainite / % (Mass balance)	$C_{Bainite}$ / wt% (Mass balance)
275	0.36	18.34	0.0014	4.1	1.2418	77.5	**0.3981**
300	0.36	18.34	0.0014	8.4	1.2801	73.2	**0.3442**
325	0.36	18.34	0.0014	8.1	1.3736	73.5	**0.3377**
350	0.36	18.34	0.0014	12	1.5931	69.6	**0.2419**
375	0.36	18.34	0.0014	7.9	1.4507	73.7	**0.3323**
400	0.36	18.34	0.0014	7.5	1.3113	74.1	**0.3524**

In order to investigate such a possibility, the samples were treated at 170° C in a muffle furnace for 20 minutes after the cessation of bainitic transformation and then air cooled.

Immediately after this, the bulk hardness was measured for each of the samples and the results are plotted in Fig. 7.6 to compare the increment in hardness due to the baking treatment. The plot reveals that in every instance, the hardness values have increased from those obtained after the isothermal bainite transformation. The increase in hardness due to such bake hardening treatment after the isothermal bainitic transformation is shown in Table 7.5 alongwith the calculated dislocation density at each transformation temperature and the amount of C in bainite. Samek *et al* [2008] have argued that during the baking of TRIP-aided steel, C atoms from bainite can reach a dislocation due to short diffusion distance as the bainite contains a high amount of carbon. The dislocations, according to them, can therefore be easily pinned during low-temperature aging (as experienced during paint baking treatment), resulting in a high BH_0 (*i.e.* bake hardening at zero prestrain) value. Detailed investigation on the inter-relationship among these parameters (dislocation density, amount of C in solution and the bake hardening response, BH_0) could be an interesting topic for future research.
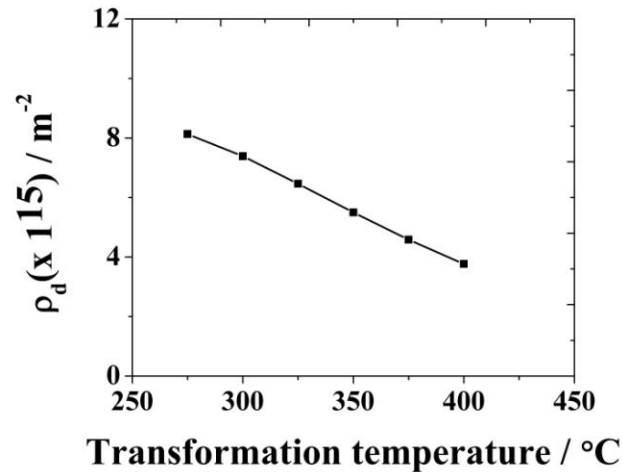
Fig.7.13: *Calculated dislocation density (ρ_d) in Delta-TRIP steel as a function of bainite transformation temperature [Bhadeshia, 2001]*

It is worth mentioning here that in the previous chapters (Chapters 5 and 6) as well as Das *et al* [2008, 2011] have previously argued that a larger prestrain would leave more free dislocations which are not pinned by the carbon atoms and hence a diminished bake hardening response could be observed. It has to be mentioned here that in those cases the amount of free solute carbon was extremely small (only a few ppm) [Das *et al.,* 2008;

Das *et al.,* 2011] which might not be able to lock all the dislocations produced by higher prestrain [Das *et al* 2008, Das *et al* 2011]. In the current study, however, the amount of C in bainite is quite high (~ 0.24 – 0.40 wt%), therefore, the bake hardening effect is also high because of combination of high dislocation density and high amount of carbon in bainite.

Table 7.5 Bake hardening results along with dislocation density and C in bainite

Transformation temperature / ^{o}C	C in bainite / wt%	Dislocation density / x 10^{15} m^{-2}	Bake hardening / MPa
275	0.3981	8.1324	60 ± 3.0
300	0.3442	7.38742	24 ± 3.1
325	0.3377	6.46304	29 ± 1.5
350	0.2419	5.4993	33 ± 1.7
375	0.3323	4.58524	32 ± 1.3
400	0.3524	3.76801	23 ± 0.8

7.6   Conclusion

A detailed study on the kinetics of bainitic transformation and its effect on the subsequent bake hardening event in TRIP-assisted steel was carried out. The resultant microstructures were characterised by several techniques and compared with the theoretical understanding. The following results can be summarised from the above discussion.

i.   Bainitic transformation in TRIP-assisted steel can lead to a very good bake hardening response. Such a high bake hardening response can be attributed to the occurrence of large number of dislocations generated due to the bainite transformation and the presence of high amount of carbon in bainitic ferrite.

ii. Calculation of the amount of carbon present in bainite was based on the experimental findings obtained utilizing XRD and 3-DAP. It was confirmed that the carbon content of bainite is greater than the equilibrium concentration.

However, dislocation density was calculated exploiting the theory of bainitic transformation only.

iii. Migration of these higher than equilibrium amount of C atoms to the dislocation sites under the thermal condition prevailing during aging condition led to a strong BH effect.

iv. The novelty of the work is that here no extra prestraining was needed; dislocations were generated *in-situ* during the transformation itself. It can be observed that high degree of BH response can be obtained in this way.

Chapter 8

Summary, Conclusion and Future Work

Chapter 8

Summary, Conclusion and Future Work

8.1 Summary and major findings

The work presented in this thesis deals with the bake hardening phenomena observed in automotive grade steels during paint baking process. Bake hardening is essentially a strain aging process where the increase in strength during BH ($\Delta\sigma_{BH}$) occurs in two stages, namely Cottrell atmosphere formation and subsequent precipitation of fine carbides. Experimental schemes were designed to observe different aspects of bake hardening phenomena in some of these grades of steels. In order to understand the bake hardening process in a better way, a theoretical model has been developed which can differentiate the individual contributions of Cottrell atmosphere and precipitate formation. Two neural network models were also developed in order to study the effect of various controlling parameters on the measured BH response. In another attempt, BH response was studied without providing any additional prestrain after isothermal bainitic transformation in a novel TRIP-assisted steel. Major findings of the entire work are summarised below.

1. One theoretical and two neural network models were developed to understand the BH phenomena. The models were used to predict the BH response of a number of steels. The model predictions were in close agreement with the actual experimental values. The models were also used to rationalize divergent results reported in literature.

2. The theoretical model described in Chapter 4 can form the basis of understanding the bake hardening phenomena. With the help of this model, it is possible to quantify the individual contribution of Cottrell atmosphere and subsequent precipitate formation to the final BH response.

3. It was observed that Cottrell atmosphere formation has greater effect than the subsequent precipitate formation on the final BH response and kinetics of Cottrell atmosphere formation is much faster than that of precipitation.

4. Effect of free solute carbon on the BH response was investigated. It was found out that increasing amount of free carbon improves the BH property significantly. However, the effect of increasing the total carbon content was not very clear. It can be concluded that free carbon is more important than the total carbon content of the steel in controlling the BH process and steel composition should be designed in such a way that optimum amount of free carbon is available for better BH response.

5. The aging condition is best represented by the parameter Dt (where D is the diffusion co-efficient of carbon atoms in α-iron and t is the aging time in second). Result of increasing Dt on the corresponding BH response was studied in detail. It was observed that major part of BH response can be obtained within a very short Dt range.

6. It was found that higher amount of Mn deteriorates the BH response whereas P enhances it. These observations can help in designing the steel composition intended to show better BH response.

7. Investigations on the effect of prestrain indicate that higher prestraining may lead to decrease the BH response. However, if adequate aging condition (temperature and time) is provided, this deterioration in BH response can be prevented.

8. Addition of microalloying elements like Nb, Ti is detrimental for good BH response. This may due to be the fact that they consume carbon atoms to form carbides or other precipitates which in turn reduces the amount of free carbon.

9. It was observed from the current study that higher annealing temperatures improve the BH response. Thus, annealing treatment should be carried out at the highest possible temperatures in order to maximise the BH effect.

10. Prestrain is not needed in TRIP-assisted steel with carbide-free bainite microstructure to achieve a good BH response. Bainite transformation generates large amount of dislocations which can be locked during subsequent aging treatment by migration of carbon atoms trapped inside bainite.

11. Compared with BH or EDD grades of steels, DP steel shows a significantly higher temperature at which its BH response becomes saturated during the baking operation. This may be attributed to the higher carbon content of DP steel.

12. The BH effect can be induced in IF steel by increasing the annealing temperature. It is believed that it may due to be the fact that at higher annealing temperatures, carbon atoms which were previously residing in grain boundary regions in the fine grain material may be pushed inside the grains due to grain coarsening during annealing and thus they contribute to the BH response.

8.2 Suggested future work

There are some limitations in the current work as well. These limitations may form the basis of the future research work in this exciting field which has the potential of direct industrial application. Some of the most important areas that require further study in this subject are listed below:

1. Cooling rate after annealing operation can greatly affect the concentration of carbon atoms in ferrite. However, the available data mentioning the cooling rate is very sparse.

2. In all BH related experiments, 2% prestrain is normally given in tension. However, during actual forming, the straining may well be in any direction, including even compression. Thus, effect of strain path on BH response may be an exciting topic to study.

3. The theoretical model developed in Chapter 4 in the current study did not take into account tempering of bainite and/or martensite which are present in DP and TRIP steel. However, the temperature at which BH experiments are carried out can have the potential to temper such hard microstructural constituents. Consequently, the model described in Chapter 4 may over-predict the BH response for such steels. Thus, developing a new model incorporating the tempering effect would make the current model much more general.

4. Effect of P on the final BH response can be an interesting subject to study.

5. Investigating the interrelationship between dislocation density, amount of carbon in solution and bake hardening response

References

References

Abe and Suzuki, 1980	H. Abe and T. Suzuki; *Trans. ISIJ,* Vol. 20, 1980, pp. 691
Abe *et al.,* 1984	Hideo Abe, Takeshi Suzuku and Kentaro Tobimatsu; *Trans. Of Japan Institute of Metals,* Vol. 25, 1984, pp. 458 – 466,
AHSS, 2006	Advanced High Strength Steel Application Guidelines, Version 3, Committee on Automotive Application, International Iron and Steel Institute, September 2006, www.ulsab-avc.org
Al-Shalfan, 2001	W. Al-Shalfan; *Ph.D Thesis*, Colorado School of Mines, Golden, Colorado, USA, 2001
Al-Shalfan *et al.,* 2006	W. Alshalfan, J. G. Speer, K. Findley and D. K. Matlock; *Metallurgical and Materials Transactions A,* Vol. 37A, 2006, pp 207 – 216
ASTM E8	*Standard Test Methods for Tension Testing of Metallic Materials,* Designation: E 8M-03, ASTM International, PA, USA
Baker *et al.,* 2002 a	L. J. Baker, S. R. Daniel and J. D. Parker; *Materials Science and Technology,* Vol. 18, 2002, pp. 355 – 367
Baker *et al.,* 2002 b	L. J. Baker, J. D. Parker and S.R.Daniel; *Materials Science and Technology,* Vol. 18, 2002, pp. 541 - 547
Barnett, 1971	D. M. Barnett; *Scripta Metallurgica,* Vol. 5, 1971, pp. 261 – 266
Benkirat *et a.,l* 1988	D. Benkirat, P. Merle and R. Borrelly; *Acta Metallurgica.*, Vol. 36, 1988, pp. 613
Berbenni, 2009	S. Berbenni; *Personal communication through E-Mail*, 18.02.2009
Berbenni *et al.,* 2004	S. Berbenni, V. Favier, X. Lemoine and M. Berveiller; *Scripta Materialia*, Vol. 51, 2004, pp. 303 – 308
Bhadeshia and Edmonds, 1983	H. K. D. H. Bhadeshia and D. V. Edmonds; *Metal Science,* Vol. 17, 1983, pp. 411 - 419
Bhadeshia *et al.,* 1991	H. K. D. H. Bhadeshia, S. A. David, J. M. Vitek and R. W. Reed; *Materials Science and Technology,* Vol. 7, 1991, pp. 686 - 698
Bhadeshia, 1999	H. K. D. H. Bhadeshia; *ISIJ International,* Vol. 39, 1999, pp. 966 - 979
Bhadeshia, 2001	H. K. D. H. Bhadeshia; *Bainite in Steels*, 2nd edition, 2001, IOM Communication, The Institute of Materials, London, SW1Y 3DB

Bhadeshia and Charistian, 1990	H. K. D. H. Bhadeshia and J. W. Christian; *Metallurgical Transactions A*, Vol. 21 A, 1990, pp. 767 – 797
Bhadeshia and Honeycombe, 2006	H. K. D. H. Bhadeshia and R. W. K. Honeycombe; *Steels: Microstructure and Properties*, 3rd edition, Butterworth-Heinemann, Oxford, UK, 2006.
Bhadeshia and Waugh,1982	H. K. D. H. Bhadeshia and A. R. Waugh; *Acta Metallurgica,* Vol. 30, 1982, pp. 775 – 784
Bhadeshia *et al.,* 2009	H. K. D. H. Bhadeshia, R. C. Dimitriu, S. Forsik, J. H. Pak and J. H. Ryu; *Materials Science and Technology,* Vol. 25, 2009, pp. 504 - 510
Bhattacharya, 2009	B. Bhattacharya; *Physical Metallurgy of Interstitial Free Steel: A Monograph*, Tata Steel Limited, 2009
Bleck and Brühl, 2008	W. Bleck and S. Brühl; in "*New Developments on Metallurgy and Applications of High Strength Steels*", Buenos Aires, 2008, edited by T. Perez, Argentina
Borrelly and Benkirat, 1985	R. Borrelly and D. Benkirat; *Acta Metallurgica,* Vol. 33, 1985, pp. 855
Bullough and Newman, 1959	R. Bullough and R. C. Bullough; *Proceedings of the Royal Society of London: Series A,* Vol. 249, 1959, pp. 427 - 440
Caballero *et al.,* 2002	F. G. Caballero, H. K. D. H. Bhadeshia, K. J. A. Mawella, D. G. Jones and P. Brown; *Materials Science and Technology,* Vol. 18, 2002, pp. 279 – 284
Caballero *et al.,* 2004	F. G. Caballero, C. Capdevila, L. F. Alvarez and C. G. de Andres; *Scripta Materialia,* Vol. 50, 2004, pp. 1061 – 1066
Caballero *et al.,* 2007	F. G. Caballero, M. K. Miller, S. S. Babu and C. Garcia-Mateo; *Acta Materialia,* Vol. 55, 2007, pp. 381 – 390
Cahn, 1957	J. W. Cahn; *Acta Metallurgica,* Vol.5, 1957, pp. 169 – 172
Carabajar *et al*., 2000	S. Carabajar, J. Merlin, V. Massardier, S. Chabanet; *Materials Science and Engineering A,* Vol. 281, 2000, pp. 132
Chatterjee, 2006	S. Chatterjee; *Ph.D. thesis,* University of Cambridge, Cambridge, UK, 2006
Chatterjee *et al.,* 2007	Sourabh Chatterjee, M. Murugunanth and H. K. D. H. Bhadeshia; *Materials Science and Technology*, Vol. 23, 2007, pp.
Cocks, 1969	U. F. Cocks; *A Statistical Theory of Alloy Hardening* in "Physics of Strength and Plasticity", edited by Ali S. Argon, The M. I. T. Press, Massachusetts, USA, 1969
Conrad, 1964	H. Conrad; *Journal of Metals,* July-1964, 1964, pp. 582 - 588

Cottrell, 1948	A.H. Cottrell; *Report of a Conference on Strength of Solids,* Physical Society, London, 1948, pp. 30 – 38
Cottrell, 1963	A. H. Cottrell; *Dislocations and Plastic Flow in Crystals,* Oxford University Press, London EC4, 1963
Cottrell and Bilby, 1949	A. H. Cottrell and B. A. Bilby; *Proceedings of Physical Society A,* Vol. 62, 1949, pp. 49 – 62
Cuddy and Leslie, 1972	L. J. Cuddy and W. C. Leslie; *Acta Metallurgica*, Vol. 20, 1972, pp. 1157-1167
Das *et al.,* 2008	S. Das, S. B. Singh, O. N. Mohanty and H. K. D. H. Bhadeshia; *Materials Science and Technology,* Vol. 24, 2008, pp. 107 – 111
Das *et al.,* 2011	S. Das, S. B. Singh and O. N. Mohanty; *Ironmaking and Steelmaking,* Vol. 38, 2011, pp. 139 - 143
De *et al.,* 1999	A. K. De, S. Vandeputte and B. C. De Cooman; *Scripta Materialia,* Vol. 41, 1999, pp. 831 - 837
De *et al.,* 2000	A. K. De, K. De Blauwe, S. Vandeputte and B. C. De Cooman; *Journal of Alloys and Compounds*, Vol. 310, 2000, pp. 405 - 410
De *et al.,* 2001	A. K. De, S. Vandeputte and B. C. De Cooman; *Scripta Materialia*, Vol. 44, 2001, pp. 695 - 7
De *et al.,* 2004	A. K. De, S. Vandeputte, B. Soenen and B. C. De Cooman; *Z. Metallkunde*, Vol. 95, 2004, pp. 713 – 71
De Cooman, 2004	B. C. De Cooman; *Current Opinion in Solid State and Materials Science,* Vol. 8, 2004, pp. 285 - 303
De Meyer *et al.,* 2000	M. De Meyer, K. De Wit and B. C. De Cooman; *Steel Research*, Vol. 71, 2000, pp. 511 - 518
Dehghani and Jonas, 2000	K. Dehghani and J. J. Jonas; *Metallurgical and Materials Transactions A,* Vol. 31A, 2000, pp. 1375 – 1384
Dollins, 1970	C. C. Dollins; *Acta Metallurgica,* Vol. 18, 1970, pp. 1209 – 1215
Edmonds and Speer, 2010	D. V. Edmonds and J. G. Speer; *Materials Science and Technology,* Vol. 26, 2010, pp. 386 - 391
Eloot *et al.,* 1998	K. Eloot, K. Okuda, K. Sakata and T. Obara; *ISIJ International,* Vol. 38, 1998, pp. 602 – 609
Elsen, 1993	P. Elsen; *Ph.D Thesis,* RWTH Aachen, 1993
Elsen and Hougardy, 1993	P. Elsen and H. P. Hougardy; *Steel Research*, Vol. 64, 1993, pp. 431 – 436
Farias, 2006	D. Farias; *Master's Thesis Report,* Technische Universiteit Eindhoven, 2006
Ferrer *et al.,* 2007	J. P. Ferrer, T. De Cook, C. Capdevila, F. G. Caballero and C. G. de Andres; *Acta Materialia*, Vol. 55, 2007, pp. 2075 – 2083

Fuji *et al.,* 1996	H. Fuji, H.K.D.H. Bhadeshia, D.J.C. Mackay; *ISIJ International,* Vol. 36, 1996, pp. 1373 - 1382.
Garcia-Mateo *et al.,* 2003	C. Garcia-Mateo, F. G. Caballero and H. K. D. H. Bhadeshia; *Journal de Physique IV,* Vol. 112, 2003, pp. 285 – 288
Gladman, 1997	T. Gladman; *The Physical Metallurgy of Microalloyed Steels*, The Institute of Materials, London, 1997
Gladman, 1999	T. Gladman; *Materials Science and Technology*, Vol.15, 1999, pp. 30 – 36
Hanai *et al.,* 1984	S. Hanai, N. Takemoto, Y. Tokunaga and Y. Mizuyama; *Trans ISIJ*, Vol. 24, 1984, pp. 17 - 23.
Harper, 1951	S. Harper; *Physical Review,* Vol. 83, 1951, pp. 709 - 712
Hartley, 1966	S. Hartley, *Acta Metallurgica*, Vol.14, 1966, pp. 1237-1246
Hill and Howard, 1987	R. J. Hill and C. J. Howard; *Journal of Applied Crystallography*, Vol. 20, 1987, pp. 467-474
Hoile, 2000	S. Hoile; *Materials Science and Technology,* Vol. 16, 2000, pp. 1079 – 1093
Honeycombe, 1984	R. W. K. Honeycombe; *The plastic deformation of Metals*, Edward Arnold, London, 2nd edition, 1984, pp. 293
Hutchinson *et al.,* 1990	W. B. Hutchinson, K. I. Nilson and J. Hirsch; "*Metallurgy of vacuum degassed products",* 109-126, 1990, Warrendale, PA, TMS
Irie *et al.,* 1981	T. Irie, S. Satoh, K. Hashiguchi, I. Takahashi and O. Hashimoto; *Kawasaki Steel Technical Report,* No. 2, 1981, pp. 14 - 22
Jeong, 1998	W. C. Jeong; *Metallurgical and Materials Transactions A*, Vol. 29A, 1998, pp. 463 - 467
Kalish and Cohen, 1970	D. Kalish and M. Cohen; *Materials Science and Engineering,* Vol. 6, 1970, pp. 156 – 166
Kinoshita and Nishimoto, 1988	M. Kinoshita and A. Nishimoto; *CAMP-ISIJ*, Vol. 3, 1990, pp. 1780 – 1785
Krausz and Karusz, 1996	A. S. Krausz and K. Krausz; The Constitutive Law of Deformation Kinetics in "*Unified Constitutive Laws of Plastic Deformation*" edited by A. S. Krausz and K. Krausz, Academic Press, London, 1996
Kurosawa *et al.,* 1988	M. Kurosawa, S. Satoh, T. Obara and K. Tsunoyama; *Kawasaki Steel Technical Report,* No. 18, 1988, pp. 61 - 65
Leslie, 1981	W. C. Leslie; *The Physical Metallurgy of Steels,* 1981, McGraw Hill Book Company, New York
Li and Leslie, 1978	C. C. Li and W. C. Leslie; *Metallurgical Transactions A*, Vol. 9A, 1978, pp. 1765 - 1775

Mackay, 1992 a	D. J. C. Mackay; Neural Comput., Vol. 4, 1992, pp. 415 - 447.
Mackay, 1992 b	D. J. C. Mackay; Neural Comput., Vol. 4, 1992, pp. 448 - 472.
Mackay, 1994	D.J.C. Mackay; *American Society for Heating, Refrigerating and Air Conditioning Engineering Transactions (ASHRAE)*, Vol. 100 (2), 1994, pp. 1053 - 1062.
MacKay, 2003	D. J. C. MacKay; *'Information theory, inference and learning algorithms'*, 2003, Cambridge, Cambridge University Press
Mahieu *et al.,* 2001	J. Mahieu, S. Claessens and B. C. De Cooman; *Metallurgical Transactions A*, Vol. 32A, 2001, pp. 2905 - 2907
Massardier *et al.,* 2004	V. Massardier, N. Lavaire, M. Sober, J. Merlin; *Scripta Materialia*, Vol. 50, 2004, pp. 1435 - 1439
Matlock *et al.,* 1998	D. K. Matlock, B. J. Allen and J. G. Speer; Proc. Conf. On *"Modern LC and ULC sheet steels for cold forming: processing and properties"*,(ed. W. Bleck), Institute of Ferrous Metallurgy, Aachen, Germany, 1998, pp. 265 – 276
McCusker *et al.,* 1999	L. B. McCusker, R. B. Von Dreele, D. E. Cox, D. Louer and P. Scardi; *Journal of Applied Crystallography*, Vol. 32, 1999, pp. 36 - 50
Meissen and Leroy, 1989	P. Meissen and V. Leroy; *Steel Research*, Vol. 60, 1989, pp. 320 - 328
Miller, 2000	M. K. Miller; *Atom Probe Tomography*, New York, Kluwer Academic / Plenum Press, 2000
MUCG-83	www.msm.cam.ac.uk/phase-trans
Mukherjee, 2006	M. Mukherjee; *Ph.D. Thesis,* IIT-Kharagpur, 2006
Mukherjee *et al.,* 2008	M. Mukherjee, S. B. Singh and O. N. Mohanty; *Materials Science and Engineering A*, Vol 486 (1-2), 2008, pp. 32 – 37
Nabarro, 1948	F. R. N. Nabarro; *Report on Strength of Solids*, Physical Society, London, 1948, pp. 38 - 45
Nakada and Keh, 1967	Y. Nakada and A. S. Keh; *Acta Metallurgica,* Vol. 15, 1967, pp. 879 – 883
Neife *et al.,* 1994	S. I. Neife, E. Pink and H. P. Stüwe; *Scripta Metallurgica et Materialia,* Vol. 30, 1994, pp. 361 - 366
Nordheim and Gorter, 1935	L. Nordheim, C. J. Gorter; *Physica*, Vol. 2, 1935, pp. 383 - 390
Obara *et al.,* 1985	T. Obara, K. Sakata, M. Nishida and T. Irie; *Kawasaki Steel Technical Report*, No. 12, 1985, pp. 25-35

Okamoto *et al.,* 1981	A. Okamoto, M. Takahashi and T. Hino; *Transactions ISIJ,* Vol. 21, 1981, pp. 802 - 809
Osawa *et al.,* 1989	K. Osawa, S. Satoh, T. Obara, T. Katoh, H. Abe and K. Tsunoyama; in Proceedings of *International Symposium on Metallurgy of Vacuum Degassed Steel Products*, Ed. R. Pradhan, TMS, 1989, pp. 181 – 195
Pereloma *et al.,* 2007	E. V. Pereloma, I. B. Timokhina, M. K. Miller and P. D. Hodgson; *Acta Materialia,* Vol. 55, 2007, pp. 2587 – 2598
Pereloma *et al.,* 2008 *a*	E. V. Pereloma, K. F. Russsel, M. K. Miller and I. B. Timokhina; *Scripta Materialia*, Vol. 58, 2008, pp. 1078 - 1081
Pereloma *et al.,* 2008 *b*	E. V. Pereloma, M. K. Miller and I. B. Timokhina; *Metallurgical and Materials Transactions A,* Vol. 39, 2008, pp. 3210 – 3216
Rana, 2006	R. Rana, S. B. Singh and O. N. Mohanty; *Scripta Materialia,* Vol. 55, 2006, pp. 1107 - 1110
Rana, 2007	R. Rana; *Ph.D thesis,* IIT Kharagpur, India, 2007
Rana *et al.,* 2008	R. Rana, W. Bleck, S. B. Singh and O. N. Mohanty; *Materials Letters,*Vol. 62, 2008, pp. 949 - 952
Rubianes and Zimmer, 1996	J. M. Rubianes and P. Zimmer; *Rev. Metall. Cah. Int. Tech*., 1996, 99-109
Sakata *et al.,* 1994	K. Sakata, S. Satoh, T. Kato and O. Hashimoto; *"Physical Metallurgy of IF steels"*, Tokyo, Iron and Steel Institute of Japan, 1994, pp. 279 - 288
Samek *et al.,* 2008	L. Samek, E. De Moor, J. Penning, J. G. Speer and B. C. De Cooman; *Metallurgical and Materials Transactions A,* Vol. 39A, 2008, pp. 2542 - 2554
Seal, 2006	R. K. Seal; *MS Thesis,* University of Pittsburgh, 2006
Singh *et al.,* 1998	S. B. Singh, H. K. D. H. Bhadeshia, D. J. C. MacKay, H. Carey and I. Martin; *Ironmaking and Steelmaking,* Vol. 25, 1998, pp. 355 - 365.
Snoek, 1941	J. L. Snoek; *Physica VIII,* No. 7, 1941, pp. 711 – 733
Soenen *et al.,* 2004	B. Soenen, A. K. De, S. Vandeputte and B. C. De Cooman; *Acta Materialia,* Vol. 52, 2004, pp 3482 – 3492
Takahashi and Bhadeshia, 1989	M. Takahashi and H. K. D. H. Bhadeshia; *Journal of Materials Science Letters,* Vol. 8, 1989, pp. 477 – 478
Takahashi *et al.,* 2005	Jun Takahashi, Masaaki Sugiyama and Naoki Maruyama; *Nippon Steel Technical Report,* No. 91, 2005, pp. 28 – 33
Taniguchi *et al.,* 2005	H. Taniguchi, T. Kiyokawa, M. Mizutani and R. Okamoto; *Tetsu-to-Hagane*, Vol. 91, 2005, pp. 662-669

Terao and Baugnet, 1990	N. Terao and A. Baugnet; *Journal of Material Science*, Vol. 25, 1990, pp. 848
Thermo-Calc	Thermo-Calc Software AB; Stockholm Technology Park, Bjornasvagen 21, SE-11347, Stockholm, Sweeden
Timokhina *et al.,* 2010	I. B. Timokhina, E. V. Pereloma, S. P. Ringer, R. K. Zheng and P. D. Hodgson; *ISIJ International,* Vol. 50, 2010, pp. 574 - 582
Tsuchida *et al.,* 2005	N. Tsuchida, E. Baba, K. Nagai and Y. Tomota; Acta Materialia, Vol. 53, 2005, pp. 265 – 270
Urabe and Jonas, 1994	T. Urabe and J. J. Jonas; *ISIJ International,* Vol. 34, 1994, pp. 435 - 442
Van Snick *et al.,* 1998	A. Van Snick, K. Lips, S. Vandeputte, B. C. De Cooman and J. Dilewijns; Proc. Conf. On *"Modern LC and ULC sheet steels for cold forming: processing and properties"*, Vol. II (ed. W. Bleck), Institute of Ferrous Metallurgy, Aachen, Germany, 1998, pp. 413 - 424
Wert, 1949	C. A. Wert; *Journal of Applied Physics,* Vol. 20, 1949, pp. 943 – 949
Wert, 1950	C. A. Wert; *Physical Review,* Vol. 79, 1950, pp. 601 - 605
Wilson and Russel, 1959	D. V. Wilson and B. Russell; *Acta Metallurgica,* Vol. 7, 1959, pp. 628 – 631
Wilson and Russel, 1960	D. V. Wilson and B. Russell; *Acta Metallurgica*, Vol. 8, 1960, pp. 36-45
X'Pert	X'Pert High Score Plus Software; PANalytical BV, Lelyweg 1, 7602 EA ALMELO, The Netherlands
Young, 2002	R. A. Young; *The Rietveld Method,* Oxford University Press, New York, 2002
Zener, 1949	C. Zener; *Journal of Applied Physics*, Vol. 20, 1949, pp. 950 – 953
Zhang *et al.,* 2008	J. Zhang, R. Fu, M. Zhang, R. Liu, X. Wei and L. Li; *Journal of University Science and Technology Beijing*, Vol. 15, 2008, 132-137.
Zhao *et al.,* 2000	J. Z. Zhao, A. K. De and B. C. De Cooman; *ISIJ International*, Vol. 40, 2000, pp. 725-730
Zhao *et al.,* 2001	J. Z. Zhao, A. K. De and B. C. De Cooman; *Metallurgical and Materials Transactions A*, Vol- 32A, 2001, 417-423

Research publications

A number of publications, including journal and conference proceedings, were obtained from the current work. These publications are listed below with their full details.

1. **Published in peer reviewed journals**

   i.   S. Das, S. B. Singh, O. N. Mohanty and H. K. D. H. Bhadeshia, *Materials Science and Technology,* Vol. 24, 2008, pp. 107 - 111

   ii. S. Das, S. B. Singh and O. N. Mohanty, *Ironmaking and Steelmaking,* Vol. 38, 2011, pp. 139 – 143

   iii. S. Das, I. Timokhina, S. B. Singh, E. Pereloma and O. N. Mohanty, *Materials Science and Engineering A,* Vol. 534, 2012, pp. 485 – 494

2. **Communicated to peer reviewed journals**

   i.   S. Das, S. B. Singh and O. N. Mohanty, "*Bake Hardening: A Theoretical Model*"

   ii. S. Das, S. B. Singh and O. N. Mohanty, "*Low temperature aging in ultra low carbon bake hardenable steel*"

3. **Published in conference proceedings**

   i.   S. Das, S. B. Singh and O. N. Mohanty, "Bake hardening: An overview"**,** Invited paper in International Conference on *Interstitial Free Steel 2010*, organised by Tata Steel Limited, Jamshedpur,2010

   ii. S. Das, S. B. Singh and O. N. Mohanty, "Thermoelectric power measurements in an ultra low carbon, bake hardenable steel", in International Conference on Advances in Materials and Materials Processing (ICAMMP) 2011, organised by IIT-Kharagpur, 8-10th November, 2011